Original Article

Clinico-pathologic study of 252 resected thymomas with emphasis on atypical A and AB group: a single institution experience

Andrea Bille[1,2], Camilla Cavalli[3], George Papaxoinis[4], Emma McLean[5], Daisuke Nonaka[2,5]

[1]Department of Thoracic Surgery, Guy's and St Thomas' National Health Service Foundation Trust, London, UK; [2]King's College London, School of Cancer & Pharmaceutical Sciences, Great Maze Pond, London, UK; [3]King's College London, Strand Campus, London, UK; [4]Medical Oncology, Agios Savvas Anticancer Hospital, Athina, Greece; [5]Department of Cellular Pathology, Guy's and St Thomas' National Health Service Foundation Trust, London, UK

Contributions: (I) Conception and design: D Nonaka; (II) Administrative support: A Bille; (III) Provision of study materials or patients: D Nonaka, A Bille; (IV) Collection and assembly of data: D Nonaka, E McLean, C Cavalli; (V) Data analysis and interpretation: D Nonaka, E McLean, G Papaxoinis; (VI) Manuscript writing: All authors; (VII) Final approval of manuscript: All authors.

Correspondence to: Daisuke Nonaka, MD. King's College London, School of Cancer & Pharmaceutical Sciences, Great Maze Pond, London, UK; Department of Cellular Pathology, Guy's and St Thomas' National Health Service Foundation Trust, North Wing, 2nd Floor, Westminster Bridge Road, London, SE1 7EH, UK. Email: DNonaka@msn.com.

Background: World Health Organization (WHO) classification defines subdivision of type B group (B1, B2, and B3) based on proportion of neoplastic epithelial cells and non-neoplastic lymphocytes, and a number of studies have demonstrated correlation between the subtype and prognosis, with type B3 being unfavorable. Type A and AB tumors share similar clinico-pathological features, with generally indolent behavior, and both are characterized by GTF2I mutation. A subset of type A and AB tumors shows atypical features such as increased mitotic activity, cytologic atypia and necrosis, and the term atypical type A has been proposed; however, the atypical category is not well-defined. Aim of the study is to establish criteria for atypical type A thymoma.

Methods: A total of 252 thymomas resected from 247 patients were retrieved and reviewed. A variety of clinical and histopathologic parameters were recorded and analyzed, and prognostic factors in type A and AB group were investigated in order to better define the atypical category.

Results: Median age was 63 years (range, 14–84 years), equal male:female ratio (121:129), median tumor size 65 mm (range, 10–300 mm). There were 46 tumors (type A), 105 (AB), 22 (B1), 47 (B2), and 32 (B3). The majority of patients with A/AB subtypes were above 63 years old, whereas the majority of patients with B group were below 63 years old. Type B group was more often of advanced stage compared to A/AB. Vascular invasion was shown more often in subtype A and necrosis in subtype B1. AB group included larger tumors than the other subtypes. Paraneoplastic syndromes were reported in 71 (28.4%) patients and were more frequently seen in subtypes B2 and B3. In A/AB group, multivariate Cox proportional hazard models demonstrated that mitotic count was the only independent prognostic factor as continuous variable [hazard ratio (HR) 1.15, 95% confidence interval (CI): 1.07–1.24, P<0.001]. A/AB cases were further classified by mitotic count in 4 groups (1–4, 5–9, 10–19 and ≥20 mitotic figures per 2 mm^2). Patients with mitotic count 1–4, 5–9 and 10–19 had similarly favorable progression free survival (PFS), while those with ≥20 mitotic figures per 2 mm^2 had remarkably worse outcomes. Therefore, A/AB patients were classified as typical if mitotic count was 0–19/2 mm^2 and atypical if ≥20 mitotic figures per 2 mm^2. Multivariate Cox proportional hazard models were performed in the entire population. The strongest prognostic factors were the new subtype classification, the presence of necrosis, the status of surgical margins and neoadjuvant treatment.

Conclusions: Our results suggest atypical type A and AB could be defined as tumors with ≥20 mitotic figures per 2 mm^2.

Keywords: Thymoma; type A; type AB; atypical thymoma

Received: 30 May 2024; Accepted: 27 January 2025; Published online: 17 September 2025.
doi: 10.21037/med-24-22
View this article at: https://dx.doi.org/10.21037/med-24-22

Introduction

Thymomas are thymic epithelial tumors characterized by the presence of organotypical features similar to those seen in either the active or the senescent thymic gland. According to the World Health Organization (WHO) classification, thymomas are divided into type A, type B, and type AB (1). Type B is further subdivided into types B1, B2, and B3. The 3 types of type B thymomas have been found to correlate with clinical outcome in several studies and are therefore thought to represent an increasing stage of "tumor progression" or tumor grade. Type A thymomas are regarded as being generally associated with a histologically bland appearance and a favorable clinical outcome. In 2012, 13 cases of type A thymomas with atypical features, including cytologic atypia, increased mitotic activity and necrosis, were described (2). Since the publication, several articles regarding atypical features in type A have emerged but so far, a definition of atypia and its relation to clinical behavior have yet to be established (3-5). In this study, we investigated a variety of clinical and pathologic features in resected thymomas to find a correlation between atypia and clinical outcome in type A and AB groups. The goal was to attempt to define atypia in this thymoma subgroup. We present this article in accordance with the STROBE reporting checklist (available at https://med.amegroups.com/article/view/10.21037/med-24-22/rc).

Highlight box

Key findings

- Atypical type A and AB could be defined as tumors with ≥20 mitotic figures per 2 mm^2.

What is known and what is new?

- Type A thymomas are regarded as tumors with a histologically bland appearance and a favorable clinical course.
- When thymomas were divided into 3 prognostic groups, i.e., a favorable prognosis group (typical A/AB), an intermediate prognostic group (poor prognostic subtypes without necrosis) and a poor prognostic group (poor prognostic subtypes with necrosis), this model was prognostically important in AJCC or Masaoka stage I–II).

What is the implication, and what should change now?

- Atypical type A and AB could be defined as tumors with ≥20 mitotic figures per 2 mm^2.

Methods

Thymomas were retrieved from the histopathology archives at St Thomas's Hospital during the period from 1997 to 2017. Inclusion criteria for the study were a thymoma treated by resection for curative intent and availability of histologic slides. A total of 255 thymomas from 250 patients were collected and analyzed. Local institutional review board (IRB) ethical consent was not required for this study, but local hospital audit committee consent (Guy's and St Thomas' NHS Foundation Trust, REC reference 18/EE/0025) was obtained. The study conformed to the provisions of the Declaration of Helsinki and its subsequent amendments. Individual consent for this retrospective analysis was waived. Hematoxylin and eosin (H&E) stained sections from resected tumors were reviewed, and according to the 2021 World Health Organization classification of thymic tumors (1). In general, a resected tumor was sliced and submitted entirely if it was <3 cm, and submitted 1 section per cm if >3 cm. The number of tumor slides ranged 2 to 26, with a median of 7. Two senior histopathologists specialized in thoracic pathology reviewed all the cases individually, and when there were discrepancies in thymoma histotype and other features, the cases were reviewed with dual-head microscope for consensus. Mitotic count was evaluated by the same two histopathologists using dualhead microscope. A variety of clinical and histopathologic parameters were recorded and analyzed. The mitotic count in 2 mm^2, that is, 8 high-power fields (×400) by NIKON Eclipse (10× eyepiece and 40× objective: 0.25 mm^2), was evaluated in areas of highest mitotic density (hotspot) in type A and AB thymomas. In type AB thymomas, the mitotic count was evaluated in lymphocyte-poor areas, as it is difficult to distinguish between mitotic figures of the tumor cells and of the lymphocytes. The evaluation of vascular invasion followed the protocol routinely used for thyroid follicular neoplasms, i.e., a vessel within or beyond capsule that contains a tumor covered with endothelium, attached to the wall or with thrombus. Low-grade cellular atypia was defined as uniform nuclei in size and shape,

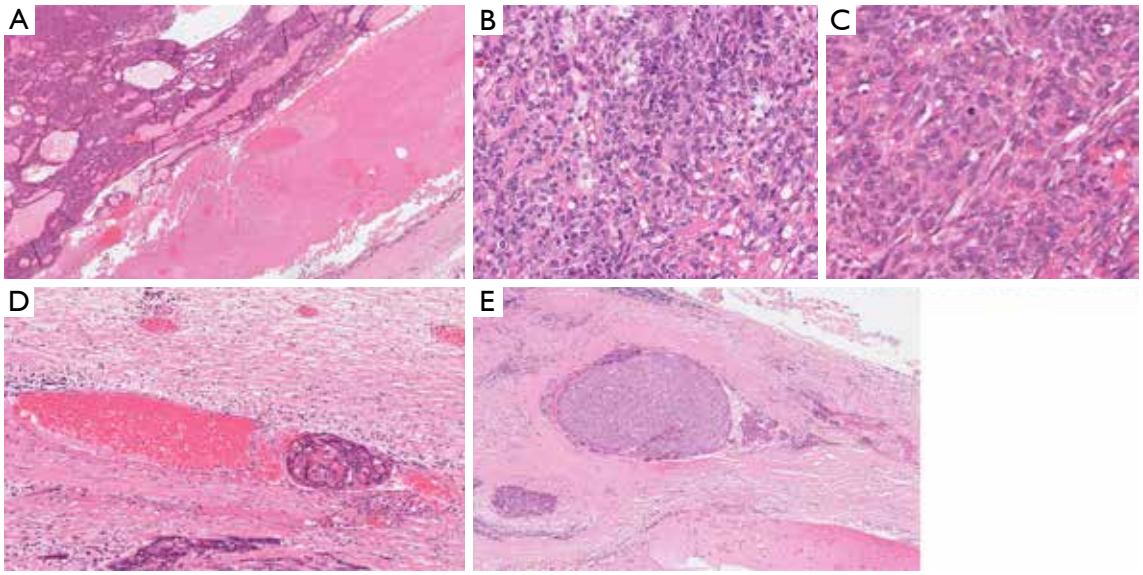

Figure 1 Representative pictures of various histologic features in hematoxylin & eosin stain. (A) Large coagulative necrosis (×40); (B,C) low grade and high grade cytologic atypia with mitotic activity, respectively (×400); (D,E) vascular invasion covered by thrombus and endothelium, respectively (×100).

while high-grade atypia was defined as enlarged nuclei of varied sizes and shapes, often accompanied by conspicuous nucleoli. Predominant pattern was assigned in each case. Microscopic photographs of examples of necrosis, cytologic atypia and vascular invasion are demonstrated in *Figure 1*.

Statistical analysis

The statistical analysis was performed using Statistical Package for the Social Sciences for Windows version 22 (SPSS, Inc., Chicago, IL, USA). Chi-square test was used to compare categorical variables. Progression-free survival (PFS) was defined as the time from surgery to disease progression or death from disease. Disease-specific survival (DSS) was defined as the time from surgery to death from disease. Median survival times were calculated by the Kaplan-Meier estimator method and compared by log-rank test. Univariate and multivariate Cox proportional hazard models were used to assess the prognostic significance of baseline parameters. The forward selection procedure with a selection criterion of P<0.10 was used in multivariable Cox proportional hazard models. The parameters examined were age (median ≥63 *vs.* <63 years), sex (male *vs.* female), American Joint Committee on Cancer (AJCC) stage (III–IV *vs.* I–II), Masaoka stage (III–IV *vs.* I–II), mitotic count as continuous variable, cellular atypia (high *vs.* low), vascular invasion (present *vs.* absent), necrosis (present *vs.* absent), tumour size (>50 *vs.* ≤50 mm), surgical margin (R1 *vs.* R0), paraneoplastic syndrome (present *vs.* absent), neoadjuvant treatment (yes *vs.* no) and thymoma subtype (A/AB *vs.* B1/2 *vs.* B3). Please note that both TNM 8th and Masaoka stages were assigned to all cases while reviewing the clinical charts, macroscopic descriptions in the original histology reports, and glass slides. All analyses were two-tailed, and p values of <0.05 were considered significant. The Bonferroni correction was applied when appropriate.

Results

The study included 247 patients who underwent surgical resection of thymoma. Median age was 63 years (range, 14–84 years). Median tumor size was 65 mm (range, 10–300 mm). The AB subtype (41.2%) was the most common, followed by B2 (18.8%), A (17.2%), B3 (12.8%) and B1 (8.8%). The basic demographic and tumor characteristics according to the thymoma subtype are demonstrated in *Table 1*. There was a substantial difference in age distribution between different thymoma subtypes. The majority of patients with A and AB subtypes were above 63 years old, whereas the majority of patients with subtypes B1, B2 and B3 were below 63 years old. Subtypes B1-B2-B3 were often of an advanced stage compared to

Table 1 Basic demographic, disease and treatment characteristics by thymoma subtype

Clinico-pathologic features	Thymoma subtype, n (%)					Total, n (%)	P value
	A	AB	B1	B2	B3		
Age (years)							<0.001
<63	8 (18.6)	48 (46.6)	13 (59.1)	30 (63.8)	20 (62.5)	119 (48.2)	
≥63	35 (81.4)	55 (53.4)	9 (40.9)	17 (36.2)	12 (37.5)	128 (51.8)	
Sex							0.34
Female	20 (46.5)	61 (59.2)	9 (40.9)	22 (46.8)	15 (46.9)	127 (51.4)	
Male	23 (53.5)	42 (40.8)	13 (59.1)	25 (53.2)	17 (53.1)	120 (48.6)	
AJCC stage							<0.001
I	38 (88.4)	101 (98.1)	16 (72.7)	33 (70.2)	18 (56.3)	209 (83.6)	
II	1 (2.3)	0	1 (4.5)	4 (8.5)	1 (3.1)	7 (2.8)	
IIIA	4 (9.3)	1 (1.0)	4 (18.2)	6 (12.8)	6 (18.8)	21 (8.4)	
IIIB	0	0	0	0	1 (3.1)	1 (0.4)	
IVA	0	1 (1.0)	1 (4.5)	4 (8.5)	6 (18.8)	12 (4.8)	
Masaoka stage							<0.001
I	16 (37.2)	48 (46.6)	2 (9.1)	5 (10.6)	3 (9.4)	76 (30.4)	
IIA	19 (44.2)	51 (49.5)	14 (63.6)	22 (46.8)	13 (40.6)	120 (48.0)	
IIB	3 (7.0)	2 (1.9)	0	5 (10.6)	2 (6.3)	12 (4.8)	
III	5 (11.6)	1 (1.0)	5 (22.7)	11 (23.4)	7 (21.9)	29 (11.6)	
IVA	0	1 (1.0)	1 (4.5)	4 (8.5)	6 (18.8)	12 (4.8)	
IVB	0	0	0	0	1 (3.1)	1 (0.4)	
Vascular invasion							0.02
Absent	36 (83.7)	99 (96.1)	22 (100.0)	47 (100.0)	30 (93.8)	237 (94.8)	
Present	7 (16.3)	4 (3.9)	0	0	2 (6.3)	13 (5.2)	
Necrosis							0.02
Absent	31 (72.1)	85 (82.5)	13 (59.1)	41 (87.2)	28 (87.5)	199 (79.6)	
Present	12 (27.9)	18 (17.5)	9 (40.9)	6 (12.8)	4 (12.5)	51 (20.4)	
Mitotic count (per 2 mm^2)							0.16
0–4	19 (44.2)	70 (68.0)	NA	NA	NA	NA	
5–9	11 (25.6)	20 (19.4)	NA	NA	NA	NA	
10–19	10 (23.2)	10 (9.7)	NA	NA	NA	NA	
≥20	3 (7.0)	3 (2.9)	NA	NA	NA	NA	
Tumor size (mm)							0.04
≤50	18 (41.9)	23 (22.3)	10 (45.5)	18 (38.3)	13 (40.6)	82 (33.2)	
>50	25 (58.1)	80 (77.7)	12 (54.5)	29 (61.7)	19 (59.4)	165 (66.8)	

Table 1 (*continued*)

Table 1 (*continued*)

Clinico-pathologic features	Thymoma subtype, n (%)					Total, n (%)	P value
	A	AB	B1	B2	B3		
Surgical margin							<0.001
R0	35 (81.4)	94 (91.3)	13 (59.1)	27 (57.4)	15 (46.9)	187 (74.8)	
R1	8 (18.6)	9 (8.7)	9 (40.9)	15 (31.9)	15 (46.9)	56 (22.4)	
R2	0	0	0	5 (10.6)	2 (6.3)	7 (2.8)	
Paraneoplastic syndrome							<0.001
Absent	35 (81.4)	81 (78.6)	19 (86.4)	22 (46.8)	19 (59.4)	179 (71.6)	
Present	8 (18.6)	22 (21.4)	3 (13.6)	25 (53.2)	13 (40.6)	71 (28.4)	
Total	43 (100.0)	103 (100.0)	22 (100.0)	47 (100.0)	32 (100.0)	250 (100.0)	

AJCC, American Joint Committee on Cancer; NA, not assessed.

Table 2 Univariate analysis of prognostic factors for progression-free survival in the entire population

Covariates	HR	95% CI	P value
Age (≥63 *vs.* <63 years[†])	0.41	0.18–0.93	0.03
Sex (male *vs.* female)	1.11	0.52–2.37	0.78
AJCC stage (III–IV *vs.* I–II)	9.04	4.18–19.54	<0.001
Masaoka stage (III–IV *vs.* I–II)	6.68	3.11–14.34	<0.001
Vascular invasion (present *vs.* absent)	1.68	0.40–7.10	0.48
Necrosis (present *vs.* absent)	2.80	1.30–6.04	0.009
Size (>50 *vs.* ≤50 mm)	1.46	0.16–13.12	0.74
Surgical margin			
R1 *vs.* R0	7.09	3.19–15.77	<0.001
R2 *vs.* R0	4.00	0.51–31.55	0.19
Thymoma subtype			
B1/2 *vs.* A/AB	8.01	2.85–22.49	<0.001
B3 *vs.* A/AB	9.35	3.01–29.02	<0.001
B1/2 *vs.* B3	0.86	0.36–2.05	0.73
Paraneoplastic syndrome (present *vs.* absent)	2.19	1.03–4.69	0.04
Neoadjuvant treatment (yes *vs.* no)	10.20	4.72–22.05	<0.001

[†], median age was 63 years. AJCC, American Joint Committee on Cancer; CI, confidence interval; HR, hazard ratio.

subtypes A and AB. Additionally, patients with subtypes B1-B2-B3 more frequently had microscopically positive surgical resection margins (R1) or macroscopic residual disease (R2). In contrast, vascular invasion was more often seen in subtype A and necrosis in subtype B1. Finally, AB group was characterized by a larger size than the other subtypes. Paraneoplastic manifestations were reported in 71 (28.4%) patients. These included myasthenia gravis in 56 (22.4%) patients, 5 with pure red cell aplasia (1 co-existing with myasthenia gravis and 1 with Goods syndrome), 2 with systemic lupus erythematosus, 3 with pemphigus vulgaris (1 co-existing with myasthenia gravis), 3 with Goods syndrome, 2 with idiopathic thrombocytopenia, 1 autoimmune hepatitis, 1 polymyalgia, and 1 multi-organ autoimmunity. Subtypes B2 and B3 had a higher incidence of paraneoplastic phenomena. Neoadjuvant treatment was given in 26 (10.4 %) patients; 25 received chemotherapy and 1 radiotherapy. Neoadjuvant chemotherapy was administered in 10 (31.3%) of the patients with B3 subtype, in 12 (17.6%) of B1/2 and only 3 (2.0%) of A/AB (P<0.001).

Of 247 patients included in the study, 242 (98%) were followed for a median time of 56 months (range, 2–254 months). During this time, 27 (10.9%) patients progressed/relapsed and 62 (25.1%) died: 15 (6.1%) from disease and 47 (19.0%) from other causes. Five-year PFS was 88% and 5-year DSS was 94%. Prognostic factors are shown in *Table 2*. As shown in *Figure 2*, PFS of patients with A and AB was similar and better than B1, B2 and B3

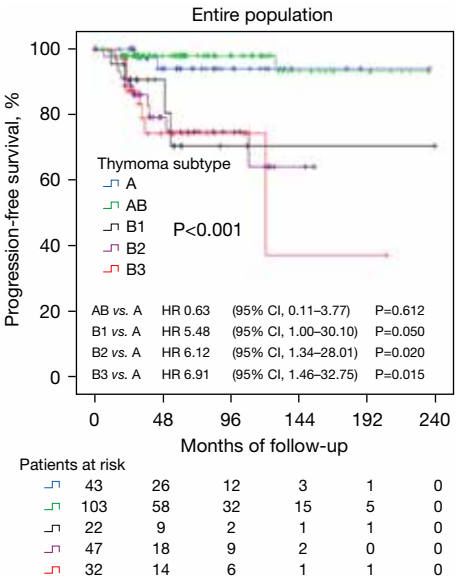

Figure 2 Progression-free survival in each thymoma subtype. CI, confidence interval; HR, hazard ratio.

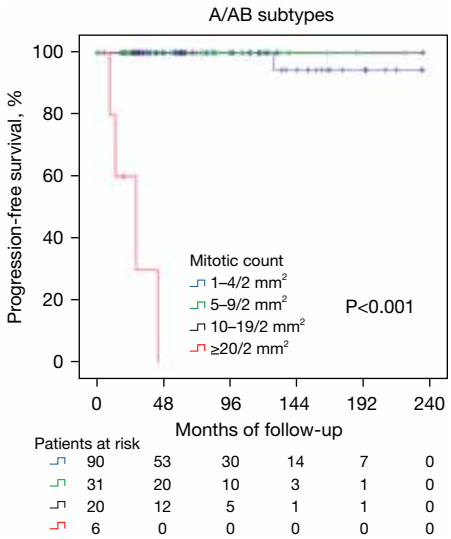

Figure 3 Progression-free survival according to mitotic count.

Table 3 Univariate analysis of prognostic factors for progression-free survival in patients with A/AB subtypes

Covariates	HR	95% CI	P value
Age (≥63 *vs.* <63 years[†])	2.70	0.30–24.20	0.37
Sex (male *vs.* female)	0.29	0.03–2.55	0.26
AJCC stage (III–IV *vs.* I–II)	9.91	1.02–96.00	0.048
Masaoka stage (III–IV *vs.* I–II)	7.72	0.80–74.36	0.08
Mitotic count (increasing)	1.14	1.07–1.21	<0.001
Cellular atypia (high *vs.* low)	15.87	1.65–152.65	0.02
Vascular invasion (present *vs.* absent)	3.57	0.39–32.37	0.26
Necrosis (present *vs.* absent)	2.54	0.42–15.23	0.31
Size (>50 *vs.* ≤50 mm)	2.12	0.23–19.30	0.50
Surgical margin (R1 *vs.* R0)	6.04	1.00–36.44	0.050
Paraneoplastic syndrome (present *vs.* absent)	0.90	0.10–8.03	0.92

[†], median age was 63 years. AJCC, American Joint Committee on Cancer; CI, confidence interval; HR, hazard ratio.

subtypes. B1 and B2 subtypes also had similar PFS. Thus, A and AB subtypes and B1 and B2 subtypes were analyzed as single subgroups. A simplified subtype classification was created, i.e., A/AB, B1/2 and B3 subtypes for further analysis.

Prognostic factors within the A/AB subgroup were analyzed to identify patients with poor characteristics, as shown in *Table 3*. Multivariate Cox proportional hazard models demonstrated that mitotic count was the only independent prognostic factor as continuous variable [hazard ratio (HR) 1.15, 95% confidence interval (CI): 1.07–1.24, P<0.001]. A/AB cases were classified by mitotic count in 4 groups (1–4, 5–9, 10–19 and ≥20 mitotic figures per 2 mm^2). As shown in *Figure 3*, patients with mitotic count 1–4, 5–9 and 10–19 had similarly favorable PFS, while those with ≥20 mitotic figures per 2 mm^2 had remarkably worse outcome. Therefore, A/AB patients were classified as typical if mitotic count was 0–19/2 mm^2 and atypical if ≥20 mitotic figures per 2 mm^2. PFS curves of patients with typical A/AB, atypical A/AB, B1/2, B3 and rare subtypes are shown in *Figure 4*.

Multivariate Cox proportional hazard models were performed in the entire population, including the new subtype classification, as shown in *Table 4*. The strongest prognostic factors were the new subtype classification, the presence of necrosis, the status of surgical margins and neoadjuvant treatment. For simplicity, the thymoma subtypes were classified into favorable prognosis (typical A/AB, unusual subtypes) and poor prognosis subtypes (atypical A/AB, B1/2, B3) and were combined with the presence or absence of necrosis in a prognostic model. Although necrosis was present at the same rate in the favorable prognosis (29/143 cases, 20.3%) and the poor prognosis subtypes (22/107, 20.6%, P=1.000), it was associated with shorter

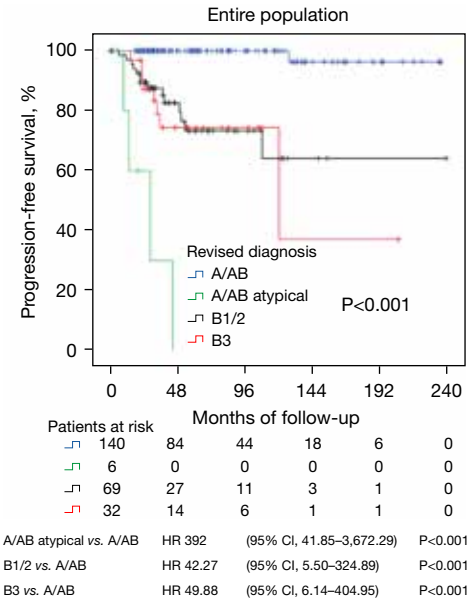

Figure 4 Progression-free survival according to typical A/AB, atypical A/AB, B1/B2 and B3 subtypes. CI, confidence interval; HR, hazard ratio.

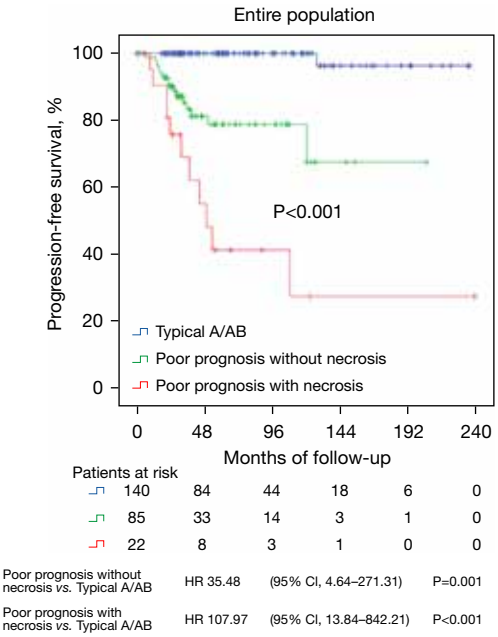

Figure 5 Progression-free survival according to each prognostic subgroup, that is, typical A/AB (favorable prognostic group), poor prognosis subtypes without necrosis (intermediate prognostic group) and poor prognosis subtypes with necrosis (poor prognostic group). CI, confidence interval; HR, hazard ratio.

Table 4 Multivariate Cox proportional hazard model of independent prognostic factors for progression-free survival in the entire population

Covariates	HR	95% CI	P value
Age (≥63 *vs.* <63 years)	1.20	0.42–3.44	0.73
Sex (male *vs.* female)	0.82	0.32–2.12	0.82
AJCC stage (III–IV *vs.* I–II)	0.88	0.27–2.86	0.84
Vascular invasion (present *vs.* absent)	0.14	0.02–0.99	0.048
Necrosis (present *vs.* absent)	5.73	1.85–17.74	0.002
Size (>50 *vs.* ≤50 mm)	1.39	0.40–4.86	0.61
Surgical margin (R1 *vs.* R0)	3.18	0.93–10.83	0.06
Paraneoplastic syndrome (present *vs.* absent)	3.81	1.38–10.51	0.010
Neoadjuvant treatment (yes *vs.* no)	9.15	2.79–29.98	<0.001
Thymoma subtype			
Atypical *vs.* typical A/AB	1,636.52	113.92–23,508.79	<0.001
B1/2 *vs.* typical A/AB	23.38	2.61–209.79	0.005
B3 *vs.* typical A/AB	33.65	3.24–349.86	0.003

AJCC, American Joint Committee on Cancer; CI, confidence interval; HR, hazard ratio.

PFS only in the poor prognosis subtypes (P=0.003) and not in the favorable prognosis group (P=0.602). Therefore, the new prognostic classification included 3 groups, a favorable prognosis group (typical A/AB, rare subtypes), an intermediate prognostic group (poor prognostic subtypes without necrosis) and a poor prognostic group (poor prognostic subtypes with necrosis), as shown in the respective PFS curves in *Figure 5*. The proposed classification was prognostic only in early clinical stages (AJCC or Masaoka stage I–II, difference of PFS in each prognostic group was statistically significant (P<0.001, respectively) (*Figure 6A,6B*). In contrast, the model was not prognostically important in advanced AJCC or Masaoka stages (III–IV) (P=0.35 and P=0.23, respectively), probably because in these stages typical A/AB subtype are under-represented (*Figure 6C,6D*). Nevertheless, none of the patients with typical A/AB subtype in advanced stage resulted in progression.

Discussion

Among all thymoma subtypes, type A and AB are regarded as a clinically indolent group, and although both represent

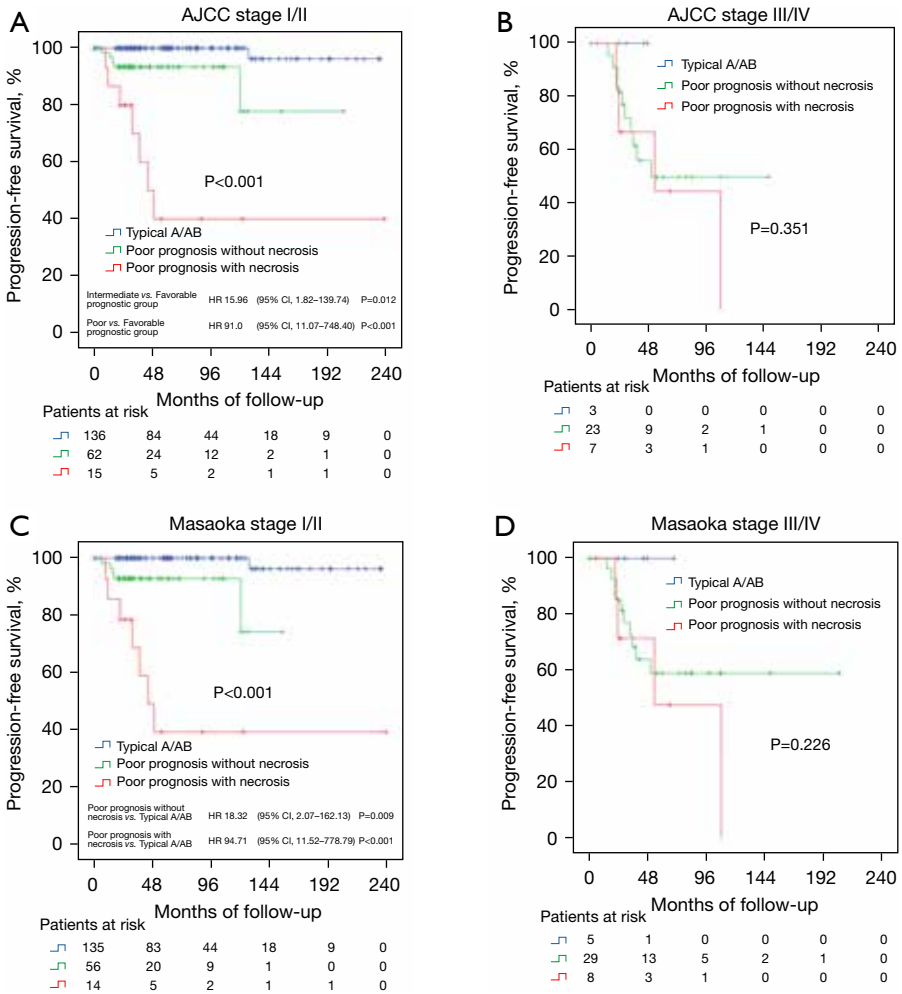

Figure 6 PFS according to each prognostic subgroup in stages. (A) PFS according to each prognostic subgroup in AJCC stage I and II; (B) PFS according to each prognostic subgroup in AJCC stage III and IV; (C) PFS according to each prognostic subgroup in Masaoka stage I and II; (D) PFS according to each prognostic subgroup in Masaoka stage III and IV. AJCC, American Joint Committee on Cancer; CI, confidence interval; HR, hazard ratio; PFS, progression-free survival.

separate subtype in the WHO classification scheme, they share a number of clinical, pathological and genetic features, including favorable behavior, infrequent association with myasthenia gravis, spindle cell morphology and GTF2I mutation. Until recently, both subtypes were regarded as being clinically benign and the majority of the literature had described no atypia or no/rare mitotic activity in those subtypes (6-8). However, a small subset of type A and AB thymomas present at stage IV, with the reported frequency being 1.4% (9) and 1.6% (10). In a recent worldwide database, approximately 1% of 443 patients with type A thymoma had stage IVb disease (Masaoka's staging system) (11,12). These data suggest that a small proportion of type A and AB thymomas may be biologically malignant; therefore, type A and AB thymomas cannot be considered to be benign neoplasms.

Approximately 10 years ago, the late Professor Juan Rosai and one of the authors in the current study reported a series of type A thymoma with atypical features, including increased mitotic activity, necrosis and cellular atypia, to expand the morphological spectrum of this subtype and to describe that not all type A thymomas were bland in appearance (2). Since then, several published articles, most of which are case reports, have been added to the literature to support the existence of atypical type A thymoma (4,13-21). However, histopathologic definition of atypical type A

thymoma in relation to the prognostic significance and the clinical and therapeutic implications has yet to be established (4). In type A group, the presence of necrosis was correlated with advanced stage at the time of surgery (5) and an increased ratio of recurrence and extrathoracic metastases (22). According to one study, there was no significant difference between the median mitotic count of stage I thymomas and that of stage II–IV thymomas based on Masaoka-Koga staging system (5). Nuclear atypia was not associated with increasing stage of disease (5). One series of five type A thymomas with distant metastases (Masaoka stage IVb) demonstrated that metastases could occur in the absence of atypical histological features, as three of their five cases were ordinary type A thymomas; and that metastatic cases had a tendency to show slightly genetic instability than non-metastatic counterparts (4).

Our study demonstrated that in multivariate Cox proportional hazard models, mitotic count was the only independent prognostic factor as a continuous variable (HR 1.15, 95% CI: 1.07–1.24, P<0.001). When A/AB cases were classified by mitotic count into 4 groups (1–4, 5–9, 10–19 and ≥20 mitotic figures per 2 mm^2), patients with mitotic count 1–4, 5–9 and 10–19 had similarly favorable PFS, but those with ≥20 mitotic figures per 2 mm^2 had remarkably worse outcomes. Therefore, A/AB thymomas are classified as typical if mitotic count was 0–19/2 mm^2 and atypical if ≥20 mitotic figures per 2 mm^2.

The study also demonstrated that the strongest prognostic factors were the proposed subtype classification (i.e., the atypical A and AB incorporated into the WHO scheme), the presence of necrosis, the status of surgical margins and neoadjuvant treatment. For practical purposes, the thymoma subtypes were classified into favorable prognosis (typical A/AB) and poor prognosis histological subtypes (atypical A/AB, B1/2, B3) and were combined with the presence or absence of necrosis in a prognostic model. This model included 3 prognostic groups: a favorable prognosis group (typical A/AB), an intermediate prognostic group (poor prognostic subtypes without necrosis) and a poor prognostic group (poor prognostic subtypes with necrosis). In AJCC or Masaoka stage I–II, the model was prognostically important while in advanced AJCC or Masaoka stages (III–IV) this model did not work.

Our study revealed that neoadjuvant treatment was an unfavorable factor, which was not expected, as some studies showed favorable outcomes. As complete resection is pivotal for improving the prognosis of thymomas, induction therapy is increasingly performed in locally advanced disease in order to downstage the tumor and make it amenable to surgical resection. Since thymomas are uncommon, in the majority of studies, there is obvious selection bias with a shrinking denominator, and the level of evidence is restricted in most publications (23). Furthermore, some studies revealed no apparent treatment-related histologic response (24). Further studies are required to establish the optimal protocol.

High mitotic count seems to be a rare occurrence in thymoma, including type A and AB, and in our study, ≥20 mitotic figures per 2 mm^2 was seen in only 4% of type A and B (6/151 tumors). As such, this cut-off value was based on a small number of cases, although the results were supported by multivariate analysis. A further study with a large number of cases is needed to verify our data.

Conclusions

In summary, our study demonstrated that type A and AB thymomas with ≥20 mitotic figures per 2 mm^2 were associated with poorer outcomes, therefore, the mitotic count of 20/2 mm^2 may serve as a cut-off value to divide type A/AB and atypical A/AB subtypes.

Acknowledgments

None.

Footnote

Reporting Checklist: The authors have completed the STROBE reporting checklist. Available at https://med.amegroups.com/article/view/10.21037/med-24-22/rc

Data Sharing Statement: Available at https://med.amegroups.com/article/view/10.21037/med-24-22/dss

Peer Review File: Available at https://med.amegroups.com/article/view/10.21037/med-24-22/prf

Funding: None.

Conflicts of Interest: All authors have completed the ICMJE uniform disclosure form (available at https://med.amegroups.com/article/view/10.21037/med-24-22/coif). The authors have no conflicts of interest to declare.

Ethical Statement: The authors are accountable for all

aspects of the work in ensuring that questions related to the accuracy or integrity of any part of the work are appropriately investigated and resolved. Local institutional review board (IRB) ethical consent was not required for this study, but local hospital audit committee consent (Guy's and St Thomas' NHS Foundation Trust, REC reference 18/EE/0025) was obtained. The study conformed to the provisions of the Declaration of Helsinki and its subsequent amendments. Individual consent for this retrospective analysis was waived.

References

1. WHO Classification of Tumours Editorial Board. Thoracic Tumours., editor. Epithelial tumours. In: Thoracic Tumours WHO Classification of Tumours, 5th Edition, Volume 5. Lyon: IARC; 2021:319-98.
2. Nonaka D, Rosai J. Is there a spectrum of cytologic atypia in type a thymomas analogous to that seen in type B thymomas? A pilot study of 13 cases. Am J Surg Pathol 2012;36:889-94.
3. Su YC, Di JX, Da JP. Clinicopathologic features of atypical type A thymoma. Zhonghua Bing Li Xue Za Zhi 2017;46:314-7.
4. Bürger T, Schaefer IM, Küffer S, et al. Metastatic type A thymoma: morphological and genetic correlation. Histopathology 2017;70:704-10.
5. Green AC, Marx A, Ströbel P, et al. Type A and AB thymomas: histological features associated with increased stage. Histopathology 2015;66:884-91.
6. Chalabreysse L, Roy P, Cordier JF, et al. Correlation of the WHO schema for the classification of thymic epithelial neoplasms with prognosis: a retrospective study of 90 tumors. Am J Surg Pathol 2002;26:1605-11.
7. Moran CA, Kalhor N, Suster S. Invasive spindle cell thymomas (WHO Type A): a clinicopathologic correlation of 41 cases. Am J Clin Pathol 2010;134:793-8.
8. Verley JM, Hollmann KH. Thymoma. A comparative study of clinical stages, histologic features, and survival in 200 cases. Cancer 1985;55:1074-86.
9. Ströbel P, Bauer A, Puppe B, et al. Tumor recurrence and survival in patients treated for thymomas and thymic squamous cell carcinomas: a retrospective analysis. J Clin Oncol 2004;22:1501-9.
10. Jain RK, Mehta RJ, Henley JD, et al. WHO types A and AB thymomas: not always benign. Mod Pathol 2010;23:1641-9.
11. Radovich M, Pickering CR, Felau I, et al. The Integrated Genomic Landscape of Thymic Epithelial Tumors. Cancer Cell 2018;33:244-258.e10.
12. Weis CA, Yao X, Deng Y, et al. The impact of thymoma histotype on prognosis in a worldwide database. J Thorac Oncol 2015;10:367-72.
13. Hashimoto M, Shimizu S, Takuwa T, et al. A case of atypical type A thymoma variant. Surg Case Rep 2016;2:116.
14. Hashimoto M, Tsukamoto Y, Matsuo S, et al. Lung metastases in an atypical type A thymoma variant. J Thorac Dis 2017;9:E805-7.
15. Grajkowska W, Matyja E, Kunicki J, et al. AB thymoma with atypical type A component with delayed multiple lung and brain metastases. J Thorac Dis 2017;9:E808-14.
16. Kawakita N, Kondo K, Toba H, et al. A case of atypical type A thymoma with vascular invasion and lung metastasis. Gen Thorac Cardiovasc Surg 2018;66:239-42.
17. Chiappetta M, Marino M, Facciolo F. Unique case of atypical type A thymoma with vertebral metastasis and high 18-fluorodeoxyglucose avidity. ANZ J Surg 2019;89:E450-1.
18. Kar A, Pandita A. Report of a Type AB Thymoma with an Atypical Type A component. Clin Med Reports 2020;5. doi:10.15761/cmr.1000156.
19. Yanagiya M, Hamaya H, Matsuzaki H, et al. Atypical Type A Thymoma Variant Manifesting Polymyalgia Rheumatica. Ann Thorac Surg 2020;110:e253-5.
20. Jimbo N, Tateyama H, Komatsu M, et al. A case of type AB thymoma with atypical histological features: Is atypical type AB thymoma an acceptable variant of thymoma? Pathol Int 2021;71:272-4.
21. Yanagiya M, Horiuchi H, Hiyama N, et al. Histopathological heterogeneity in an atypical type A thymoma variant with pulmonary metastases. Pathol Int 2021;71:438-40.
22. Vladislav IT, Gökmen-Polar Y, Kesler KA, et al. The role of histology in predicting recurrence of type A thymomas: a clinicopathologic correlation of 23 cases. Mod Pathol

2013;26:1059-64.
23. Ajimizu H, Sakamori Y. Narrative review of indication and management of induction therapy for thymic epithelial tumors. Mediastinum 2024;8:44.
24. Johnson GB, Aubry MC, Yi ES, et al. Radiologic Response to Neoadjuvant Treatment Predicts Histologic Response in Thymic Epithelial Tumors. J Thorac Oncol 2017;12:354-67.

doi: 10.21037/med-24-22
Cite this article as: Bille A, Cavalli C, Papaxoinis G, McLean E, Nonaka D. Clinico-pathologic study of 252 resected thymomas with emphasis on atypical A and AB group: a single institution experience. Mediastinum 2025;9:22.

Review Article

When rarity meets thoracic cancers: a narrative review from ITMIG 2024

Margaret Ottaviano[1]^, Paolo Antonio Ascierto[1], Erica Pietroluongo[2]

[1]Department of Melanoma, Cancer Immunotherapy and Development Therapeutics, Istituto Nazionale Tumori-IRCCS Fondazione "G. Pascale", Naples, Italy; [2]Department of Clinical Medicine and Surgery, University Federico II, Naples, Italy

Contributions: (I) Conception and design: M Ottaviano; (II) Administrative support: None; (III) Provision of study materials or patients: None; (IV) Collection and assembly of data: M Ottaviano, E Pietroluongo; (V) Data analysis and interpretation: M Ottaviano, E Pietroluongo; (VI) Manuscript writing: All authors; (VII) Final approval of manuscript: All authors.

Correspondence to: Margaret Ottaviano, MD, PhD. Department of Melanoma, Cancer Immunotherapy and Development Therapeutics, Istituto Nazionale Tumori-IRCCS Fondazione "G. Pascale", Via Mariano Semmola, 80131 Naples, NA, Italy. Email: margaretottaviano@gmail.com.

Background and Objective: Rare thoracic cancers (RTCs) comprise a heterogeneous group of malignancies characterized by low incidence, high histological diversity, and significant clinical challenges. Their rarity often results in delayed diagnoses, lack of standardized therapeutic approaches, and limited prospective clinical trials. The absence of robust data is compounded by the fragmentation of expertise across institutions, underscoring the need for centralized, multidisciplinary management and international collaboration. This article aims to provide an overview of three representative RTC models, highlighting their unique clinical, pathological, and therapeutic features, and to discuss strategies for optimizing clinical care.

Methods: A narrative review was conducted based on a targeted search of PubMed, MEDLINE, and major conference proceedings up to January 2025. The search focused on selected RTCs highlighted during the 2024 ITMIG annual meeting, using terms such as "SMARCA4-deficient undifferentiated tumors", "thymic neuroendocrine neoplasms", and "mediastinal germ cell tumors". Eligible sources included case reports, retrospective series, and narrative reviews. Only English-language publications were considered.

Key Content and Findings: We focus on SMARCA4-deficient undifferentiated tumors as examples of rare entities newly defined by molecular profiling; thymic neuroendocrine neoplasms as ultra-rare and biologically aggressive neoplasms; and mediastinal germ cell tumors, which share biological traits with their gonadal counterparts but exhibit unique clinical behaviors. Through these models, we highlight common themes in RTCs management, including diagnostic uncertainty, limited therapeutic options, and emerging directions.

Conclusions: We discuss the strengths and limitations of current evidence and future perspectives aimed at enhancing outcomes through dedicated registries and tailored therapeutic strategies.

Keywords: Rare thoracic cancers (RTCs); SMARCA4-deficient tumors; thymic neuroendocrine neoplasms (TNENs); mediastinal germ cell tumors (mediastinal GCTs)

Received: 15 April 2025; Accepted: 28 July 2025; Published online: 25 September 2025.

doi: 10.21037/med-25-22

View this article at: https://dx.doi.org/10.21037/med-25-22

^ ORCID: 0000-0001-9589-0808.

Introduction

Thoracic malignancies encompass over 100 different histotypes in the World Health Organization (WHO) 5th Classification of 2021, which covers tumors of the lung, thymus, heart, and pleura (1). Rare cancers, as defined by the European Rare Cancer Surveillance Project (RARECARE), represent a highly heterogeneous group of diseases with an incidence of fewer than six cases per 100,000 individuals annually (2). Overall, the estimated incidence of all rare tumors in Europe accounts for 24% of all cancers and, according to the results of RARECARE and Surveillance, Epidemiology, and End Results (SEER) databases, in Europe and the United States of America the 5-year survival is lower (48.5% and 55%, respectively) compared with all cancers with higher incidence (63.4% and 74%, respectively) (3). This worse survival may be mainly related to the lack of adequate and standardized treatments and delays in diagnosis (4). Rare thoracic cancers (RTCs) represent 8% of all thoracic malignancies (2,3), with a crude incidence in Europe of 6.8 per 100 000 people per year (2-4), while the SEER database reports an incidence of 0.22–0.25 cases per 100,000 per year for thymomas (5), 0.04–0.09 for mediastinal germ-cell tumors, and 0.03–0.80 for thoracic sarcomas (6), highlighting how this low incidence is the result of limited literature data with small case series and no prospective studies neither dedicated rare registry studies (7). The low frequency, the high prevalence of different subtypes, and the extreme unpredictability of clinical manifestation make RTCs an excellent challenge for most clinicians (8), who often have to manage complex decision-making processes. Tools largely proposed and accepted by the scientific community to try to fill the gap between common and RTCs are the centralization of diagnostic work-up and treatment in reference centers with high volume, expertise, and multidisciplinary approach (7). Moreover, worthy of consideration is that at the national and international level, some histological subtypes of RTCs may be studied in networks to organize individual efforts and make collation of personal experiences and global collaboration possible. The International Thymic Malignancy Interest Group (ITMIG), founded in 2010 and committed to research and guidelines development in the field of mediastinal cancers, has opened the way for building national-level infrastructure dedicated to reaching scientifically robust progress for rare cancers (9). The Italian network ThYmic MalignanciEs (TYME) is born in the wake of ITMIG to improve the current knowledge and provide a multidisciplinary consensus for the best treatment strategies for thymic epithelial tumors (TETs) (10). While significant efforts have been carried on scientific networking for TETs, which represent the most common mediastinal solid malignancies (8), most histological subtypes belonging to RTCs do not benefit from this organization, and data about them are based on small retrospective cohorts or cases reports (11). In this narrative review, we aim to discuss the epidemiology and the treatment strategies of three oncological models of RTCs selected by the scientific community of ITMIG for the 2024 annual conference to highlight the most critical emerging needs for RTCs: SMARCA4-deficient undifferentiated tumors (SMARCA4-dUT) as a model of rare entities characterized by new molecular profiles discoveries of common cancers; thymic neuroendocrine neoplasms (TNENs) a model of ultra-rare malignancies with an incidence rate less than one case per 100,000 individuals per year; mediastinal germ cell tumors (GCTs) as a model of rare cancers with unfavorable prognosis compared with gonadal counterparts. We present this article in accordance with the Narrative Review reporting checklist (available at https://med.amegroups.com/article/view/10.21037/med-25-22/rc).

Methods

In this narrative review, we discussed the epidemiology, diagnostic complexity, and treatment strategies of selected RTCs presented at the 2024 ITMIG conference. A targeted literature search was conducted using PubMed, MEDLINE, and relevant conference proceedings up to January 2025 (*Table 1*). Search terms included "rare thoracic cancers", "SMARCA4-deficient undifferentiated tumors", "thymic neuroendocrine neoplasms", and "mediastinal germ cell tumors". No restrictions were applied regarding study design or publication status. Only articles published in English were considered. Given the rarity of the selected tumor subtypes, case reports, retrospective studies, and narrative reviews were included. Literature selection was performed independently by two authors, with disagreements resolved by consensus.

SMARCA4-dUT

SMARCA4-dUT are a rare and aggressive subgroup of thoracic malignancies characterized by mutations in the *SMARCA4* gene (12). While nosologically related to SMARCA4-deficient non-small cell lung cancer (SD-

Table 1 The search strategy summary

Items	Specification
Date of search	Up to January 31, 2025
Databases and other sources searched	PubMed, MEDLINE, major international conference proceedings (e.g., ITMIG Annual Meeting)
Search terms used	"Rare thoracic cancers", "SMARCA4-deficient undifferentiated tumors", "thymic neuroendocrine neoplasms", "mediastinal germ cell tumors"
Timeframe	From inception of each database to January 31, 2025
Inclusion and exclusion criteria	Included: English-language publications such as case reports, retrospective series, narrative reviews, and relevant conference abstracts
	Excluded: non-English publications, editorials without original data, and studies not focused on the selected rare thoracic cancers
Selection process	All articles were independently reviewed by two authors (M.O., E.P.). Discrepancies were resolved by discussion and consensus
Additional considerations	Selection was focused on tumor entities presented at the 2024 ITMIG meeting to ensure clinical and scientific relevance

ITMIG, International Thymic Malignancy Interest Group.

NSCLC), they remain a distinct entity. Indeed, SD-NSCLC accounts for approximately 5% of NSCLC cases and is characterized by aggressive clinical features and poor prognosis (13,14).

SMARCA4 is part of the SWI/SNF chromatin remodeling complex, which plays a critical role in suppressing tumor progression. These genes are among the most frequently mutated in human cancers, with alterations occurring in 20–24% of cases across various malignancies (15,16). These mutations are predominantly loss-of-function events, leading to disruptions in transcriptional regulation and DNA repair, thereby driving tumorigenesis. Thus, the defining molecular hallmark of SMARCA4-dUT is the mutation of *SMARCA4*, which leads to the loss of BRG1 protein expression (17). SD-NSCLC are usually adenocarcinomas and often form glandular structures showing a strong expression of cytokeratins in contrast to SMARCA4-dUT. The solid component does not differentiate between carcinoma and SMARCA4-dUT. Immunoexpression of SOX2, CD34, and SALL4 in SMARCA4-dUT is common but may not occur (18). In contrast, SD-NSCLC often harbors co-occurring mutations, including the KRAS G12C variant, which has therapeutic implications, particularly in the context of KRAS inhibitors (19).

Recent studies have further delineated the genomic and morphological distinctions of SMARCA4-dUT compared to other malignancies. For instance, while poorly-differentiated neuroendocrine carcinoma (NEC) and SMARCA4-dUT may share histological overlap and thoracic localization, SMARCA4-dUT lacks majority of the neuroendocrine markers (e.g., CD56 and chromogranin A), and is defined by the absence of BRG1 expression. Similarly, although morphologically similar to SMARCA4-dUT, malignant rhabdoid tumors are distinguished by SMARCB1/INI1 loss rather than SMARCA4 mutations (20). Another extensively studied and potentially targetable SMARCA4-deficient malignancy is small cell carcinoma of the ovary, hypercalcemic type (SCCOHT), which shares notable morphologic, immunophenotypic, and molecular similarities with thoracic SMARCA4-dUT (21).

SMARCA4-dUT predominantly affects young males to middle-aged adults and is strongly associated with smoking history (18). These tumors are most frequently characterized by the presence of large, compressive masses localized within the mediastinum, pleura, or lungs, and they often present clinically with a constellation of symptoms such as dyspnea, chest pain, and superior vena cava syndrome, all of which are indicative of their highly invasive and infiltrative behavior (22). The prognosis for patients diagnosed with SMARCA4-dUT remains poor, as evidenced by a median overall survival (OS) of merely six months, further emphasizing the urgent need for novel and more effective therapeutic interventions to improve clinical outcomes (23).

From a histopathological perspective, SMARCA4-

dUT poses significant diagnostic challenges due to its morphological overlap with poorly differentiated carcinomas and carcinomas of unknown primary origin, and requires immunohistochemical confirmation using a well-defined panel of antibodies, as well as correlation of histological image with clinical and radiological findings .Recent advancements in molecular diagnostics, mainly through the application of next-generation sequencing (NGS), have greatly enhanced the ability to detect *SMARCA4* mutations along with associated co-alterations, thereby facilitating a more precise understanding of the molecular landscape of these tumors (14). Moreover, the development and refinement of liquid biopsy technologies, which enable the non-invasive detection and analysis of circulating tumor DNA (ctDNA), have emerged as tools for both the early diagnosis of SMARCA4-deficient malignancies and the real-time monitoring of treatment responses (24).

Radiologically, SMARCA4-dUT often presents as a large, heterogeneous mass with necrotic and calcified areas. While not pathognomonic, these features are distinctive and aid in diagnosis (25). These tumors exhibit a strong affinity for ^{18}F-fluorodeoxyglucose (FDG), rendering positron emission tomography (PET) a helpful imaging modality for clinical staging and disease monitoring, particularly in the context of assessing tumor burden and metastatic spread (26). These radiological characteristics alone are insufficient for a definitive diagnosis. However, when combined with clinical, histopathological, and molecular data, they enhance diagnostic accuracy and support therapeutic decision-making. The treatment management of SMARCA4-dUT is evolving in response to the challenges posed by the tumor's inherent resistance to conventional treatments. Surgery, while a potentially curative approach in localized Stage I disease, offers limited benefits in advanced stages due to high rates of recurrence and early metastases (27). Radiotherapy has similarly shown limited utility due to widespread resistance reported in several clinical cases (27). Preclinical data suggest that SMARCA4-knockdown lung cancer cells exhibit sensitivity to cisplatin, attributed to impaired DNA repair mechanisms (28). In real-world settings, responses are limited, likely due to BRG1 loss, which reduces chromatin accessibility and disrupts calcium signaling pathways critical for chemotherapy-induced apoptosis.

A retrospective study of SMARCA4-dUT and SD-NSCLC highlighted the poor outcomes associated with chemotherapy alone. Patients receiving exclusive chemotherapy had significantly lower progression-free survival (PFS) (median PFS: 2.73 months) than those receiving chemo-immunotherapy (median PFS: 26.8 months, P=0.0437) (29).

Indeed, immunotherapy has emerged as a promising strategy for SMARCA4-dUT, leveraging the tumor's high tumor mutation burden (TMB) and genomic instability, even without programmed death-ligand 1 (PD-L1) expression. Immune checkpoint inhibitors (ICIs) have demonstrated durable responses, with case reports describing rapid symptomatic improvements and significant tumor regression following their use (30,31). Naito *et al.* reported a complete response in SMARCA4-dUT patients who received nivolumab after three cycles of chemotherapy despite undetectable PD-L1 expression (31). Similarly, Yang *et al.* successfully treated a PD-L1-negative SMARCA4-dUT patient with a second-line therapy with tislelizumab, etoposide, and carboplatin after four cycles of liposomal paclitaxel and cisplatin failed. Both patients had a high TMB (32).

Currently, there is a lack of randomized controlled trials (RCTs) focused on SMARCA4-dUT, with most evidence coming from retrospective studies. Nonetheless, several targeted therapies are being researched for SMARCA4 deficiency. Xue *et al.* demonstrated that SCCOHT cells exhibit limited CDK4/6 activity and respond to CDK4/6 inhibitors, suggesting their potential repurposing for SMARCA4-deficient tumors. In a case report, a patient with SMARCA4-deficient SCCOHT responded well to the combination of abemaciclib and nivolumab after multiple failed treatments, and this sensitivity was later confirmed in NSCLC with SMARCA4 loss (33).

However, a nonrandomized trial showed limited clinical benefit of palbociclib and ribociclib alone in tumors with CDK4/6 pathway alterations, including SMARCA4-deficient cases (34). AURKA inhibitors have demonstrated increased efficacy in preclinical studies due to BRG1 loss, which sensitizes tumors to these agents (35). Similarly, ATR targeting replication stress responses show potential as a therapeutic strategy for SMARCA4-dUT (36). Lastly, oxidative phosphorylation (OXPHOS) inhibitors (010759) and PARP inhibitors have been explored, although clinical use is currently limited by toxicity and insufficient data (37,38).

SMARCA4-deficient undifferentiated tumors remain a clinical challenge due to their aggressive behavior and limited responsiveness to conventional therapies. However, recent advancements in immunotherapy, targeted agents, and combination strategies have highlighted new

potential avenues for therapeutic intervention. A deeper understanding of the molecular mechanisms underlying SMARCA4 deficiency will be essential to guide future research and improve clinical outcomes in this rare and aggressive tumor entity.

TNENs

TNENs are ultra-rare malignancies with an estimated incidence of 0.02 per 100,000 individuals (39). They represent only 2–5% of all thymic tumors and account for less than 0.5% of all neuroendocrine neoplasms (NENs) (40). These tumors are highly aggressive and have a poor prognosis, with approximately 50% of patients failing to reach a 5-year survival rate (41). Due to their rarity and histological complexity, accurate diagnosis remains challenging. TNENs typically occur in middle-aged individuals, with a slight male predominance and a preference for the white population (42). The 2021 WHO classification divides TNENs into two main categories based on their histopathological features: neuroendocrine tumors (NETs) grade 1 (typical carcinoid) and grade 2 (atypical carcinoid) (collectively referred to as TNETs); and NECs [small cell carcinoma and large cell neuroendocrine carcinoma (LCNEC)]. Typical carcinoids are well-differentiated tumors with a low mitotic rate, whereas atypical carcinoids exhibit higher mitotic activity and focal necrosis (43). Small cell carcinoma and LCNECs are highly aggressive neoplasms characterized by a high mitotic rate and extensive necrosis. Immunohistochemical markers, including chromogranin A, synaptophysin, CD56, retinoblastoma protein (RB), are used to differentiate TNENs. A newly described subset, NET G3, shares morphological characteristics with well-differentiated NETs but displays higher proliferative activity and distinct molecular features, including an intermediate Ki-67 index (44). Although this category is recognized in the gastro-entero-pancreatic (GEP) system, it is not formally included in the 2021 WHO classification for thymic tumors. Notably, in contrast to GEP and pulmonary NENs, the Ki-67 index is currently not used for diagnostic or grading purposes in TNENs (45). Given the limited data on "thymic NET G3", future studies should clarify its molecular characteristics, clinical behavior, and optimal therapeutic strategies, which are currently unexplored.

Additionally, distinguishing primary TNENs from metastatic pulmonary NENs remains a diagnostic challenge, particularly in the absence of definitive immunohistochemical markers. TNENs frequently present non-specific symptoms, including cough, chest pain, dyspnea, and superior vena cava syndrome due to their anterior mediastinal location. These tumors may also exhibit functional activity; in 25% of cases, they can present Cushing's syndrome due to ectopic adrenocorticotropic hormone (ACTH) production, while carcinoid syndrome is relatively rare (46). The potential association with autoimmune disorders and paraneoplastic syndromes related to the thymic gland further complicates the clinical presentation. Genetic testing for MEN1 should be considered in patients with TNENs, particularly in those with a family history of endocrine neoplasms or multiple primary NETs. This evaluation can guide screening for associated tumors in both patients and at-risk relatives, preventing misclassification of recurrences as new malignancies (43).

Imaging studies play a crucial role in the diagnosis and staging of TNENs. Computed tomography (CT) and magnetic resonance imaging (MRI) provide essential morphological details, while functional imaging with FDG-PET, particularly in highly aggressive tumors, and gallium-68 DOTA-(Tyr^3)-Octreotate (DOTATATE) PET/CT in more differentiated tumors, enhances diagnostic accuracy. Gallium-68 DOTATATE PET/CT has become particularly valuable in evaluating NETs. It facilitates the precise identification of tumors of somatostatin receptors (SSTRs), helping select patients for somatostatin analogs [somatostatin analogs long-acting release (SSA-LAR)] and peptide receptor radionuclide therapy (PRRT) (47). The management of TNENs requires a multidisciplinary approach involving thoracic surgeons, oncologists, radiologists, and pathologists. Surgery is the preferred primary treatment for all potentially radically resectable, well-differentiated TNETs, as complete resection significantly improves survival outcomes (48). Adjuvant therapy is generally not recommended for typical and atypical carcinoids unless there is a high risk of recurrence. Radiotherapy is mainly used for incompletely resected or unresectable TNENs, particularly in cases with local invasion or symptom burden. However, its impact on long-term survival remains uncertain (49).

The high recurrence rates of TNENs (40–70% at 5 years) highlight the need for effective systemic therapies, especially for high-grade subtypes. Several treatments have been explored for metastatic TNENs, including chemotherapy, targeted therapies, and PRRT. SSA-LAR are widely used in well-differentiated, SSTR-positive TNENs, particularly in slowly progressing or indolent disease. Although no

randomized trials evaluate SSA-LAR monotherapy in TNENs, data from pulmonary carcinoids suggest that this treatment may delay disease progression in well-differentiated tumors, particularly in low-grade NETs with SSTR expression (SPINET trial) (50). However, for progressive or high-grade tumors, SSAs are potentially combined with targeted agents [e.g., everolimus (EVE)] or PRRT.

Platinum-based chemotherapy remains the cornerstone of first-line treatment for high-grade TNENs, particularly LCNEC and small cell carcinoma. The most used regimen is etoposide combined with either cisplatin or carboplatin, which has shown an objective response rate (ORR) around 30% and a median PFS of 7.2 months in retrospective analyses (51). While cisplatin-based regimens are traditionally preferred due to their higher response rates, carboplatin-based regimens offer better tolerability, especially in patients with comorbidities or poor performance status (52). Second-line chemotherapy options for TNENs are not well established. Treatment decisions for platinum-refractory cases are guided mainly by evidence extrapolated from pulmonary and thymic NETs (53,54).

Among targeted therapies, the mTOR inhibitor EVE has demonstrated activity in pulmonary and TNETs. The LUNA trial evaluated pasireotide (PAS) and EVE in progressive bronchial and thymic carcinoids as monotherapy or combined. The PAS + EVE combination improved both PFS and biochemical PFS (BPFS) compared to monotherapies, suggesting a potential benefit in disease control (55). However, dose reductions were required in over 50% of patients, and 65.9% discontinued treatment due to disease progression.

The Phase III CABINET trial was a randomized, double-blind study evaluating cabozantinib versus placebo in patients with previously treated advanced NETs. The trial included two cohorts, one with pancreatic NETs (pNETs) and another with extra-pancreatic NETs (epNETs), including TNENs. In the epNET cohort [n=203], cabozantinib demonstrated a median PFS of 8.4 months, significantly improving over the 3.9 months observed in the placebo group (HR 0.38; 95% CI 0.25–0.59; P<0.0001). These findings highlight cabozantinib as a potential therapeutic option in advanced TNENs, particularly for patients progressing on SSAs and EVE (56).

PRRT is also being investigated as a promising therapeutic approach in TNENs. The phase 3 LEVEL trial (GETNE-T2217) is an ongoing study investigating the efficacy and safety of ^{177}Lu-edotreotide versus EVE in patients with advanced, well-differentiated NETs of lung or thymic origin. Eligible patients must have progressive, SSTR-positive NETs (WHO grade 1 or 2) and are randomized 3:2 to receive either six cycles of ^{177}Lu-edotreotide or daily EVE (10 mg) until disease progression or intolerable toxicity. The primary endpoint is PFS, with secondary endpoints including OS, ORR, and patient-reported outcomes (57). If positive, the LEVEL trial could position PRRT as a key therapeutic option for well-differentiated TNETs, particularly in patients progressing on SSAs or EVE, potentially redefining the treatment algorithm. Despite therapeutic advancements, TNENs management relies heavily on data extrapolated from extra-thymic NETs, underscoring the urgent need for dedicated trials and biomarker-driven approaches investigating the early integration of PRRT.

Mediastinal GCTs

Histopathogenesis and epidemiology

GCTs are the most common cancers among young adults, with less than 2% diagnosed over the age of 55–60 years (58). They represent a distinct category of solid tumors that are highly responsive to chemotherapy (59). Consequently, GCTs have a high cure rate, even in advanced stages, with nearly 80% of metastatic patients successfully treated with chemotherapy, radiotherapy, and surgery (60). Based on clinical presentation, pathology, and cytogenetics, human GCTs can be classified into five types: (I) teratoma/yolk sac tumor of infancy (mostly in females); (II) seminoma and non-seminomatous of young adults (mostly in males); (III) spermatocytic seminoma in older men, found solely in the testis; (IV) dermoid cyst, almost exclusively occurring in the ovary; (V) gestational trophoblastic tumors (61). Type I GCTs are more frequently found in extragonadal locations than in the gonads, whereas type II GCTs primarily occur in the gonads. Outside the gonads, type II GCTs are only identified in two areas: the anterior mediastinum and the midline of the brain, including the pineal gland and suprasellar regions (61). The anterior compartment of the mediastinum is the most common site for extragonadal GCTs, although cases involving the middle mediastinum have also been reported (62).

Primary mediastinal GCTs (PMGCTs) account for only 1–3% of GCTs and 16% of mediastinal tumors (63). They are predominantly found in males (3) and may be associated with metachronous testicular cancer within a 10-year timeframe in approximately 10% of patients (62).

The average age at diagnosis is between 25 and 35 years, and unlike testicular GCTs, there has been no recorded increase in incidence (63).

Clinical features and diagnostic considerations

Individuals with Klinefelter syndrome are particularly vulnerable, and this syndrome should be excluded in young patients diagnosed with PMGCTs (62). Women are less affected by PMGCTs and typically, though not always present with type I GCTs. The most common histotype found in both men and women with PMGCTs is mature teratoma, a pattern also observed in those with Klinefelter syndrome (61). PMGCTs generally present as an anterior mediastinal mass, associated with symptoms such as chest pain, shortness of breath, and cough. These tumors are primarily diagnosed in males, exhibiting a male-to-female ratio of 9:1 (64). Interestingly, PMGCTs may relate to Klinefelter syndrome and hematologic malignancies (58). In terms of histological features, non-seminomatous types are more prevalent than seminomas in PMGCTs, making up 60–70% of cases, with mature teratoma—which is often treated surgically—being the most common histotype.

In contrast, immature teratomas are a rarer and more aggressive subtype with worse outcomes (65,66). PMCGTs with seminoma histology demonstrate excellent cure rates, comparable to those of their testicular counterparts, with a 5-year survival rate surpassing 90% (65). Typically, they are slow-growing tumors and may present with elevated levels of beta-human chorionic gonadotropin (hCG), particularly if syncytiotrophoblast cells are present in the tumor, as well as elevated lactate dehydrogenase (LDH) at the time of diagnosis. Conversely, non-teratomatous non-seminomatous PMGCTs (NS-PMGCTs) are aggressive tumors with a poor prognosis and an estimated 5-year OS rate of approximately 40–50%.

They may have highly elevated levels of alpha-fetoprotein (AFP), which favours the diagnosis of yolk sac tumor component and beta-hCG, pointing to the coexistence of choriocarcinoma component (67-69). According to the most accepted theory, PMGCTs develop when germ cells halt their descent and remain in the anterior mediastinum, becoming malignant (58), which explains the presence of normal testes in these patients. Several similarities exist between testicular cancers and PMGCTs. Both cancers show the isochromosome 12p [i(12p)], a cytogenetic aberration found in approximately 80% of PMGCTs, regardless of the histological subtype (70). In challenging diagnostic cases, the persistence of i(12p), usually identified through fluorescence *in situ* hybridization, serves as a valuable tool for differentiating mediastinal masses, and confirming a diagnosis of PMGCTs (71,72). Additionally, PMGCTs, when compared to testicular GCTs, display a higher TMB and distinct pathogenic oncogene alterations, including TP53 (46%), c-KIT (18%), KRAS (18%), PTEN (11%), NRAS (4%), and PIK3CA (4%). These alterations are more commonly seen in NS-PMGCTs than in seminomas and non-seminomatous testicular GCTs (6).

Molecular pathogenesis and prognostic implications

Recent literature has emphasized the importance of TP53 mutations and MDM2 alterations in GCTs' cisplatin resistance. While TP53 mutations are mainly associated with PMGCTs, MDM2 amplifications are predominantly found in the testis (73). A retrospective multi-center study found TP53 genomic alterations in 56% of non-seminomatous tumors, which were linked to significantly shorter OS compared to patients with wild-type TP53 PMGCTs, suggesting a distinct genomic background associated with poor prognosis in PMGCT patients (73,74).

Treatment strategies

In the case of PMGCT diagnosis, the most appropriate treatment should be started as soon as possible, aiming for a curative intent. While the cure rate can reach 80% even in cases of extensive disease for seminoma PMGCT, this drops to 40–50% for patients with NS-PMGCTs, who often require a multimodal approach. PMGCTs with mature teratoma histology can be cured with surgery alone, resulting in an excellent prognosis. Teratomas with somatic-type malignancy are treated with surgery +/– chemotherapy, depending on the type and percentage of the transformed tumor (58). The complete or near-complete *en bloc* excision after normalized or decreased serum tumor markers (AFP; beta-hCG; LDH) plays a crucial role in curing patients with PMGCTs (64). Although NS-PMGCTs are less sensitive to cisplatin-based chemotherapies, patients are most often treated with standard-dose chemotherapy (SDCT), according to the BEP protocol (bleomycin, etoposide, cisplatin), or etoposide and cisplatin (EP), based on the IGCCCG risk group. Chemotherapy, according to the VIP schedule (etoposide, ifosfamide, and cisplatin), using ifosfamide

instead of bleomycin, should be considered as the primary option for the potential of subsequent thoracic surgery (65). For non-seminomatous histotype, it is recommended to administer four cycles of cisplatin-based chemotherapy followed by surgical resection of any remaining mediastinal mass, as the residual tumor could still contain viable germ cells, whether immature or mature, or teratoma with somatic differentiation, all of which are associated with a poor prognosis. Radiation therapy should be used in specific cases, such as managing brain metastases.

High-dose chemotherapy (HDCT) and future directions

The need for testing HDCT has been emphasized due to the known chemosensitivity of GCTs and the goal of achieving a higher rate of long-term remissions, even in cases with poor prognosis like NS-PMGCTs (64). Consequently, since the early 1970s, HDCT protocols have been evaluated in advanced GCT patients. However, it is crucial to acknowledge that NS-PMGCT serves as a negative prognostic indicator, suggesting unfavorable outcomes for patients undergoing HDCT and autologous stem cell transplantation (ASCT). Therefore, some specialists do not recommend HDCT for NS-PMGCTs (66), and the role of HDCT in PMGCTs remains debated due to the absence of well-defined prognostic indicators and the limited research available. Recently, results from the largest series of NS-PMGCTs treated with HDCT (including 69 adult males) have been reported, showing an OS of 43.3% at 2 years, and 34.7% at 5 and 10 years. An analysis of outcomes revealed that patients who received HDCT as initial therapy experienced better PFS and OS than those treated during subsequent relapses (with a 5-year PFS of 51.8% compared to 26.8% and a 5-year OS of 51.3% against 25.9%). Consequently, the authors propose that HDCT with ASCT could serve as a viable treatment option either after the first relapse or even as a front-line strategy (75). In conclusion, PMGCTs include heterogeneous histological entities with distinct clinical and molecular features that differentiate non-seminomatous and seminoma PMGCTs, with NS-PMGCTs being the poorest prognostic group due to their low sensitivity to cisplatin and greater tendency to relapse. For this patient population, optimizing therapeutic strategies is crucial for improving survival outcomes while preserving quality of life. Therefore, identifying biological and genetic factors to investigate novel therapies in centers with expertise in the care of GCTs should be essential for achieving better results (76).

Conclusions

RTCs represent a heterogeneous group of malignancies with distinct clinical presentation, molecular features, and treatment strategies. Despite the relative differences among the three models of RTCs here analyzed, a careful basal evaluation, with specific expertise in the context of multidisciplinary management in reference centers, is the best way to improve outcomes in these rare tumors. Additionally, international registries should be promoted in order to consolidate clinical data, facilitate patient recruitment, and support large-scale trials.

Acknowledgments

E.P. is supported by a scholarship from Associazione TUTOR for the academic year 2024–2025.

Footnote

Provenance and Peer Review: This article was commissioned by the Guest Editor (Malgorzata Szolkowska) for "The Series Dedicated to the 14th International Thymic Malignancy Interest Group Annual Meeting (ITMIG 2024)" published in *Mediastinum*. The article has undergone external peer review.

Reporting Checklist: The authors have completed the Narrative Review reporting checklist. Available at https://med.amegroups.com/article/view/10.21037/med-25-22/rc

Peer Review File: Available at https://med.amegroups.com/article/view/10.21037/med-25-22/prf

Funding: None.

Conflicts of Interest: All authors have completed the ICMJE uniform disclosure form (available at https://med.amegroups.com/article/view/10.21037/med-25-22/coif). "The Series Dedicated to the 14th International Thymic Malignancy Interest Group Annual Meeting (ITMIG 2024)" was commissioned by the editorial office without any funding or sponsorship. M.O. reports speaker fees from MSD and Novartis; consulting fees and participation on an advisory board for Regeneron. P.A.A. reports receiving consulting fees from Bristol-Meyers Squibb, Roche-Genentech, Merck Sharp & Dohme, Novartis, Merck Serono, Pierre-Fabre, AstraZeneca, Sun Pharma,

Sanofi, Sandoz, Immunocore, Italfarmaco, Nektar, Boehringer-Ingelheim, Eisai, Regeneron, Daiichi Sankyo, Pfizer, OncoSec, Nouscom, Lunaphore, Seagen, iTeos, Medicenna, Bio-Al Health, ValoTx, Replimmune, Bayer, Erasca, Philogen, Biontech, and Anaveon. He also reports receiving support for attending meetings and travel from Pfizer, Bio-Al Health, Replimmune, MSD, and Pierre Fabre. In addition, he serves as President of Fondazione Melanoma Onlus (Naples, Italy) and the Campania Society of ImmunoTherapy of Cancer (SCITO), and is a Member of the Steering Committee of the Society for Melanoma Research (SMR), and a Member of the Board of Directors for the Society of Immuno-Therapy of Cancer (SITC). E.P. is supported by a scholarship from Associazione TUTOR for the academic year 2024–2025. The authors have no other conflicts of interest to declare.

Ethical Statement: The authors are accountable for all aspects of the work in ensuring that questions related to the accuracy or integrity of any part of the work are appropriately investigated and resolved.

References

1. Nicholson AG, Tsao MS, Beasley MB, et al. The 2021 WHO Classification of Lung Tumors: Impact of Advances Since 2015. J Thorac Oncol 2022;17:362-87.
2. Gatta G, Capocaccia R, Botta L, et al. Burden and centralised treatment in Europe of rare tumours: results of RARECAREnet-a population-based study. Lancet Oncol 2017;18:1022-39.
3. Buchalet C, Durdux C. Role of radiotherapy in the management of rare solid thoracic tumors of the adults. Cancer Radiother 2023;27:614-21.
4. AIRTUM Working Group; Busco S, Buzzoni C, et al. Italian cancer figures--Report 2015: The burden of rare cancers in Italy. Epidemiol Prev 2016;40:1-120.
5. DeSantis CE, Kramer JL, Jemal A. The burden of rare cancers in the United States. CA Cancer J Clin 2017;67:261-72.
6. Stiller CA, Trama A, Serraino D, et al. Descriptive epidemiology of sarcomas in Europe: report from the RARECARE project. Eur J Cancer 2013;49:684-95.
7. Pastorino U, Leuzzi G, Sabia F, et al. Long term outcome of complex surgical resection and reconstruction for rare thoracic cancers. Tumori 2023;109:450-7.
8. Roden AC, Fang W, Shen Y, et al. Distribution of Mediastinal Lesions Across Multi-Institutional, International, Radiology Databases. J Thorac Oncol 2020;15:568-79.
9. Detterbeck FC. The international thymic malignancy interest group. J Natl Compr Canc Netw 2013;11:589-93.
10. Imbimbo M, Ottaviano M, Vitali M, et al. Best practices for the management of thymic epithelial tumors: A position paper by the Italian collaborative group for ThYmic MalignanciEs (TYME). Cancer Treat Rev 2018;71:76-87.
11. Palmieri G, Tortora M, Parola S, et al. Mediastinal soft tissue sarcoma: dark sides and future lights. Mediastinum 2020;4:9.
12. Ye R, Wu A, Lin C, et al. SMARCA4-deficient non-small cell lung cancer: a case description and literature analysis. Quant Imaging Med Surg 2024;14:4215-22.
13. Kim JH, Woo JH, Lim CY, et al. SMARCA4-deficient non-small cell lung carcinoma: clinicodemographic, computed tomography, and positron emission tomography-computed tomography features. J Thorac Dis 2024;16:1753-64.
14. Schoenfeld AJ, Bandlamudi C, Lavery JA, et al. The Genomic Landscape of SMARCA4 Alterations and Associations with Outcomes in Patients with Lung Cancer. Clin Cancer Res 2020;26:5701-8.
15. Shain AH, Pollack JR. The spectrum of SWI/SNF mutations, ubiquitous in human cancers. PLoS One 2013;8:e55119.
16. Kadoch C, Crabtree GR. Mammalian SWI/SNF chromatin remodeling complexes and cancer: Mechanistic insights gained from human genomics. Sci Adv 2015;1:e1500447.
17. Mardinian K, Adashek JJ, Botta GP, et al. SMARCA4: Implications of an Altered Chromatin-Remodeling Gene for Cancer Development and Therapy. Mol Cancer Ther 2021;20:2341-51.
18. Yadav R, Sun L, Salyana M, et al. SMARCA4-deficient undifferentiated tumor of lung mass—a rare tumor with the rarer occurrence of brain metastasis: a case report and review of the literature. J Investig Med High Impact Case

Rep 2022. doi:10.1177/23247096221074864.
19. Negrao MV, Araujo HA, Lamberti G, et al. Comutations and KRASG12C Inhibitor Efficacy in Advanced NSCLC. Cancer Discov 2023;13:1556-71.
20. Shinno Y, Ohe Y; Lung Cancer Study Group of the Japan Clinical Oncology Group (JCOG). Thoracic SMARCA4-deficient undifferentiated tumor: current knowledge and future perspectives. Jpn J Clin Oncol. 2024;54:265-70.
21. Auguste A, Blanc-Durand F, Deloger M, et al. Small Cell Carcinoma of the Ovary, Hypercalcemic Type (SCCOHT) beyond SMARCA4 Mutations: A Comprehensive Genomic Analysis. Cells 2020;9:1496.
22. Al-Shbool G, Krishnan Nair H. SMARCA4-Deficient Undifferentiated Tumor: A Rare Malignancy With Distinct Clinicopathological Characteristics. Cureus 2022;14:e30708.
23. Marumo Y, Yoshida T, Ina K, et al. Diagnosis of a SMARCA4-deficient undifferentiated tumor using multigene panel testing: A case report. Clin Case Rep 2023;11:e7854.
24. Filipska M, Rosell R. Mutated circulating tumor DNA as a liquid biopsy in lung cancer detection and treatment. Mol Oncol 2021;15:1667-82.
25. Kwon HJ, Jang MH. SMARCA4-deficient undifferentiated thoracic tumor: A case report. World J Clin Cases 2023;11:2521-7.
26. Guo J, Liao Z, Chen Q, et al. FDG PET/CT in a Case of Thoracic SMARCA4-Deficient Undifferentiated Tumor. Clin Nucl Med 2023;48:1111-3.
27. Longo V, Catino A, Montrone M, et al. Treatment of Thoracic SMARCA4-Deficient Undifferentiated Tumors: Where We Are and Where We Will Go. Int J Mol Sci 2024;25:3237.
28. Kothandapani A, Gopalakrishnan K, Kahali B, et al. Downregulation of SWI/SNF chromatin remodeling factor subunits modulates cisplatin cytotoxicity. Exp Cell Res 2012;318:1973-86.
29. Lin Y, Yu B, Sun H, et al. Promising efficacy of immune checkpoint inhibitor plus chemotherapy for thoracic SMARCA4-deficient undifferentiated tumor. J Cancer Res Clin Oncol 2023;149:8663-71.
30. Shi L, Lin L, Ding Y, et al. Case report: A rapid response to immunotherapy in a thoracic SMARCA4-deficient undifferentiated tumor with respiratory failure. Front Oncol 2022;12:1020875.
31. Naito T, Umemura S, Nakamura H, et al. Successful treatment with nivolumab for SMARCA4-deficient non-small cell lung carcinoma with a high tumor mutation burden: A case report. Thorac Cancer 2019;10:1285-8.
32. Yang P, Xiong F, Lin Y, et al. Effectiveness of tislelizumab when combined with etoposide and carboplatin in patients with SMARCA4-deficient undifferentiated thoracic tumor: a case report. Transl Cancer Res 2023;12:1041-8.
33. Xue Y, Meehan B, Macdonald E, et al. CDK4/6 inhibitors target SMARCA4-determined cyclin D1 deficiency in hypercalcemic small cell carcinoma of the ovary. Nat Commun 2019;10:558.
34. Lee EK, Esselen KM, Kolin DL, et al. Combined CDK4/6 and PD-1 Inhibition in Refractory SMARCA4-Deficient Small-Cell Carcinoma of the Ovary, Hypercalcemic Type. JCO Precis Oncol 2020;4:736-42.
35. Tagal V, Wei S, Zhang W, et al. SMARCA4-inactivating mutations increase sensitivity to Aurora kinase A inhibitor VX-680 in non-small cell lung cancers. Nat Commun 2017;8:14098.
36. Gupta M, Concepcion CP, Fahey CG, et al. BRG1 Loss Predisposes Lung Cancers to Replicative Stress and ATR Dependency. Cancer Res 2020;80:3841-54.
37. Pilié PG, Gay CM, Byers LA, et al. PARP Inhibitors: Extending Benefit Beyond BRCA-Mutant Cancers. Clin Cancer Res 2019;25:3759-71.
38. Lissanu Deribe Y, Sun Y, Terranova C, et al. Mutations in the SWI/SNF complex induce a targetable dependence on oxidative phosphorylation in lung cancer. Nat Med 2018;24:1047-57.
39. Tartarone A, Lerose R, Lettini AR, et al. Current Treatment Approaches for Thymic Epithelial Tumors. Life (Basel) 2023;13:1170.
40. Hsu CH, Chan JK, Yin CH, et al. Trends in the incidence of thymoma, thymic carcinoma, and thymic neuroendocrine tumor in the United States. PLoS One 2019;14:e0227197.
41. Bakhos CT, Salami AC, Kaiser LR, et al. Thymic Neuroendocrine Tumors and Thymic Carcinoma: Demographics, Treatment, and Survival. Innovations (Phila) 2020;15:468-74.
42. Brcic L, Heidinger M, Popper H. Neuroendocrine neoplasms of the mediastinum. Pathologe 2016;37:434-40.
43. Bohnenberger H, Ströbel P. Recent advances and conceptual changes in the classification of neuroendocrine tumors of the thymus. Virchows Arch 2021;478:129-35.
44. Dinter H, Bohnenberger H, Beck J, et al. Molecular Classification of Neuroendocrine Tumors of the Thymus. J Thorac Oncol 2019;14:1472-83.
45. Marx A, Chan JKC, Chalabreysse L, et al. The 2021 WHO Classification of Tumors of the Thymus and

Mediastinum: What Is New in Thymic Epithelial, Germ Cell, and Mesenchymal Tumors? J Thorac Oncol 2022;17:200-13.
46. Dutta R, Kumar A, Julka PK, et al. Thymic neuroendocrine tumour (carcinoid): clinicopathological features of four patients with different presentation. Interact Cardiovasc Thorac Surg 2010;11:732-6.
47. Strange CD, Ahuja J, Shroff GS, et al. Imaging Evaluation of Thymoma and Thymic Carcinoma. Front Oncol 2021;11:810419.
48. Sullivan JL, Weksler B. Neuroendocrine Tumors of the Thymus: Analysis of Factors Affecting Survival in 254 Patients. Ann Thorac Surg 2017;103:935-9.
49. NCCN Clinical Practice Guidelines in Oncology: Neuroendocrine and Adrenal Tumors. Version 1.2025. Plymouth Meeting (PA): NCCN; 2025. Available online: https://www.nccn.org/professionals/physician_gls/pdf/neuroendocrine.pdf
50. Baudin E, Capdevila J, Hörsch D, et al. Treatment of advanced BP-NETS with lanreotide autogel/depot vs placebo: the phase III SPINET study. Endocr Relat Cancer 2024;31:e230337.
51. Filosso PL, Yao X, Ahmad U, et al. Outcome of primary neuroendocrine tumors of the thymus: a joint analysis of the International Thymic Malignancy Interest Group and the European Society of Thoracic Surgeons databases. J Thorac Cardiovasc Surg 2015;149:103-9.e2.
52. Guan Y, Yao Q, Hao Y, et al. The combination of etoposide and platinum for the treatment of thymic neuroendocrine neoplasms: A retrospective analysis. Cancer Med 2023;12:16011-8.
53. Sun W, Lipsitz S, Catalano P, et al. Phase II/III study of doxorubicin with fluorouracil compared with streptozocin with fluorouracil or dacarbazine in the treatment of advanced carcinoid tumors: Eastern Cooperative Oncology Group Study E1281. J Clin Oncol 2005;23:4897-904.
54. Bajetta E, Catena L, Procopio G, et al. Are capecitabine and oxaliplatin (XELOX) suitable treatments for progressing low-grade and high-grade neuroendocrine tumours? Cancer Chemother Pharmacol 2007;59:637-42.
55. Baudin E, Berruti A, Giuliano M, et al. First long-term results on efficacy and safety of long-acting pasireotide in combination with everolimus in patients with advanced carcinoids (NET) of the lung/thymus: Phase II LUNA trial. J Clin Oncol https://ascopubs.org/doi/10.1200/JCO.2021.39.15_suppl.8574
56. Chan JA, Geyer S, Zemla T, et al. Phase 3 Trial of Cabozantinib to Treat Advanced Neuroendocrine Tumors. N Engl J Med 2025;392:653-65.
57. García-Álvarez A, García-Carbonero R, Anton-Pascual B, et al. ^{177}Lu-edotreotide versus everolimus in patients with advanced neuroendocrine tumors of lung or thymic origin: the phase 3 randomized LEVEL, GETNE-T2217 trial. J Clin Oncol 2024;42:TPS3177.
58. Rosti G, Secondino S, Necchi A, et al. Primary mediastinal germ cell tumors. Semin Oncol 2019;46:107-11.
59. Rescigno P, Ottaviano M, Palmieri G. Platinum drug sensitivity and resistance in testicular germ cell tumors: two sides of the same coin. Cancer Drug Resist 2020;3:672-5.
60. Condello C, Rescigno P, Ottaviano M, et al. Clinical features and psychological aspects of the decision-making process in stage I testicular germ cell tumors. Future Oncol 2018;14:1591-9.
61. Oosterhuis JW, Stoop H, Honecker F, et al. Why human extragonadal germ cell tumours occur in the midline of the body: old concepts, new perspectives. Int J Androl 2007;30:256-63; discussion 263-4.
62. Pini GM, Colecchia M. Mediastinal germ cell tumors: a narrative review of their traits and aggressiveness features. Mediastinum 2022;6:5.
63. McKenney JK, Heerema-McKenney A, Rouse RV. Extragonadal germ cell tumors: a review with emphasis on pathologic features, clinical prognostic variables, and differential diagnostic considerations. Adv Anat Pathol 2007;14:69-92.
64. Giunta EF, Ottaviano M, Mosca A, et al. Standard versus high-dose chemotherapy in mediastinal germ cell tumors: a narrative review. Mediastinum 2022;6:6.
65. Ozgun G, Nappi L. Primary Mediastinal Germ Cell Tumors: A Thorough Literature Review. Biomedicines 2023;11:487.
66. Kesler KA, Rieger KM, Hammoud ZT, et al. A 25-year single institution experience with surgery for primary mediastinal nonseminomatous germ cell tumors. Ann Thorac Surg 2008;85:371-8.
67. Gillessen S, Sauvé N, Collette L, et al. Predicting Outcomes in Men With Metastatic Nonseminomatous Germ Cell Tumors (NSGCT): Results From the IGCCCG Update Consortium. J Clin Oncol 2021;39:1563-74.
68. Ko JJ, Bernard B, Tran B, et al. Conditional Survival of Patients With Metastatic Testicular Germ Cell Tumors Treated With First-Line Curative Therapy. J Clin Oncol 2016;34:714-20.
69. International Germ Cell Cancer Collaborative Group: A prognostic factor-based staging system for metastatic germ cell cancers. J Clin Oncol 1997;15:594-603.

70. International Prognostic Factors Study Group; Lorch A, Beyer J, et al. Prognostic factors in patients with metastatic germ cell tumors who experienced treatment failure with cisplatin-based first-line chemotherapy. J Clin Oncol 2010;28:4906-11.
71. Houldsworth J, Korkola JE, Bosl GJ, et al. Biology and genetics of adult male germ cell tumors. J Clin Oncol 2006;24:5512-8.
72. Bosl GJ, Ilson DH, Rodriguez E, et al. Clinical relevance of the i(12p) marker chromosome in germ cell tumors. J Natl Cancer Inst 1994;86:349-55.
73. Ottaviano M, Giunta EF, Rescigno P, et al. The Enigmatic Role of TP53 in Germ Cell Tumours: Are We Missing Something? Int J Mol Sci 2021;22:7160.
74. Bacon JVW, Giannatempo P, Cataldo G, et al. TP53 Alterations Are Associated With Poor Survival in Patients With Primary Mediastinal Nonseminoma Germ Cell Tumors. Oncologist 2022;27:e912-5.
75. Secondino S, Badoglio M, Rosti G, et al. High-dose chemotherapy with autologous stem cell transplants in adult primary non-seminoma mediastinal germ-cell tumors. A report from the Cellular Therapy and Immunobiology working party of the EBMT. ESMO Open 2024;9:103692.
76. Parola S, Oing C, Rescigno P, et al. PARP inhibitors in testicular germ cell tumors: what we know and what we are looking for. Front Genet 2024;15:1480417.

doi: 10.21037/med-25-22
Cite this article as: Ottaviano M, Ascierto PA, Pietroluongo E. When rarity meets thoracic cancers: a narrative review from ITMIG 2024. Mediastinum 2025;9:23.

Review Article

Mediastinal tumors: why, when, and how to biopsy?

Dirk Van Raemdonck[1,2]^, Paul M. Clement[3,4]^

[1]Department of Thoracic Surgery, University Hospitals Leuven, Leuven, Belgium; [2]Department of Chronic Diseases and Metabolism, KU Leuven, Leuven, Belgium; [3]Department of General Medical Oncology, University Hospitals Leuven, Leuven, Belgium; [4]Department of Oncology, Leuven Cancer Institute, KU Leuven, Leuven, Belgium

Contributions: (I) Conception and design: D Van Raemdonck; (II) Administrative support: D Van Raemdonck; (III) Provision of study materials or patients: Both authors; (IV) Collection and assembly of data: Both authors; (V) Data analysis and interpretation: Both authors; (VI) Manuscript writing: Both authors; (VII) Final approval of manuscript: Both authors.

Correspondence to: Emeritus Prof. Dr. Dirk Van Raemdonck, MD, PHD. Department of Thoracic Surgery, University Hospitals Leuven, Gasthuisberg, Herestraat 49, B-3000 Leuven, Belgium; Department of Chronic Diseases and Metabolism, KU Leuven, Leuven, Belgium. Email: dirk.vanraemdonck@uzleuven.be.

Abstract: The finding of a mediastinal mass often poses a diagnostic challenge for clinicians. A correct diagnosis on the nature of a mediastinal tumor is important prior to initiating any treatment. Therefore, good knowledge is needed on mediastinal anatomy and its different compartments as well as on the differential diagnosis of a wide variety of benign and malignant mediastinal lesions. A complete history of the symptoms and a full clinical examination together with imaging and laboratory tests can guide the clinician towards a final diagnosis at presentation. Pretreatment tissue biopsy of a mediastinal tumor is not always required in case the clinical diagnosis is highly probable based on the above findings and when the tumor looks well encapsulated and of non-invasive nature amenable to upfront complete surgical resection as judged by the thoracic surgeon. Tissue diagnosis is recommended for a clinically and radiographically for cancer suspected, locally advanced or unresectable mediastinal mass in order to confirm the diagnosis and to guide induction therapy or definitive systemic treatment. An ultrasound or computed tomography (CT)-guided core needle biopsy may result in sufficient tissue for definitive cytopathological diagnosis. Otherwise, a minimally invasive procedure by video-assisted thoracoscopy (VATS) or robot-assisted thoracoscopy (RATS) or occasionally an open surgical biopsy may be necessary to obtain more tissue for pathological examination and molecular testing. Depending on the location of the mediastinal mass in any of the mediastinal compartments, various surgical approaches can be chosen to biopsy. A frozen section is helpful to check the quality of the biopsy but is less effective for a precise diagnosis. The definitive pathological report needs to be awaited prior to initiating any treatment except in case of a life-threatening condition such as critical airway compression or superior vena cava syndrome.

Keywords: Mediastinal tumors; epithelial thymic tumors; biopsy; surgery

Received: 04 May 2025; Accepted: 15 July 2025; Published online: 19 September 2025.

doi: 10.21037/med-25-29

View this article at: https://dx.doi.org/10.21037/med-25-29

^ ORCID: Dirk Van Raemdonck, 0000-0003-1261-0992; Paul M. Clement, 0000-0001-7600-0806.

Introduction

The mediastinum is like a box of Pandora. You never know what to find on the inside until you open the box (1). According to the Greek mythology Pandora received a box as a gift from the gods. Driven by curiosity Pandora opened the box thus releasing curses upon mankind (2). Likewise, opening the mediastinum to take a surgical biopsy of a well encapsulated, non-invasive tumor may initiate undesired complications like postoperative chest pain, hemorrhage, wound infection, pleural effusion, or tumor spread not becoming apparent until at a later stage during patient's follow-up.

The decision to biopsy a mediastinal mass should be well thought through in advance following discussion during a multidisciplinary tumor board conference and balanced against any possible risk.

In this short review we will discuss three questions: why, when, and how to biopsy mediastinal tumors?

Why to biopsy mediastinal tumors?

The finding of a mediastinal mass of unknown origin often poses a diagnostic challenge for clinicians. A correct diagnosis prior to initiating any treatment is important. Therefore, a good understanding of the anatomical boundaries of the three different mediastinal compartments (prevascular, visceral, paravertebral) as proposed by the International Thymic Malignancy Interest Group is of utmost importance (3). Also, profound knowledge is needed on the different structures running in each mediastinal compartment (*Table 1*) that may become the primary origin for a wide variety of benign and malignant mediastinal lesions (*Table 2*) (4).

Patients with a mediastinal mass can be completely asymptomatic when discovered at the time of an incidental finding on imaging or present with clinical symptoms that may help to guide towards correct diagnosis. These symptoms can either be systemic (so called B symptoms such as anorexia, fever, night sweating), local (dyspnea, cough, stridor, hemoptysis, dysphagia, chest pain, hoarseness, Horner's syndrome, superior vena cava syndrome), or paraneoplastic related to a wide range of auto-immune disorders (ptosis, diplopia, dysarthria, muscle weakness, neurologic syndromes, anemia, skin disorders, endocrine disorders, opportunistic infections) such as often is the case with thymic epithelial tumors (TETs). Mostly known and described syndromes are myasthenia gravis (MG), red blood cell aplasia, and hypogammaglobulinemia (Good syndrome) (5-7). With attention to patient's age and gender together with clinical characteristics, a narrowed differential diagnosis on the exact nature of the mediastinal mass becomes possible (8). Together with thoracic imaging [chest X-ray; chest computed tomography (CT), magnetic resonance imaging, positron emission tomography (PET), other nuclear scans] describing the exact localization and internal characteristics of the mass (9-12) and laboratory tests including tumor markers, antibodies, and hormones (*Table 3*) (13-16), a clinical diagnosis can be made in most patients. Increased beta human chorionic gonadotropin (beta-HCG) or alpha fetoprotein (AFP) serum levels in a

Table 1 Mediastinal structures running through three mediastinal compartments

Prevascular
Thymus
Mammary vessels
Ectopic (para)thyroid
Phrenic nerve
Lymph nodes
Fat
Visceral
Trachea & carina
Esophagus
Heart
Great vessels[†]
Pericardium
Vagal nerve
Thoracic duct
Lymph nodes
Fat
Paravertebral
Sympathetic chain
Lymph nodes
Fat

All mediastinal compartments are covered with pleura. Tumors may originate out of the mediastinal pleura: e.g., solitary fibrous tumors or localized pleural mesothelioma. These tumors should be included in the list of differential diagnosis of mediastinal tumors, mainly in the paravertebral compartment. [†], ascending aorta, aortic arch, descending aorta, superior vena cava, brachiocephalic vein, (hemi-)azygos vein, intrapericardial pulmonary arteries.

Table 2 Mediastinal tumors (real and false) presenting in three mediastinal compartments (excluding mediastinitis/mediastinal abscess)

Prevascular
Thymic tumors
Germ cell tumors[†]
Lymphoma[‡]
Thyroid (goiter)
Parathyroid adenoma
Paraganglioma
Lymphangioma
Hemangioma
Lipo(sarco)ma
Thymic hyperplasia
Thymic cyst
(Metastatic) lymph nodes
Sternal tumor
Cartilaginous tumor
Visceral
Thymic tumors (rare)
Lymphoma[‡]
Thyroid (goiter)
Paraganglioma
(Metastatic) lymph nodes
Bronchogenic cyst
Enteric cyst
Pericardial cyst
Esophageal diverticulum
Esophageal tumor
Mega-esophagus
Diaphragmatic hernia
Aneurysms[¶]
Paravertebral
Neurogenic tumors[§]
Lymphoma[‡]
Paraganglioma
Lipo(sarco)ma
Thoracic duct cyst
(Metastatic) lymph nodes
Meningocele
Vertebral tumor
Solitary fibrous tumor
Localized pleural mesothelioma

[†], including teratoma, seminoma, non-seminomatous germ cell tumors; [‡], including Hodgkin lymphoma, mediastinal T-lymphoblastic leukaemia/lymphoma, and primary mediastinal large B-cell lymphoma; [§], including neurilemoma, neurofibroma, ganglioneuroma(blastoma), (malignant) schwannoma; [¶], including aneurysms of aorta, brachiocephalic and caval veins, (hemi-)azygos vein, pulmonary artery, pulmonary veins.

Table 3 Tumor markers, antibodies and hormones in the differential diagnosis of mediastinal masses

Tumor markers
CEA
NSE
LDH
AFP
Beta-HCG
Autoantibodies
Anti-AChR (myasthenia gravis)
Anti-MuSK (myasthenia gravis)
T-cell antigens (lymphoma)
B-cell antigens (lymphoma)
Hormones
Insulin
T3–T4: thyroid hormone
PTH
Calcitonin
ACTH
Catecholamines (adrenaline)

ACTH, adrenocorticotropic hormone; AFP, alpha fetoprotein; AChR, acetylcholine receptor; Beta-HCG, beta human chorionic gonadotropin; CEA, carcinoembryonic antigen; LDH, lactate dehydrogenase; MuSK, muscle specific tyrosine kinase; NSE, neuron specific enolase; PTH, parathyroid hormone.

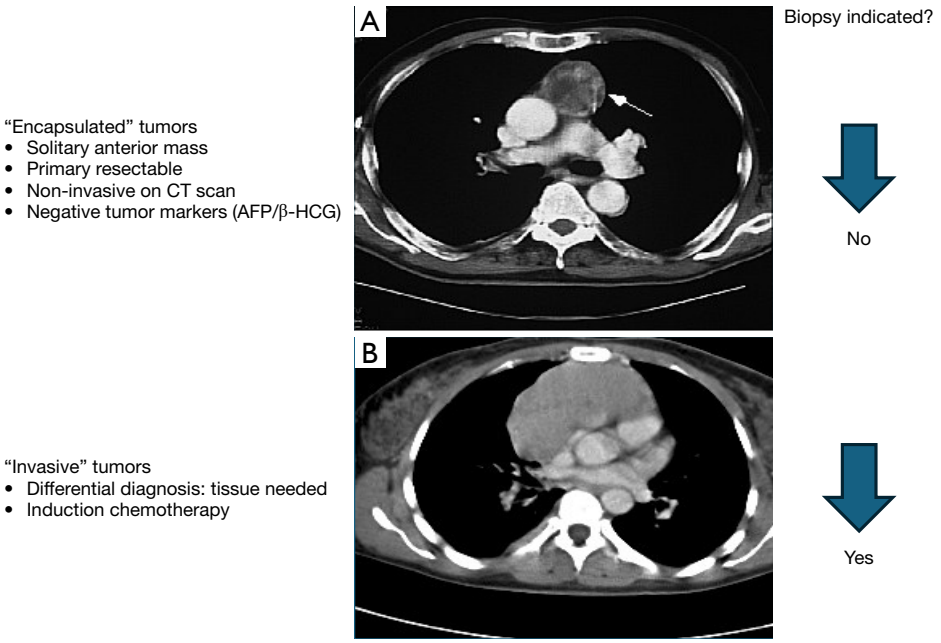

Figure 1 Two patients presenting with an epithelial thymic tumor in the prevascular mediastinum. (A) The tumor in the image was a well encapsulated stage I thymoma resected upfront with no need for preoperative biopsy (no); (B) the tumor in the image was an invasive stage III thymoma on surgical biopsy taken via right anterior mediastinotomy (yes). Patient was treated with 3 courses of induction chemotherapy prior to resection via median sternotomy. CT, computed tomography; AFP, alpha fetoprotein; HCG, human chorionic gonadotropin.

patient with a mediastinal mass are highly indicative for the presence of an extragonadal germ cell tumor. In patients with a suspicion of a TET anti-acetylcholine receptor (AChR) antibodies should be routinely analyzed prior to thymectomy, even in those without clinical symptoms or neurologic signs of MG. One in four of these patients will have anti-AChR antibodies and more than 90% will develop clinical MG within 6 years after thymectomy (17).

When to biopsy mediastinal tumors?

Pretreatment tissue biopsy of mediastinal lesions is not always required when clinical diagnosis is confirmed or highly probable based on the above-mentioned findings.

Also, an incisional biopsy in a patient with a solitary, well circumscribed, solid, non-invasive (encapsulated) and resectable mediastinal tumor on preoperative imaging and with negative tumor markers is contraindicated in order to avoid tumor spilling that may increase the risk for pleural tumor spread during late follow-up. This is especially the case for TET. Primary resection without preoperative tissue diagnosis is then advocated (*Figure 1A*). In a survey of members of the European Society of Thoracic Surgeons reported in 2011, the uselessness of a routine histologic confirmation before surgery was queried. Ninety one percent of the responding centers do not routinely look for histological confirmation when thymoma is suspected. The most frequent comment was that in case CT scan strongly suggests the presence of a thymoma (small, resectable, encapsulated lesion with no radiological sign of invasion) or when MG is associated, no preoperative histological diagnosis is required (18). Similarly, a well circumscribed lesion in the posterior mediastinum suspicious of a benign neurogenic tumor can be resected primarily without previous biopsy when resection is indicated.

On the other hand, a surgical biopsy for histopathological, immunohistochemical and molecular analysis is indicated in patients presenting with an irregular, lobular, large tumor invading mediastinal structures (*Figure 1B*). Also in patients with a mediastinal mass and elevated AFP or β-HCG serum levels indicative for the presence of an extragonadal germ cell tumor, a biopsy of the mass for further analysis may occasionally be needed to exclude morphologic mimics presenting in the mediastinum. It has been reported that solitary fibrous tumor, Ewing sarcoma, or rhabdomyosarcoma may also produce elevated AFP

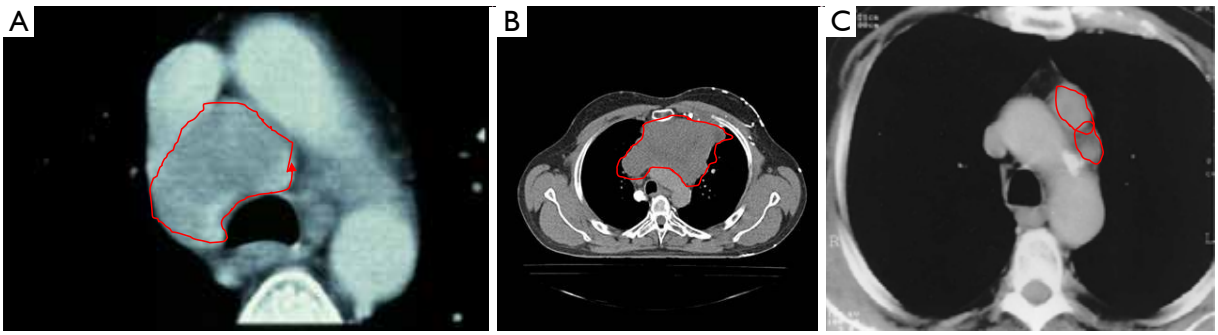

Figure 2 A different surgical approach to biopsy a mediastinal tumor is chosen according to its location in one of the mediastinal compartments. (A) A large pretracheal lymphadenopathy from a small cell lung carcinoma in the visceral mediastinum biopsied in this patient through cervical mediastinoscopy; nowadays endobronchial ultrasound core needle biopsy would be the first choice to obtain tissue; (B) a mediastinal large B cell lymphoma in the prevascular mediastinum biopsied via left anterior mediastinotomy; (C) two large para-aortic lymphadenopathies from a non-small cell lung carcinoma in the prevascular mediastinum biopsied via left video-assisted thoracoscopy. The red circles indicate tumor margins.

or β-HCG serum levels (19). However, a surgical biopsy may delay needed preoperative chemotherapy and make subsequent surgery more difficult.

Establishing the correct nature of the tumor on biopsy is needed as pathology will guide neoadjuvant therapy with the hope to enhance local resectability prior to surgical exploration at a later stage (20). Also, definitive tissue diagnosis is mandatory to exclude the need for any surgical treatment and to plan definitive systemic therapy or other methods for local tumor control (e.g., in case of lymphoproliferative disease).

How to biopsy mediastinal tumors?

An ultrasound or CT-guided core needle biopsy with multiple passages may result in sufficient tissue for definitive diagnosis of tumors in the prevascular (21,22) or paravertebral (23) mediastinum. For tumors in the visceral mediastinum, endo-bronchial (EBUS) (24) or esophageal endoscopic (EUS) (25) ultrasound-guided needle aspiration may be helpful in the diagnosis of mediastinal masses of unknown etiology. However, a false negative biopsy due to inadequate tissue sampling is always possible, but less likely with a core-needle biopsy thereby avoiding a surgical biopsy.

Making a correct diagnosis on a fragmented tissue specimen is not always an easy job for a pathologist. The sensitivity and diagnostic yield of fine needle aspiration in anterior mediastinal masses is reported to be lower compared to core needle biopsy, especially for non-carcinomatous tumors such as thymomas and lymphomas (26,27). Cases with non-definitive fine needle aspiration biopsy diagnoses are largely due to sampling error and/or insufficient cellularity (28). Making a wrong histologic diagnosis on preoperative needle sampling has been reported when compared to the postoperative pathologic analysis of the resected specimen (29).

In case more adequate tissue is desired for histology, immunohistochemistry, and molecular testing to fully characterize the tumor, a surgical biopsy either minimally-invasive or occasionally via open way may be needed to obtain more tissue for histopathology and immunological staining. Depending on the exact location of the mass in any mediastinal compartment (*Figure 2*), different surgical approaches can be chosen varying between median or lateral cervical incision for highly located prevascular tumors, anterior mediastinotomy for parasternal lesions in the prevascular mediastinum; video-assisted mediastinoscopy as an alternative to EBUS or EUS for a mass in the visceral mediastinum; or video-assisted (VATS) or robot-assisted (RATS) thoracoscopy to biopsy a lesion in the prevascular or paravertebral mediastinum. Minimally invasive procedures such as VATS and RATS offer the possibility to also sample hilar or pleural abnormalities concomitantly identified. Occasionally a partial sternotomy or limited thoracotomy may be needed to reach the tumor for adequate tissue biopsy. In one study in patients with a suspicion of a lymphoproliferative disease extending in the prevascular and visceral compartment, the authors reported that diagnostic accuracy was lower for cervical mediastinoscopy (80.4%)

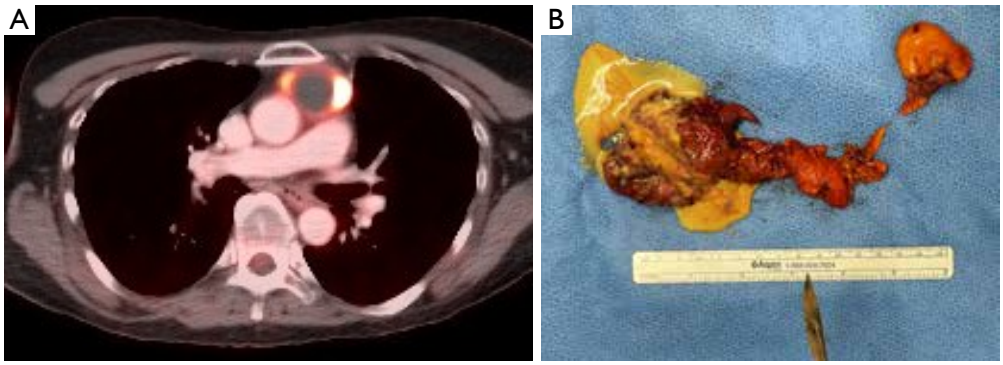

Figure 3 The case of a 56-year-old female treated with 5 cycles of chemotherapy for Hodgkin lymphoma. (A) PET-CT scan suggested a necrotic mass with residual tumor activity in the outer layer; (B) instead of taking a blind biopsy, the residual mass was completely resected with thymectomy via left thoracoscopy. A necrotic lesion with thick sterile pus was found in the resected specimen. Pathologic examination confirmed persistent Hodgkin lymphoma. PET-CT, positron emission tomography/computed tomography.

compared to anterior mediastinotomy (95.9%) (30).

Taking a biopsy of a residual lesion suspicious for lymphoma recurrence on PET imaging following definitive chemo-radiotherapy can be hazardous because of dense mediastinal fibrosis. A core biopsy by opening the fibrotic capsula is needed to sample adequate tissue. Occasionally, the residual mass can be entirely resected by thymectomy to ensure that the residual fluorodeoxyglucose (FDG)-avid zone shown on PET scan is included in the specimen (*Figure 3*).

A frozen section is helpful to check the quality of the biopsy, but is less effective for a precise tissue diagnosis of some primary mediastinal lesions, which may have a similar histologic appearance such as thymoma and lymphoma. Flow cytometry analysis on a fresh biopsy though can be done fast and add to the diagnosis of a lymphoma, particularly lymphoblastic lymphoma.

The definitive pathological report based on histology, immunohistochemistry, and molecular testing needs to be awaited prior to initiating any treatment except in case of a life-threatening condition such as critical airway compression or superior vena cava syndrome.

Conclusions

The finding of a mediastinal mass often poses a diagnostic challenge for clinicians. Pretreatment tissue biopsy of mediastinal lesions is not always required in case the diagnosis is confirmed or highly probable based on clinical symptoms and signs, thoracic imaging and laboratory tests. Upfront surgical resection without pathologic confirmation may be indicated for well encapsulated and non-invasive suspicious mediastinal lesions. Tissue diagnosis prior to surgical resection is recommended for locally advanced or unresectable mediastinal tumors in order to confirm the suspected diagnosis and to guide induction therapy or definitive systemic treatment. An ultrasound or CT-guided core needle biopsy may result in sufficient tissue for definitive diagnosis while the diagnostic yield of fine needle biopsy is lower. A surgical biopsy may be needed to obtain more tissue for histology, immunohistochemistry and molecular testing. A frozen section is helpful to check the quality of the biopsy but is less effective for a precise tissue diagnosis.

Acknowledgments

This paper was presented as an invited lecture at the 14th Annual Meeting of the International Thymic Malignancy Interest Group, October 30–November 1, 2024, Yokohama, Japan.

Footnote

Provenance and Peer Review: This article was commissioned by the Guest Editor (Malgorzata Szolkowska) for "The Series Dedicated to the 14th International Thymic Malignancy Interest Group Annual Meeting (ITMIG 2024)" published in *Mediastinum*. The article has undergone external peer review.

Peer Review File: Available at https://med.amegroups.com/article/view/10.21037/med-25-29/prf

Funding: None.

Conflicts of Interest: Both authors have completed the ICMJE uniform disclosure form (available at https://med.amegroups.com/article/view/10.21037/med-25-29/coif). "The Series Dedicated to the 14th International Thymic Malignancy Interest Group Annual Meeting (ITMIG 2024)" was commissioned by the editorial office without any funding or sponsorship. P.M.C. reports consulting fees paid to his institution from MSD, Merck, and Servier; participation in an advisory board for MSD; and service as a member of the CTG/CRM Belgium. The authors have no other conflicts of interest to declare.

Ethical Statement: The authors are accountable for all aspects of the work in ensuring that questions related to the accuracy or integrity of any part of the work are appropriately investigated and resolved.

References

1. Van Raemdonck D. What comes out of Pandora's box. J Thorac Cardiovasc Surg 2015:149:110-1.
2. Walcot, P. Pandora's jar, Hermes 1961;89:249–51.
3. Carter BW, Tomiyama N, Bhora FY, et al. A modern definition of mediastinal compartments. J Thorac Oncol 2014;9:S97-101.
4. Shields TW. Primary tumors and cysts of the mediastinum. In Shields TW. editor. General Thoracic Surgery. Philadelphia: Lea & Febiger; 1983:927-54.
5. Evoli A, Lancaster E. Paraneoplastic disorders in thymoma patients. J Thorac Oncol 2014;9:S143-7.
6. Girard N, Ruffini E, Marx A, et al. Thymic epithelial tumours: ESMO Clinical Practice Guidelines for diagnosis, treatment and follow-up. Ann Oncol 2015;26 Suppl 5:v40-55.
7. Titulaer MJ, Soffietti R, Dalmau J, et al. Screening for tumours in paraneoplastic syndromes: report of an EFNS task force. Eur J Neurol 2011;18:19-e3.
8. Carter BW, Marom EM, Detterbeck FC. Approaching the patient with an anterior mediastinal mass: a guide for clinicians. J Thorac Oncol 2014;9:S102-9.
9. Carter BW, Okumura M, Detterbeck FC, et al. Approaching the patient with an anterior mediastinal mass: a guide for radiologists. J Thorac Oncol 2014;9:S110-8.
10. Strange CD, Truong MT, Ahuja J, et al. Imaging evaluation of thymic tumors. Mediastinum 2023;7:28.
11. Ackman JB. Imaging of mediastinal masses. Magn Reson Imaging Clin N Am 2015;23:141-64.
12. Ahuja J, Strange CD, Agrawal R, et al. Approach to Imaging of Mediastinal Masses. Diagnostics (Basel) 2023;13:3171.
13. Sandoval JA, Malkas LH, Hickey RJ. Clinical significance of serum biomarkers in pediatric solid mediastinal and abdominal tumors. Int J Mol Sci 2012;13:1126-53.
14. Ying J, Huang Y, Ye X, et al. Comprehensive study of clinicopathological and immune cell infiltration and lactate dehydrogenase expression in patients with thymic epithelial tumours. Int Immunopharmacol 2024;126:111205.
15. Talerman A, van der Pompe WB, Haije WG, et al. Alpha-foetoprotein and carcinoembryonic antigen in germ cell neoplasms. Br J Cancer 1977;35:288-91.
16. Lazzarino M, Orlandi E, Klersy C, et al. Serum CA 125 is of clinical value in the staging and follow-up of patients with non-Hodgkin's lymphoma: correlation with tumor parameters and disease activity. Cancer 1998;82:576-82.
17. Marcuse F, Hochstenbag M, Hoeijmakers JGJ, et al. Subclinical myasthenia gravis in thymomas. Lung Cancer 2021;152:143-8.
18. Ruffini E, Van Raemdonck D, Detterbeck F, et al. Management of thymic tumors: a survey of current practice among members of the European Society of Thoracic Surgeons. J Thorac Oncol 2011;6:614-23.
19. Fichtner A, Marx A, Ströbel P, et al. Primary germ cell tumours of the mediastinum: A review with emphasis on diagnostic challenges. Histopathology 2024;84:216-37.
20. Yue J, Gu Z, Yu Z, et al. Pretreatment biopsy for histological diagnosis and induction therapy in thymic tumors. J Thorac Dis 2016;8:656-64.
21. Saito T, Kobayashi H, Sugama Y, et al. Ultrasonically guided needle biopsy in the diagnosis of mediastinal masses. Am Rev Respir Dis 1988;138:679-84.
22. Ben-Yehuda D, Polliack A, Okon E, et al. Image-guided core-needle biopsy in malignant lymphoma: experience with 100 patients that suggests the technique is reliable. J Clin Oncol 1996;14:2431-4.
23. Sinner WN. The direct approach to posterior mediastinal masses by fine-needle biopsy. Oncology 1985;42:187-92.

24. Yasufuku K, Nakajima T, Fujiwara T, et al. Utility of endobronchial ultrasound-guided transbronchial needle aspiration in the diagnosis of mediastinal masses of unknown etiology. Ann Thorac Surg 2011;91:831-6.
25. Hünerbein M, Ghadimi BM, Haensch W, et al. Transesophageal biopsy of mediastinal and pulmonary tumors by means of endoscopic ultrasound guidance. J Thorac Cardiovasc Surg 1998;116:554-9.
26. Nasit JG, Patel M, Parikh B, et al. Anterior mediastinal masses: A study of 50 cases by fine needle aspiration cytology and core needle biopsy as a diagnostic procedure. South Asian J Cancer 2013;2:7-13.
27. Petranovic M, Gilman MD, Muniappan A, et al. Diagnostic Yield of CT-Guided Percutaneous Transthoracic Needle Biopsy for Diagnosis of Anterior Mediastinal Masses. AJR Am J Roentgenol 2015;205:774-9.
28. Assaad MW, Pantanowitz L, Otis CN. Diagnostic accuracy of image-guided percutaneous fine needle aspiration biopsy of the mediastinum. Diagn Cytopathol 2007;35:705-9.
29. Robinson LA, Dobson JR, Bierman PJ. Fallibility of transthoracic needle biopsy of anterior mediastinal masses. Thorax 1995;50:1114-6.
30. Elia S, Cecere C, Giampaglia F, et al. Mediastinoscopy vs. anterior mediastinotomy in the diagnosis of mediastinal lymphoma: a randomized trial. Eur J Cardiothorac Surg 1992;6:361-5.

doi: 10.21037/med-25-29
Cite this article as: Van Raemdonck D, Clement PM. Mediastinal tumors: why, when, and how to biopsy? Mediastinum 2025;9:24.

Review Article

Factors distinguishing thymomas from thymic squamous cell carcinoma: a proposal for diagnosis emphasizing the immunophenotype

Yosuke Yamada^

Department of Molecular Pathology, Graduate School of Medicine and Faculty of Medicine, The University of Tokyo, Tokyo, Japan

Correspondence to: Yosuke Yamada, MD, PhD. Department of Molecular Pathology, Graduate School of Medicine and Faculty of Medicine, The University of Tokyo, 7-3-1 Hongo, Bunkyo-ku, Tokyo 113-0033, Japan. Email: yoyamada@m.u-tokyo.ac.jp.

Abstract: Thymic epithelial tumors (TETs) are rare but represent the most common neoplasms in the adult mediastinum. They are primarily classified into thymomas and thymic carcinomas, with thymic squamous cell carcinoma (SCC) being the most prevalent subtype of thymic carcinoma. Distinguishing thymomas from thymic carcinoma is critical, as it directly influences treatment strategies. However, considerable interobserver variability remains, and differentiating type A and type B3 thymomas—characterized by scattered or absent immature T cells—from thymic SCC continues to pose a diagnostic challenge. Notably, thymomas and thymic carcinomas are biologically distinct entities. Typical thymic SCC more prominently exhibits phenotypes of medullary thymic epithelial cells (mTECs) than thymomas. For example, we have demonstrated that thymic SCC frequently shows characteristics resembling tuft cells, a subset of mTECs. Moreover, these tuft cell-like phenotypes are strongly associated with KIT expression, a well-established marker of thymic SCC, which likely activates signaling pathways characteristic of this carcinoma subtype. The mTEC-like properties of thymic SCC may support the notion that it can partially mimic the cytoarchitecture of the thymus, a feature generally associated with thymoma. Therefore, immunophenotypic profiling may enhance diagnostic accuracy in distinguishing thymomas from thymic SCC. This review presents this perspective through discussion of various TET cases, focusing on type A thymoma, type B3 thymoma, and thymic SCC. Rather than asserting a definitive viewpoint, we aim to encourage constructive discussion toward a diagnostic consensus for TETs.

Keywords: Thymoma; thymic carcinoma; thymic epithelial tumors (TETs); diagnostic pathology; immunohistochemistry

Received: 20 February 2025; Accepted: 01 July 2025; Published online: 25 September 2025.
doi: 10.21037/med-24-50
View this article at: https://dx.doi.org/10.21037/med-24-50

Introduction

The thymus is a key lymphoepithelial organ responsible for T cell development. Thymic epithelial cells (TECs) play a central role in this process and can give rise to tumors commonly found in the anterior mediastinum, known as thymic epithelial tumors (TETs). Although various classification systems have been proposed for TETs (1), the World Health Organization (WHO) classification, introduced in 1999 (3rd edition) and last updated in 2021 (5th edition), has become the international standard (2). TETs are broadly categorized into thymomas and thymic carcinomas. Thymomas are further classified into types A, AB, B1, B2, and B3, along with rarer subtypes, namely, micronodular thymoma with lymphoid stroma (MNTLS) and metaplastic thymoma. Thymic carcinomas are less

^ ORCID: 0000-0001-7952-2706.

common, occurring at approximately one-fourth the frequency of thymomas, with squamous cell carcinoma (SCC) accounting for about 80% of cases. Although thymic neuroendocrine neoplasms are also epithelial tumors originating in the thymus, they are classified independently from thymomas and thymic carcinomas (2).

Clinically, the most important distinction among TET subtypes is between thymoma and thymic carcinoma, as they require different treatment approaches. Thymomas are often more suitable for repeat local ablative therapy or radiologic surveillance, whereas thymic carcinomas tend to require earlier and more aggressive systemic treatment. In addition, pemetrexed is more effective in thymomas than in thymic carcinomas (3), while sunitinib demonstrates greater efficacy in thymic carcinomas (4). These contrasting responses highlight the biological differences leading to varied therapeutic responses between thymoma and thymic carcinoma.

However, considerable interobserver variability has been reported in the diagnosis of TET, particularly in distinguishing between type A and type B3 thymomas—both characterized by a paucity or absence of immature T cells—and thymic SCC (5-8). Additionally, distinguishing MNTLS from micronodular thymic carcinoma with lymphoid hyperplasia can also be challenging, due to their histomorphological similarities, especially at low-power magnification. This difficulty is further compounded by the fact that micronodular thymic carcinoma is a recently defined subtype of thymic SCC (2,9).

To address this issue, it may be beneficial to present actual pathological images of diagnostically challenging cases and to discuss the distinguishing features between the aforementioned thymoma subtypes and thymic SCC. However, based on our review of the literature from the past decade, only a limited number of publications include such images (6,10,11). Possibly due to space constraints, the WHO classification (Blue Book) also provides limited coverage of the diagnostic challenges involved in differentiating thymoma from thymic SCC. In this review, we present a series of TET cases—focusing on type A thymoma, type B3 thymoma, and thymic SCC—and propose that pathologists should place greater emphasis on immunophenotypic profiling to aid in diagnosis, particularly in light of recent advances in TET biology.

Type A thymoma: histomorphology

Type A thymoma is defined as a TET with variable growth patterns, composed of bland spindle or oval tumor cells with few or no admixed immature T cells (2). One representative case of type A thymoma is presented as Case 1.

Type A thymoma typically shows coarse lobulation and is surrounded by a complete or incomplete fibrous capsule (*Figure 1A*). A fascicular growth pattern is often observed (*Figure 1B,1C*). In such areas, the tumor cells display spindly or oval nuclei with inconspicuous nucleoli and ill-defined eosinophilic cytoplasm. Mitoses are generally absent, and immature T cells are rarely seen (*Figure 1B*). The tumor may be compartmentalized by thick fibrous bands (*Figure 1C*), and each compartment—or even a single nest—can exhibit different growth patterns. In this case, some tumor nests consisted of cells forming glandular or microcystic structures (*Figure 1D*), in which the tumor cells tended to have rounder nuclei (*Figure 1E*).

Although perivascular spaces are not a hallmark of type A thymoma, they may occasionally be observed, particularly in areas where tumor cells form epithelial structures rather than a typical spindle cell morphology (*Figure 1F*). The current WHO classification defines "atypical type A thymoma" as a subtype characterized by cytologic atypia, increased mitotic activity, and necrosis (2). While this subtype may appear distinct, it shares molecular features and clinical behavior with conventional type A thymoma (2) and, based on current evidence, does not exhibit the immunophenotypes of thymic SCC (discussed further below). Consistent with the WHO classification, we emphasize the histological diversity of type A thymoma. Additionally, we believe that cytological features can vary, even though overt atypia is typically absent.

Type B3 thymoma: histomorphology

Type B3 thymoma is defined as a TET predominantly composed of mildly to moderately atypical polygonal tumor cells, accompanied by small numbers of non-neoplastic immature T cells (2). In this context, we present two representative cases of type B3 thymoma [Case 2 (*Figure 2A-2C*) and Case 3 (*Figure 2D-2F*)].

Type B3 thymomas typically appear pink and exhibit, at least in part, a lobular growth pattern. They are often associated with areas of type B2 thymoma, which contains a greater number of immature T cells and appears bluer (*Figure 2A*). A defining histologic feature of type B3 thymoma is the presence of vessels with occasionally dilated perivascular spaces (*Figure 2B*). Tumor cells display round to elongated, sometimes grooved nuclei, and have

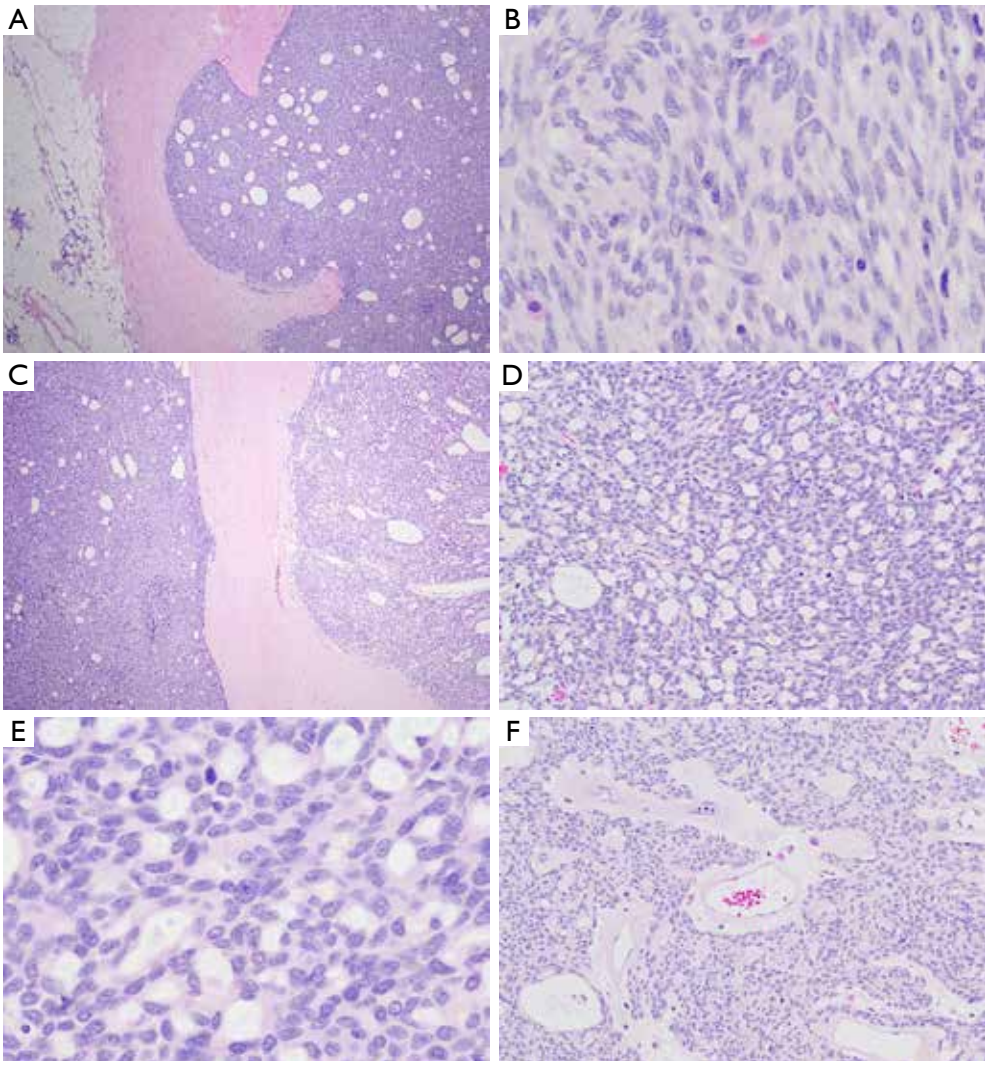

Figure 1 A case of type A thymoma. Case 1: The tumor exhibits lobular growth surrounded by a fibrous capsule (A). The tumor cells have spindle-shaped or oval nuclei with inconspicuous nucleoli, and mitotic figures are not evident. Immature T cells are almost absent (B). The tumor is separated by thick fibrous bands (C) and forms glandular or microcystic structures in some areas (right side) (D). In these regions, tumor cells may display rounder nuclei, although oval to spindle-shaped features persist (E). Dilated vessels with perivascular spaces are observed, particularly in less spindle-shaped areas (F) (A-F: hematoxylin and eosin staining; A, ×40; B, ×600; C, ×40; D, ×200; E, ×600; F, ×200).

eosinophilic or clear cytoplasm. Mitoses were not evident in these cells (*Figure 2C*). A small number of immature T cells were scattered among the tumor cells (*Figure 2B,2C*).

Although not exclusive to this subtype, type B3 thymomas can form relatively irregular nests surrounded by thick fibrous stroma (*Figure 2D*). In smaller or irregular nodules, perivascular spaces may be inconspicuous or absent (*Figure 2E*); however, the cytological features of the tumor cells remain consistent with those seen in well-demarcated lobules, and immature T cells are still present in this case (*Figure 2F*). While not observed in Cases 2 and 3, prominent nucleoli, cytologic anaplasia, and mitotic figures can occasionally be seen in otherwise typical type B3 thymomas (1,2).

Thymic SCC: histomorphology

Thymic SCC is defined as a primary malignant neoplasm of the thymus that exhibits morphological features similar to those observed in SCCs of other organs (2). Two cases of

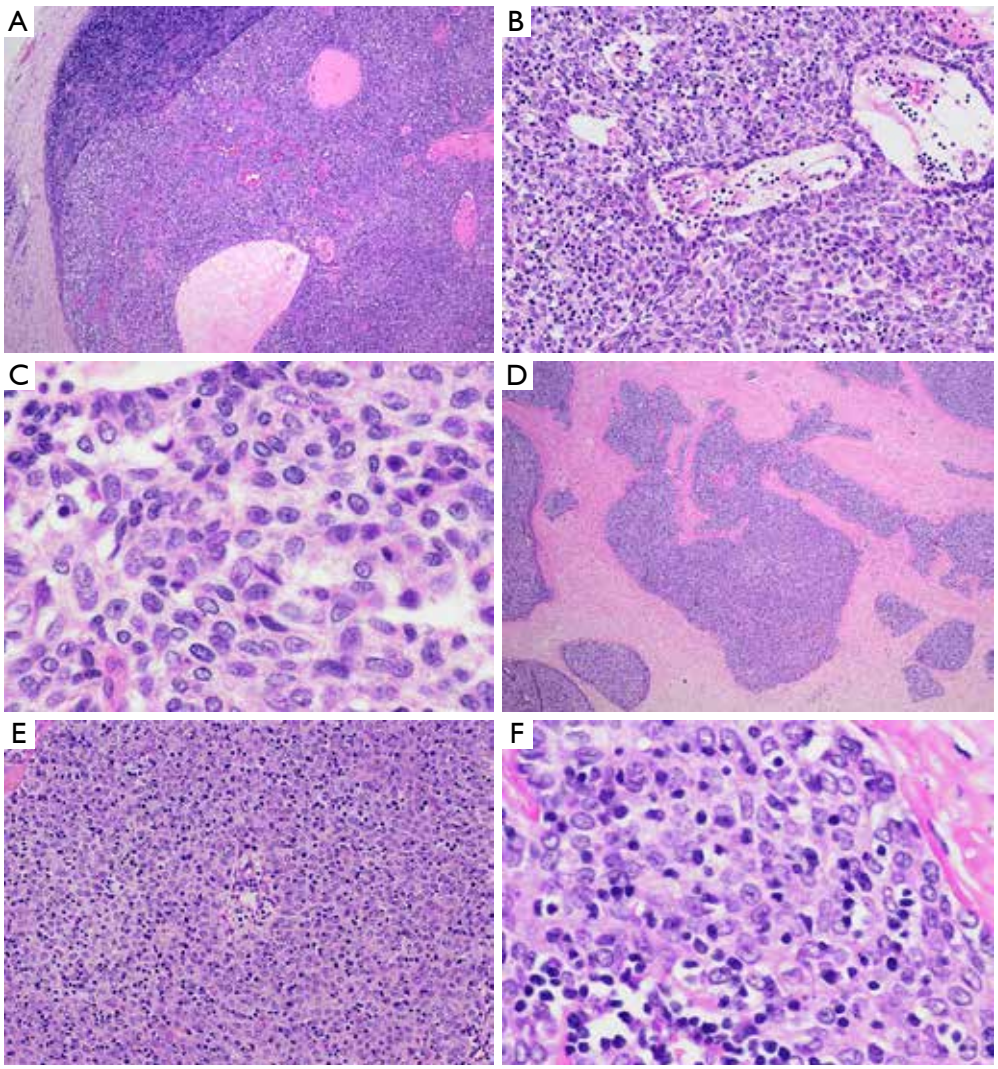

Figure 2 Two cases of type B3 thymoma. Case 2: The tumor is well-demarcated and appears pink overall, with a blue region in the upper part due to the presence of a type B2 thymoma component (A). It consists of numerous polygonal tumor cells with eosinophilic cytoplasm and accompanying immature T cells. Perivascular spaces are prominent (B). The tumor cells exhibit round to oval vesicular nuclei with slight grooves and relatively large eosinophilic cytoplasm. Nucleoli are not conspicuous, and mitotic figures are not evident (C). Case 3: The tumor invades thick fibrous stroma and forms irregularly shaped nodules (D). Perivascular spaces are small or inconspicuous within these nodules (E). The tumor cells are similar to those in Case 2 (F) (A-D: hematoxylin and eosin staining; A, ×40; B, ×200; C, ×600; D, ×40; E, ×200; F, ×600).

thymic SCC are presented: Case 4 (*Figure 3A-3D*) and Case 5 (*Figure 3E,3F*).

In straightforward cases, the tumors are clearly invasive, infiltrating the surrounding tissues and forming irregularly shaped nests (*Figure 3A*). Most thymic SCCs are poorly differentiated, with squamous differentiation often observed only focally, particularly at the periphery of the nests (*Figure 3B*). The tumor cells display large vesicular nuclei, often with prominent nucleoli, and eosinophilic-to-amphophilic cytoplasm. Mitotic figures are readily identifiable, and immature T cells are absent (*Figure 3C*).

Although not specified in the WHO classification (2), we believe that thymic SCC may contain vessels with perivascular spaces infiltrated by inflammatory cells,

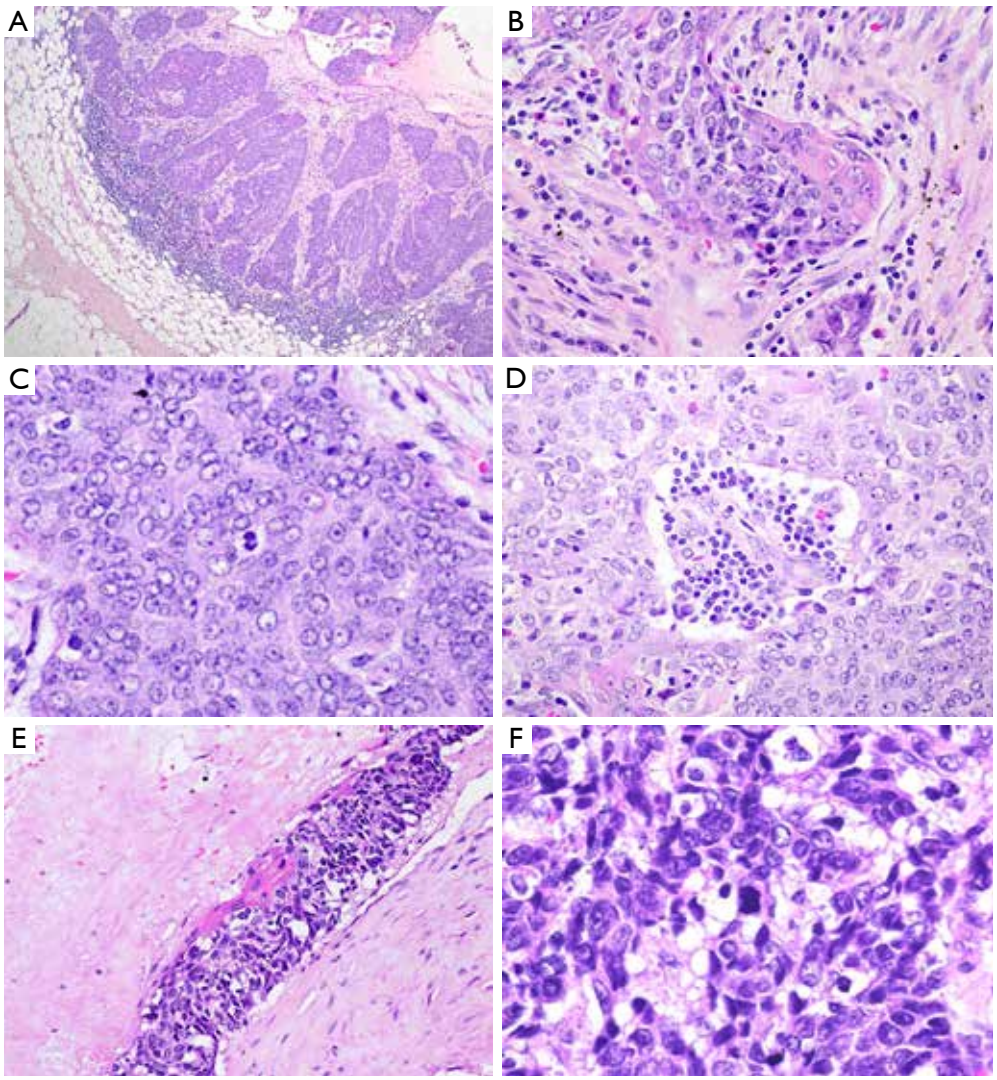

Figure 3 Two cases of thymic squamous cell carcinoma. Case 4: The tumor invades surrounding tissues and forms irregularly shaped islands (A). Focal squamous differentiation is observed, particularly at the periphery of the islands (B). Tumor cells display vesicular nuclei with prominent nucleoli and eosinophilic or amphophilic cytoplasm. Mitoses are readily identifiable (C). Although not prominent, vessels resembling perivascular spaces are present and are accompanied by inflammatory cells (D). Case 5: The tumor forms small nodules encased in sclerohyaline stroma (E). Keratinization is evident, but most tumor cells show hyperchromatic and pleomorphic nuclei with scant cytoplasm. Mitoses are frequently observed (F) (A-F: hematoxylin and eosin staining; A, ×40; B, ×400; C, ×600; D, ×400; E, ×200; F, ×600).

particularly in larger tumor nodules (*Figure 3D*). A similar observation is illustrated in a textbook (1). Thymic SCC is also frequently associated with sclerohyaline stroma (*Figure 3E*). In addition to focal squamous differentiation (*Figure 3E*), the tumor cells in this case demonstrated high-grade nuclear atypia, characterized by hyperchromatic and pleomorphic nuclei with abundant mitotic activity (*Figure 3F*).

Thymomas and thymic SCC: immunoreactivity for CD5 and KIT

It has long been recognized that thymic SCC often expresses CD5 and KIT, whereas such expression is rare in thymomas (12-14). Type B3 thymoma (Case 3), like other thymoma subtypes including type A thymoma, is negative for CD5 (*Figure 4A*) and KIT (*Figure 4B*). In contrast, thymic SCC (Case 4) demonstrates positive immunoreactivity for CD5

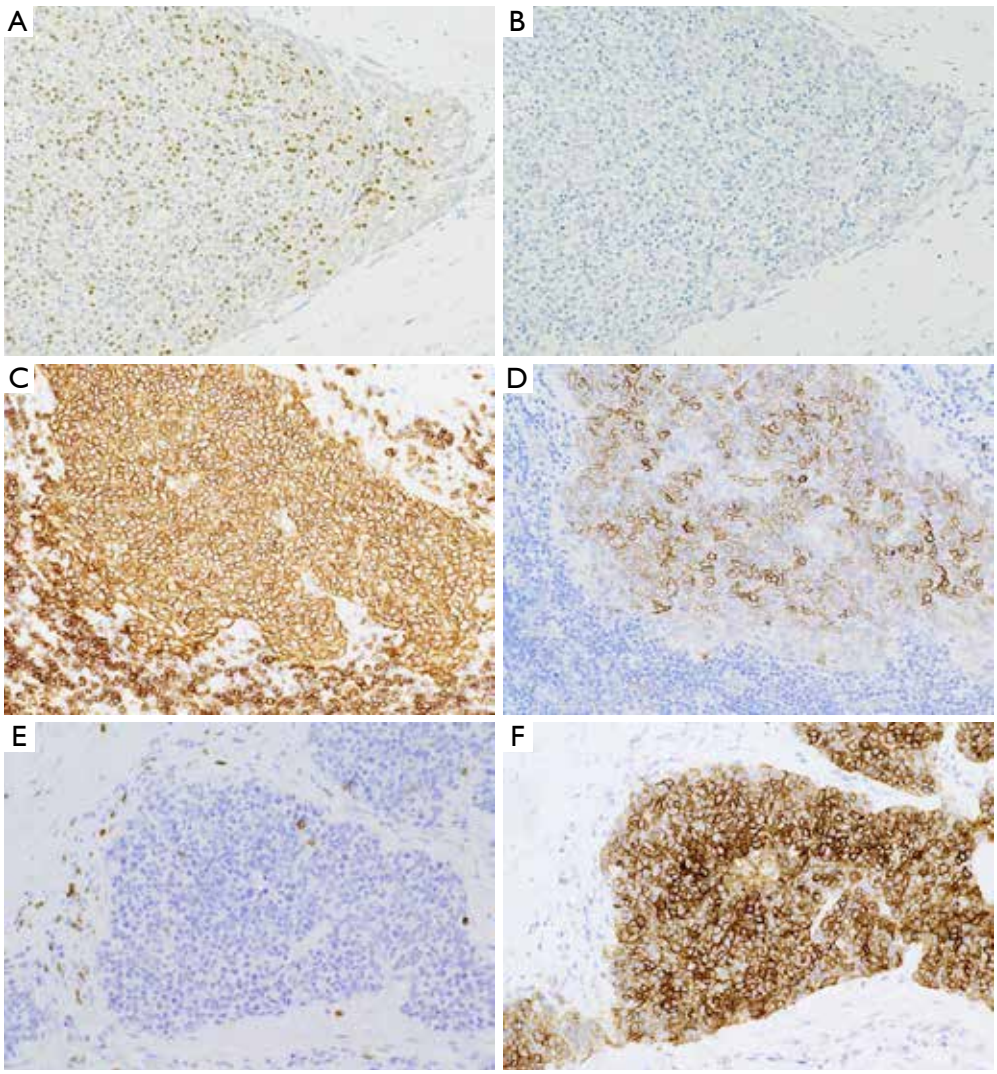

Figure 4 Immunohistochemical findings of type B3 thymoma and thymic squamous cell carcinoma. Case 3 (same as Case 3 in *Figure 2*): tumor cells are negative for CD5 (A) and KIT (B). CD5 highlights T cells within the tumor; some are also TdT-positive (not shown). Case 4 (same as Case 4 in *Figure 3*): tumor cells are diffusely positive for CD5 (C) and partially positive for KIT (D). Case 6: tumor cells are nearly negative for CD5 (E), while most express KIT (F) (A-F: immunohistochemistry; A-F: ×200).

(*Figure 4C*) and KIT (*Figure 4D*).

Although not frequently emphasized, the expression patterns of CD5 and KIT can vary among thymic SCC cases and even within a single tumor. In Case 4, tumor cells exhibited diffuse CD5 expression (*Figure 4C*), while KIT expression was relatively patchy (*Figure 4D*). Conversely, Case 6 (a different thymic SCC case) showed minimal CD5 expression (*Figure 4E*) but diffuse KIT expression (*Figure 4F*). Some authors have noted that CD5-positive cells tend to localize at the periphery of tumor nests (15), whereas this distribution pattern is not observed for KIT-positive cells. A recent study suggests that CD5 expression may serve as a prognostic marker in thymic SCC, reporting that CD5-high (>50%) SCCs are associated with better outcomes than CD5-low SCCs (16).

What factors should distinguish thymoma from thymic SCC?

We have presented six cases: type A thymoma (Case 1), type B3 thymoma (Cases 2 and 3), and thymic SCC (Cases 4 to 6). Based on these representative cases,

distinguishing thymomas from thymic carcinoma may appear straightforward. However, even in typical cases, histomorphological and cytological features can vary within a single subtype and may overlap between thymoma and thymic carcinoma.

This observation is not entirely original (6), as challenging cases have been described that display features of both typical thymoma and typical thymic SCC, making diagnosis difficult for pathologists. Wolf *et al.* investigated the reproducibility of the WHO classification among a large cohort of international pathologists specializing in thymic pathology. In their study, they presented images of eight TET cases, four of which did not achieve diagnostic consensus (6). Another study on thymic carcinoma reported a case of thymic SCC with features that complicate its distinction from type B3 thymoma (10). According to these studies, thymic SCC may exhibit thymus-like organotypic features, such as lobulation and fibrous septation, or may display cytologically bland characteristics.

As exemplified by tumors of the central nervous system (17), tumor classification and diagnosis are becoming increasingly integrative, moving beyond sole reliance on histomorphology. This trend is well justified, given that cancer biology is profoundly influenced by molecular characteristics, including genetic and epigenetic signatures, as well as comprehensive gene expression profiles (18). The classification of TETs should be no exception. A growing body of research—particularly since the advent of whole genome sequencing—has revealed previously under-recognized features of TETs, thereby enhancing our understanding and improving diagnostic accuracy.

Petrini *et al.* were the first to report that a substantial proportion of thymomas—particularly type A and AB—harbor a hotspot mutation in the general transcription factor II-I (*GTF2I*), specifically the *GTF2I* L424H variant (19). This finding was subsequently confirmed by independent studies (20-22), and the functional significance of the mutation has been demonstrated both *in vitro* (23) and, more recently, *in vivo* using genetically engineered mouse models (24,25). The absence of such mutations in thymic carcinomas suggests that type A thymoma and thymic SCC are genetically distinct, at least in typical cases. Furthermore, a recent study reported that a rare subset (6%) of type B2 or B3 thymomas harbors the *KMT2A*::*MAML2* fusion and exhibits aggressive behavior (26). This translocation seems specific to these subtypes within TETs and may further highlight the genetic differences between thymoma and thymic SCC.

A study conducted as part of The Cancer Genome Atlas (TCGA) project provided a more comprehensive analysis of the molecular features of TETs, demonstrating that thymic carcinomas form a distinct molecular cluster separate from thymomas (22). Although the limited number of thymic carcinoma cases in the TCGA study (N=9; 4 SCC, 4 undifferentiated, 1 thymic carcinoma not otherwise specified) may be a limitation, subsequent studies with larger sample sizes have confirmed substantial genetic differences between thymomas and thymic carcinomas (27,28).

Additionally, recent studies supported by molecular research and associated datasets have highlighted features of medullary TECs (mTECs) in typical thymic SCC—features that were previously under-recognized (29-35). For example, we were the first to report that most thymic SCCs exhibit gene expression profiles resembling those of tuft cells (29), a subset of mTECs present in the thymus (36,37). We further found that tuft cells physiologically express KIT at higher levels than other TEC subtypes, and that tuft cell-like phenotypes are strongly associated with KIT expression (29). An independent research group later confirmed that among TECs, only non-neoplastic tuft cells uniquely express KIT, based on reanalysis of single-cell RNA sequencing data from the normal thymus (31,38). The association between KIT and tuft cell-like carcinoma or normal tuft cells has also been validated in studies of non-thymic organs (39-43). The effectiveness of KIT inhibition in treating rare *KIT*-mutated thymic SCC (44), along with the observation that *KIT*-mutated and KIT-positive (but non-mutated) thymic SCCs show overlapping histopathological features (45), suggests that KIT plays a role in the biological behavior of thymic SCC. We believe the connection between mTECs (particularly tuft cells) and KIT further highlights the significance of KIT expression in characterizing thymic SCC.

Additionally, some authors have suggested that CD5 expression in TETs may reflect mTEC characteristics, as physiological CD5-expressing cells have been identified as a subset of neuroendocrine cells in the thymic medulla (31), although the biological significance of these findings remains unclear. The medullary features of thymic SCC may also help explain its frequent focal neuroendocrine phenotype (34,46,47), given that neuroendocrine cells constitute a subset of mTECs in the thymus (38). We hypothesize that thymic SCC is a distinct entity among TETs, characterized by both a squamous cell phenotype and mTEC properties with a tendency toward neuroendocrine differentiation—including tuft cells—for reasons that

remain to be elucidated (48).

Although the characteristics of KIT- and CD5-expressing cells in the normal thymus, as well as the functional roles of KIT and CD5 in thymic SCC, warrant further investigations, such as through digital image analysis (49) and specific transcriptomic approaches, findings from a series of recent studies already provide a strong rationale for emphasizing KIT and CD5 expression in the diagnosis of thymic SCC. Furthermore, the medullary phenotype of thymic SCC may explain its thymus-like cytoarchitecture, particularly lobulation and perivascular spaces, which are not associated with immature T cells.

Consistent with this, recent studies report that the specificity of KIT for thymic carcinomas, as compared to thymomas, can reach 100%, with a sensitivity of 86% when using a 10% cutoff criterion (9). The authors also emphasized the importance of immunostaining for immature T cells using TdT, which may be replaced by CD1a or CD99. I agree with this approach, as scattered immature T cells can often be more difficult to distinguish from mature lymphocytes than one might expect. However, some pathologists tend to differentiate thymoma from thymic carcinoma primarily based on the extent to which the tumor retains thymus-like histomorphology and bland cytology—features that often serve as a foundation for pathological diagnosis. In this context, some authors have proposed the category of atypical thymoma as an intermediate entity between thymoma and thymic carcinoma, noting that thymomas can occasionally express KIT and/or CD5 (11). In the next three sections, we present four (mainly three) TET cases that pose diagnostic challenges, and we share our reflections based on the insights discussed above. The concept of atypical thymoma may be relevant to some of these cases.

Micronodular thymic carcinoma with lymphoid hyperplasia

This newly recognized entity is classified as a subtype of thymic SCC (2,50) and has recently garnered attention (51-53). We present one case (Case 7) alongside a case of MNTLS (Case 8). Micronodular thymic carcinoma with lymphoid hyperplasia is characterized by discrete or sometimes coalescent nodules surrounded by lymphoid-rich stroma containing reactive lymphoid follicles (*Figure 5A*). The tumor cells are cytomorphologically similar to conventional thymic SCC, exhibiting large vesicular nuclei, prominent nucleoli, and eosinophilic cytoplasm (*Figure 5B*). Although mitotic figures are frequently reported (51,54), they were not evident in this case. Immunohistochemically, the tumor often expresses CD5 (*Figure 5C*) and KIT (*Figure 5D*), similar to conventional thymic SCC. The primary differential diagnosis is MNTLS (*Figure 5E,5F*). While the histological features, particularly at low magnification (*Figure 5E*), may appear similar, the cytomorphology (*Figure 5F*) and immunohistochemical patterns are markedly different; MNTLS is negative for both CD5 and KIT (2,50-53). Therefore, we believe the key to avoiding misdiagnosis is simply recognizing this entity.

Moreover, this tumor illustrates that thymic SCCs can exhibit cytoarchitectural diversity while sharing common immunohistochemical features. Clinically, micronodular thymic carcinomas with lymphoid hyperplasia may not be high-grade tumors based on previous reports (50-52,54). However, due to the small number of documented cases, definitive conclusions about their clinical behavior remain premature.

A challenging case of TETs: type A thymoma versus thymic SCC

The tumor (Case 9) was multilobulated and, although it invaded the surrounding adipose tissue, the border remained well-demarcated (*Figure 6A*). A potential concern was the presence of small, irregularly shaped islands at the periphery (*Figure 6B*). The tumor contained vessels with large perivascular spaces primarily filled with lymphocytes (*Figure 6C*). Tumor cells were spindle- or oval-shaped, proliferating in a fascicular growth pattern, occasionally forming whorl-like structures (*Figure 6D*) and rosettes (*Figure 6E*). Compared with conventional type A thymoma, the nuclei appeared larger and more monotonous, with some cells showing central nucleoli. Mitoses were readily observed (10 per 2 mm^2) (*Figure 6F*). Immunohistochemically, the tumor showed diffuse expression of CD5 (*Figure 7A*), KIT (*Figure 7B*), and p40 (*Figure 7C*). The Ki-67 labeling index was approximately 13% (*Figure 7D*). No TdT-positive cells were identified (not shown). Although not diagnostic, vascular invasion was clearly present (*Figure 7E*).

One of the pioneering studies on KIT expression in TETs reported that 1 out of 50 thymomas exhibited diffuse (>50%) KIT positivity, noting that "this thymoma is composed of spindle cells with mild atypia and is probably classified as an atypical thymoma, although it belongs to the type A histologic subtype in the (3rd) WHO classification" (13).

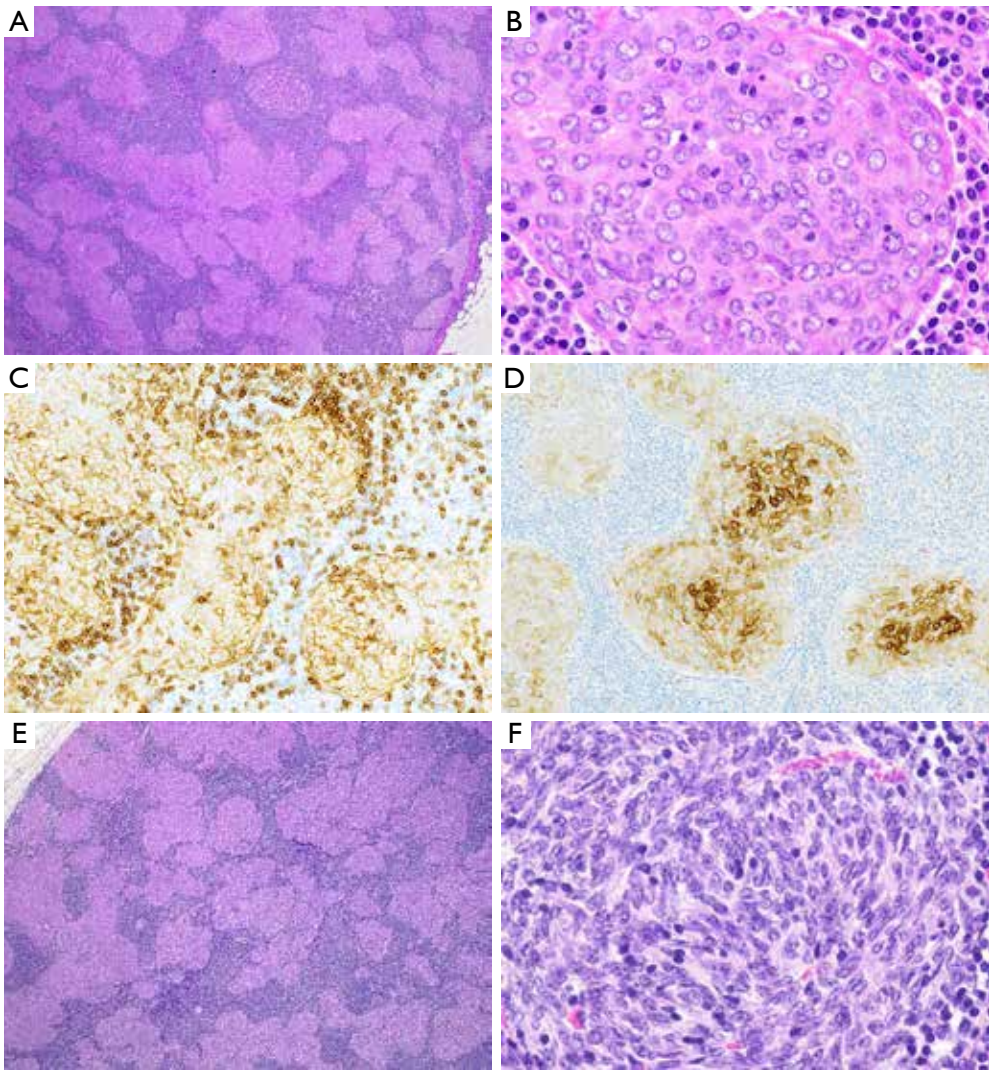

Figure 5 A case of micronodular thymic carcinoma with lymphoid hyperplasia, referencing a case of micronodular thymoma with lymphoid stroma. Case 7 (micronodular thymic carcinoma with lymphoid hyperplasia): The tumor comprises discrete or coalescent nodules separated by abundant lymphoid stroma featuring reactive lymphoid follicles (A). The tumor cells exhibit vesicular nuclei with prominent nucleoli, and mitoses are scant (B). The tumor cells express CD5 (C) and KIT (D). Case 8 (micronodular thymoma with lymphoid stroma): The tumor displays histomorphology similar to that of micronodular thymic carcinoma, particularly at low magnification (E). The tumor cells are denser than those in micronodular thymic carcinoma; however, their nuclei are spindle-shaped, and nucleoli are inconspicuous (F) (A, B, E, F: hematoxylin and eosin staining; C, D: immunohistochemistry; A, ×40; B, ×600; C, ×200; D, ×200; E, ×40; F, ×600).

This case may resemble the present one. While most pathologists would likely agree that the current case is not representative of a conventional type A thymoma, as the previous comments suggest, we are not convinced that a majority would classify it as thymic SCC either—particularly given its histomorphological resemblance to an (atypical) type A thymoma.

If a diagnosis of thymic SCC is favored for such cases, it may be worth reconsidering the current WHO definition of thymic SCC—"a primary malignant neoplasm of the thymus with morphological features of SCC as seen in other organs"—in future editions to improve diagnostic consistency. Although this definition has historical precedent, an international discussion, possibly through the International Thymic Malignancy Interest Group (ITMIG), may be warranted.

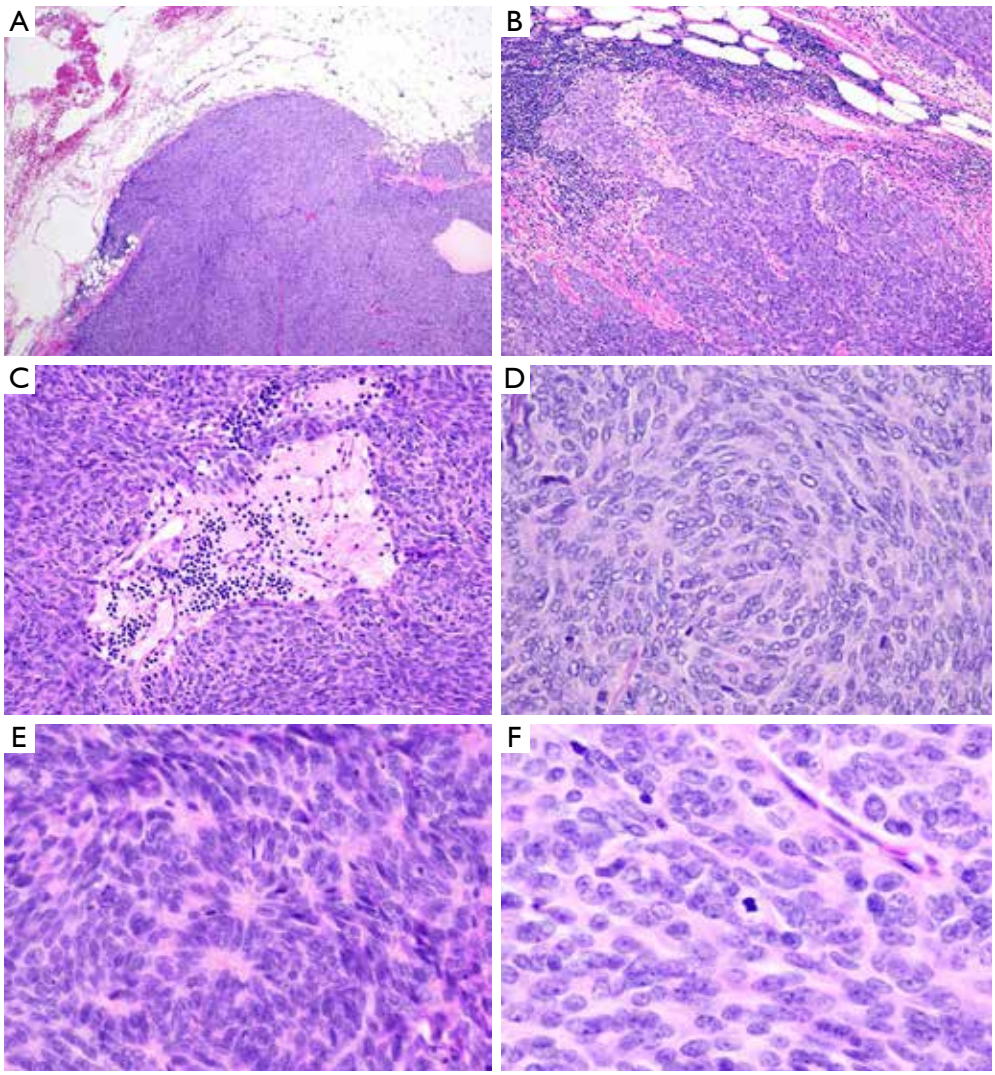

Figure 6 A challenging case of a thymic epithelial tumor: distinguishing between type A thymoma and thymic squamous cell carcinoma. Case 9: The tumor exhibits a lobulated appearance and invades the surrounding adipose tissue with pushing borders (A). A small number of irregularly shaped nodules are also present at the periphery (B). Overall, the tumor is composed of spindle cells, and perivascular spaces are apparent (C). The tumor cells proliferate in fascicles with whorls (D) and rosette-like structures (E). The tumor cells display relatively uniform oval to spindle-shaped nuclei, sometimes with prominent nucleoli and eosinophilic cytoplasm. Mitoses are readily observed (10 per 2 mm^2) (F) (A-F: hematoxylin and eosin staining; A, ×40; B, ×100; C, ×200; D, ×400; E, ×400; F, ×600).

A challenging case of TETs: thymic SCC originating from type B3 thymoma?

We have discussed the differences between thymoma and *de novo* thymic SCC. However, the possibility that thymoma may transform into thymic SCC has long been a subject of debate (1,11,55). A recent large-scale study reported that only two out of 368 thymic carcinomas were derived from type B3 thymoma (26), and the notion that thymoma-to-carcinoma transformation is rare appears to be a recent trend (56-58). However, the two cases referenced were interpreted as such (thymic SCC), and their pathological images were not provided.

The presented case (Case 10) may serve as a valuable example. It would essentially be diagnosed as a type B2 and B3 thymoma (*Figure 8A*), although invasive behavior is evident. The tumor formed variably sized nodules (lobules), with or without accompanying immature T cells and

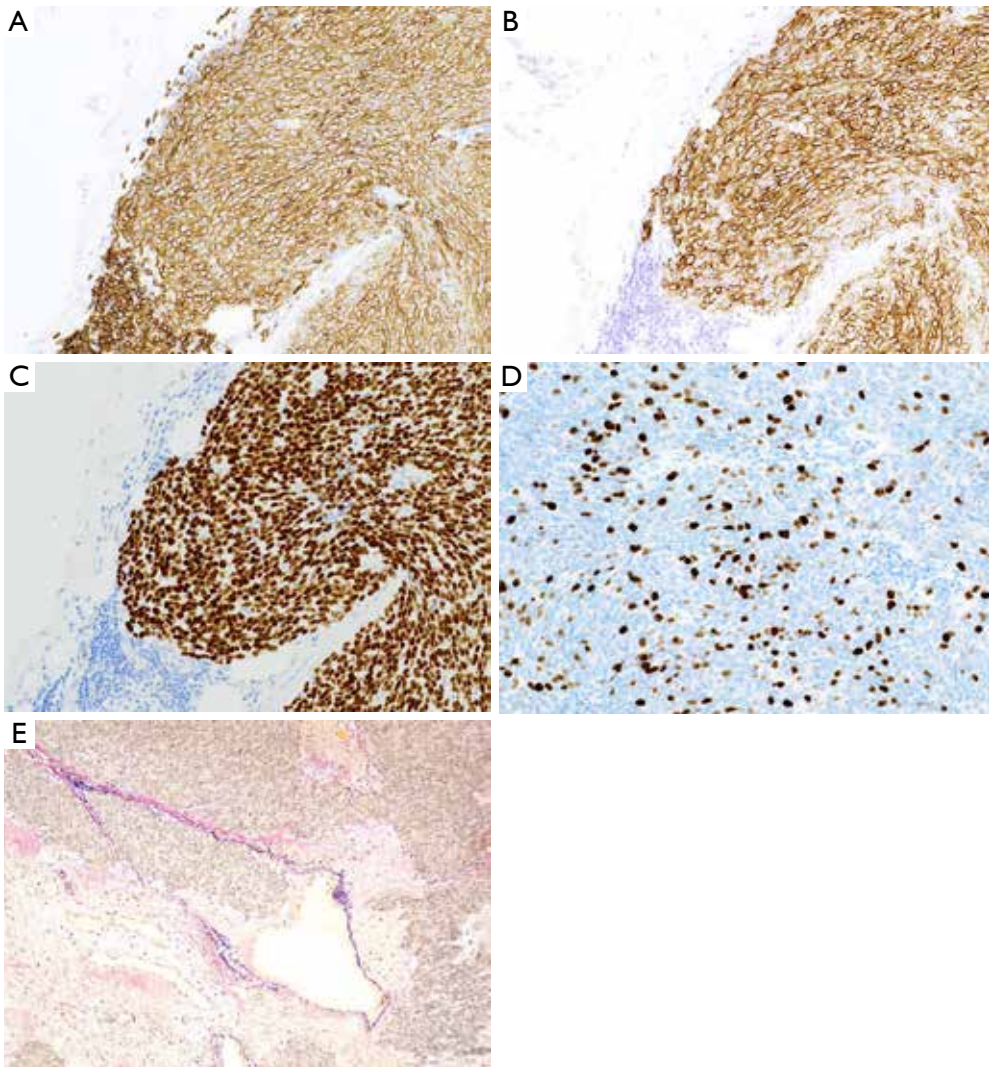

Figure 7 A challenging case of a thymic epithelial tumor distinguishing between type A thymoma and thymic squamous cell carcinoma (continued). Case 9: Immunohistochemically, the tumor cells are diffusely positive for CD5 (A), KIT (B), and p40 (C). The Ki-67 labeling index is approximately 13% in the hotspot (D). The tumor also exhibits vascular invasion (E) (A-D: immunohistochemistry; E: EVG staining; A-E, ×20).

perivascular spaces (*Figure 8B*). The tumor cells had variably sized, sometimes grooved nuclei, with occasional prominent nucleoli and relatively large pale to eosinophilic cytoplasm. Mitoses were not evident (*Figure 8C*). However, in some areas measuring 9 x 6 mm, the tumor exhibited irregularly shaped, anastomosing islands lacking the typical features of type B3 thymoma (*Figure 8D,8E*). These islands were composed of tumor cells with increased cellular density and nuclear atypia, although mitoses remained absent (*Figure 8F*). Immunohistochemically, these cells did not express CD5 (*Figure 9A*) or KIT (*Figure 9B*), as these markers may reflect mTEC characteristics that are unlikely to be present in tumors derived from type B3 thymoma. The Ki-67 labeling index in these areas was approximately 12% (*Figure 9C*), higher than that in the conventional type B3 thymoma regions (*Figure 9D*).

We believe this case might be diagnosed as focal thymic SCC arising from a type B3 thymoma, based on the loss of characteristic histological features of type B3 thymoma. However, this implies that different diagnostic

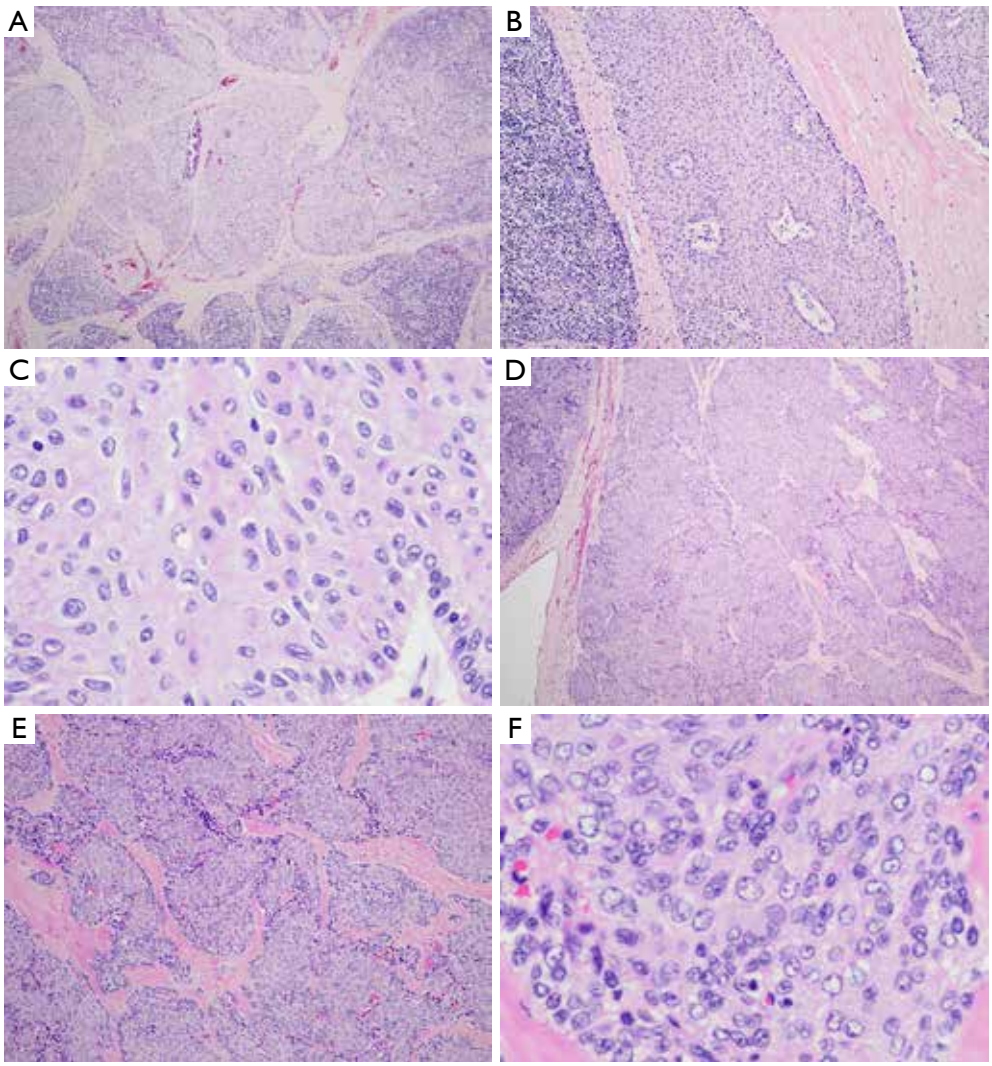

Figure 8 A challenging case of a thymic epithelial tumor: defining thymic squamous cell carcinoma derived from type B3 thymoma. Case 10: The majority of the tumor exhibits well-demarcated nodules composed of tumor cells with moderate atypia, accompanied by immature T cells and perivascular spaces (A-C), consistent with type B3 thymoma. However, some areas measuring 9 mm × 6 mm consist of irregularly shaped islands lacking typical features of type B3 thymoma (D,E). These islands contain tumor cells with increased nuclear atypia, characterized by larger nuclei, although mitoses are still not evident (F) (A-F: hematoxylin and eosin staining; A, ×40; B, ×100, C, ×600; D, ×40; E, ×100; F, ×600).

criteria must be applied to *de novo* thymic SCC and type B3 thymoma-derived thymic SCC, due to the differing histogeneses of typical thymic SCC and type B3 thymoma (59-61). Even if readers concur with this interpretation, a remaining challenge is determining the minimum size such areas should reach to justify this diagnosis. Therefore, an area larger than one low-power microscopic field (×40) may serve as a practical and clearly defined threshold. An alternative approach might be to retain the diagnosis of type B3 thymoma while noting the presence of such areas in a footnote, especially considering that the clinical significance remains unclear. Furthermore, the biological characteristics of type B3 thymoma-derived thymic SCC are likely to differ from those of typical *de novo* thymic SCC. Continued

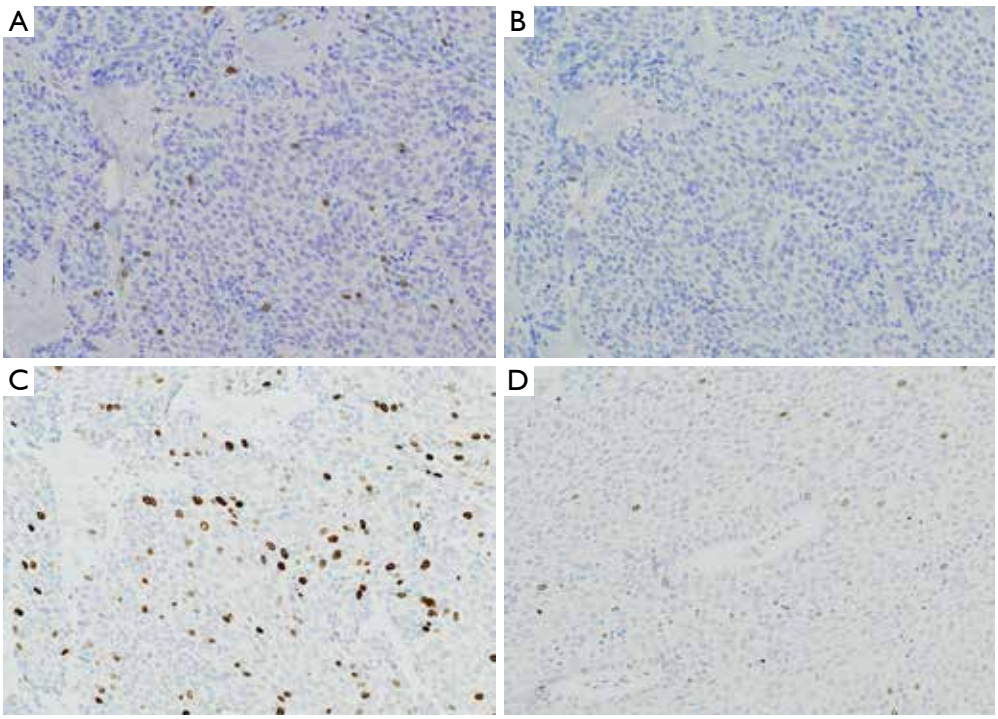

Figure 9 A challenging case of a thymic epithelial tumor: how to define thymic squamous cell carcinoma derived from type B3 thymoma (continued). Case 10: The tumor cells are negative for CD5 (A) and KIT (B), and the Ki-67 labeling index is approximately 12% in the atypical areas (C), which is higher than in typical type B3 thymoma regions (D) (A-D: immunohistochemistry, ×200).

discussion on this topic is warranted.

Conclusions

The diagnosis of TET is currently based on the WHO classification. While many TETs can be accurately diagnosed using hematoxylin and eosin staining-stained slides alone in straightforward cases, some remain diagnostically challenging. A representative example is the distinction between thymoma and thymic SCC when the TET case exhibits overlapping histomorphological features. Accumulating evidence supports the notion that thymomas and thymic carcinomas are biologically distinct neoplasms, with most thymic SCCs exhibiting features of mTECs. The commonly used immunohistochemical markers for thymic SCC, KIT and CD5, may be associated with this phenotype and offer greater diagnostic utility than previously appreciated. However, this concept may necessitate a dual standard for diagnosing thymic SCC, depending on tumor histogenesis—a topic warranting further discussion. Despite these complexities, this article contributes to ongoing discussion and facilitates the development of a consensus regarding the pathological distinctions between thymoma and thymic carcinoma.

Acknowledgments

The author would like to thank Shun Hasegawa and Masahito Hoki for kindly providing specimens for many of the thymic epithelial tumor cases.

Footnote

Provenance and Peer Review: This article was commissioned by the Guest Editor (Malgorzata Szolkowska) for "The Series Dedicated to the 14th International Thymic Malignancy Interest Group Annual Meeting (ITMIG 2024)" published in *Mediastinum*. The article has undergone external peer review.

Peer Review File: Available at https://med.amegroups.com/article/view/10.21037/med-24-50/prf

Funding: This work was supported in part by JSPS

KAKENHI (Number 24K10122) and the Takeda Science Foundation, Medical Research Grant (Number 2023044992).

Conflicts of Interest: The author has completed the ICMJE uniform disclosure form (available at https://med.amegroups.com/article/view/10.21037/med-24-50/coif). "The Series Dedicated to the 14th International Thymic Malignancy Interest Group Annual Meeting (ITMIG 2024)" was commissioned by the editorial office without any funding or sponsorship. The author has no other conflicts of interest to declare.

Ethical Statement: The author is accountable for all aspects of the work in ensuring that questions related to the accuracy or integrity of any part of the work are appropriately investigated and resolved.

References

1. Shimosato Y, Mukai K, Matsuno Y. Tumors of the mediastinum. In: Atlas of Tumor Pathology, 4th Series, Fascicle 11. Washington, DC: AFIP Press; 2010.
2. WHO Classification of Tumours. Thoracic tumours. Lyon (France): International Agency for Research on Cancer; 2021.
3. Gbolahan OB, Porter RF, Salter JT, et al. A Phase II Study of Pemetrexed in Patients with Recurrent Thymoma and Thymic Carcinoma. J Thorac Oncol 2018;13:1940-8.
4. Thomas A, Rajan A, Berman A, et al. Sunitinib in patients with chemotherapy-refractory thymoma and thymic carcinoma: an open-label phase 2 trial. Lancet Oncol 2015;16:177-86.
5. Molina TJ, Bluthgen MV, Chalabreysse L, et al. Impact of expert pathologic review of thymic epithelial tumours on diagnosis and management in a real-life setting: A RYTHMIC study. Eur J Cancer 2021;143:158-67.
6. Wolf JL, van Nederveen F, Blaauwgeers H, et al. Interobserver variation in the classification of thymic lesions including biopsies and resection specimens in an international digital microscopy panel. Histopathology 2020;77:734-41.
7. Oselin K, Girard N, Lepik K, et al. Pathological discrepancies in the diagnosis of thymic epithelial tumors: the Tallinn-Lyon experience. J Thorac Dis 2019;11:456-64.
8. Galli G, Trama A, Abate-Daga L, et al. Accuracy of pathologic diagnosis for thymic epithelial tumors: a brief report from an Italian reference Center. Lung Cancer 2020;146:66-9.
9. Naso JR, Vrana JA, Koepplin JW, et al. EZH2 and POU2F3 Can Aid in the Distinction of Thymic Carcinoma from Thymoma. Cancers (Basel) 2023;15:2274.
10. Roden AC, Szolkowska M. Common and rare carcinomas of the thymus. Virchows Arch 2021;478:111-28.
11. Suster DI, Craig Mackinnon A, DiStasio M, et al. Atypical thymomas with squamoid and spindle cell features: clinicopathologic, immunohistochemical and molecular genetic study of 120 cases with long-term follow-up. Mod Pathol 2022;35:875-94.
12. Pan CC, Chen PC, Chiang H. KIT (CD117) is frequently overexpressed in thymic carcinomas but is absent in thymomas. J Pathol 2004;202:375-81.
13. Nakagawa K, Matsuno Y, Kunitoh H, et al. Immunohistochemical KIT (CD117) expression in thymic epithelial tumors. Chest 2005;128:140-4.
14. Hishima T, Fukayama M, Fujisawa M, et al. CD5 expression in thymic carcinoma. Am J Pathol 1994;145:268-75.
15. Hosaka N, Ohe C, Miyasaka C, et al. The role of CD5 expression in thymic carcinoma: possible mechanism for interaction with CD5+ lymphoid stroma (microenvironment). Histopathology 2016;68:450-5.
16. Naso JR, Jenkins SM, Vrana JA, et al. CD5 Immunoreactivity Is Associated With Longer Overall Survival in Thymic Carcinoma: A Brief Report. JTO Clin Res Rep 2025;6:100803.
17. WHO Classification of Tumours. Central nervous system tumours. Lyon (France): International Agency for Research on Cancer; 2021.
18. Hanahan D. Hallmarks of Cancer: New Dimensions. Cancer Discov 2022;12:31-46.
19. Petrini I, Meltzer PS, Kim IK, et al. A specific missense mutation in GTF2I occurs at high frequency in thymic epithelial tumors. Nat Genet 2014;46:844-9.
20. Suster D, Mackinnon AC, Pihan G, et al. Lymphocyte-

Rich Spindle Cell Thymoma: Clinicopathologic, Immunohistochemical, Ultrastructural and Molecular Genetic Study of 80 Cases. Am J Surg Pathol 2022;46:603-16.
21. Wells K, Lamrca A, Papaxoinis G, et al. Unique correlation between GTF2I mutation and spindle cell morphology in thymomas (type A and AB thymomas). J Clin Pathol 2023;76:463-6.
22. Radovich M, Pickering CR, Felau I, et al. The Integrated Genomic Landscape of Thymic Epithelial Tumors. Cancer Cell 2018;33:244-258.e10.
23. Kim IK, Rao G, Zhao X, et al. Mutant GTF2I induces cell transformation and metabolic alterations in thymic epithelial cells. Cell Death Differ 2020;27:2263-79.
24. Giorgetti OB, Nusser A, Boehm T. Human thymoma-associated mutation of the GTF2I transcription factor impairs thymic epithelial progenitor differentiation in mice. Commun Biol 2022;5:1037.
25. He Y, Kim IK, Bian J, et al. A Knock-In Mouse Model of Thymoma With the GTF2I L424H Mutation. J Thorac Oncol 2022;17:1375-86.
26. Massoth LR, Hung YP, Dias-Santagata D, et al. Pan-Cancer Landscape Analysis Reveals Recurrent KMT2A-MAML2 Gene Fusion in Aggressive Histologic Subtypes of Thymoma. JCO Precis Oncol 2020;4:PO.19.00288.
27. Kurokawa K, Shukuya T, Greenstein RA, et al. Genomic characterization of thymic epithelial tumors in a real-world dataset. ESMO Open 2023;8:101627.
28. Girard N, Basse C, Schrock A, et al. Comprehensive Genomic Profiling of 274 Thymic Epithelial Tumors Unveils Oncogenic Pathways and Predictive Biomarkers. Oncologist 2022;27:919-29.
29. Yamada Y, Simon-Keller K, Belharazem-Vitacolonnna D, et al. A Tuft Cell-Like Signature Is Highly Prevalent in Thymic Squamous Cell Carcinoma and Delineates New Molecular Subsets Among the Major Lung Cancer Histotypes. J Thorac Oncol 2021;16:1003-16.
30. Yamada Y, Sugimoto A, Hoki M, et al. POU2F3 beyond thymic carcinomas: expression across the spectrum of thymomas hints to medullary differentiation in type A thymoma. Virchows Arch 2022;480:843-51.
31. Matsumoto M, Ohmura T, Hanibuchi Y, et al. AIRE illuminates the feature of medullary thymic epithelial cells in thymic carcinoma. Cancer Med 2023;12:9843-8.
32. Yuan X, Huang L, Luo W, et al. Diagnostic and Prognostic Significances of SOX9 in Thymic Epithelial Tumor. Front Oncol 2021;11:708735.
33. Kashima J, Hishima T, Okuma Y, et al. CD70 in Thymic Squamous Cell Carcinoma: Potential Diagnostic Markers and Immunotherapeutic Targets. Front Oncol 2021;11:808396.
34. Kashima J, Hashimoto T, Yoshida A, et al. Insulinoma-associated-1 (INSM1) expression in thymic squamous cell carcinoma. Virchows Arch 2022;481:893-901.
35. Li H, Ren B, Yu S, et al. The clinicopathological significance of thymic epithelial markers expression in thymoma and thymic carcinoma. BMC Cancer 2023;23:161.
36. Bornstein C, Nevo S, Giladi A, et al. Single-cell mapping of the thymic stroma identifies IL-25-producing tuft epithelial cells. Nature 2018;559:622-6.
37. Miller CN, Proekt I, von Moltke J, et al. Thymic tuft cells promote an IL-4-enriched medulla and shape thymocyte development. Nature 2018;559:627-31.
38. Bautista JL, Cramer NT, Miller CN, et al. Single-cell transcriptional profiling of human thymic stroma uncovers novel cellular heterogeneity in the thymic medulla. Nat Commun 2021;12:1096.
39. Yamada Y, Belharazem-Vitacolonnna D, Bohnenberger H, et al. Pulmonary cancers across different histotypes share hybrid tuft cell/ionocyte-like molecular features and potentially druggable vulnerabilities. Cell Death Dis 2022;13:979.
40. Yamada Y, Bohnenberger H, Kriegsmann M, et al. Tuft cell-like carcinomas: novel cancer subsets present in multiple organs sharing a unique gene expression signature. Br J Cancer 2022;127:1876-85.
41. Huang YH, Klingbeil O, He XY, et al. POU2F3 is a master regulator of a tuft cell-like variant of small cell lung cancer. Genes Dev 2018;32:915-28.
42. Huang L, Bernink JH, Giladi A, et al. Tuft cells act as regenerative stem cells in the human intestine. Nature 2024;634:929-35.
43. Jimbo N, Ohbayashi C, Takeda M, et al. POU2F3-Expressing Small Cell Lung Carcinoma and Large Cell Neuroendocrine Carcinoma Show Morphologic and Phenotypic Overlap. Am J Surg Pathol 2024;48:4-15.
44. Ströbel P, Hartmann M, Jakob A, et al. Thymic carcinoma with overexpression of mutated KIT and the response to imatinib. N Engl J Med 2004;350:2625-6.
45. Schirosi L, Nannini N, Nicoli D, et al. Activating c-KIT mutations in a subset of thymic carcinoma and response to different c-KIT inhibitors. Ann Oncol 2012;23:2409-14.
46. Hishima T, Fukayama M, Hayashi Y, et al. Neuroendocrine differentiation in thymic epithelial tumors with special reference to thymic carcinoma and atypical thymoma.

Hum Pathol 1998;29:330-8.
47. Lauriola L, Erlandson RA, Rosai J. Neuroendocrine differentiation is a common feature of thymic carcinoma. Am J Surg Pathol 1998;22:1059-66.
48. Yamada Y, Iwane K, Nakanishi Y, et al. Thymic Carcinoma: Unraveling Neuroendocrine Differentiation and Epithelial Cell Identity Loss. Cancers (Basel) 2023;16:115.
49. Bocchialini G, Schiefer AI, Müllauer L, et al. Tumour immune microenvironment in resected thymic carcinomas as a predictor of clinical outcome. Br J Cancer 2022;127:1162-71.
50. Weissferdt A, Moran CA. Micronodular thymic carcinoma with lymphoid hyperplasia: a clinicopathological and immunohistochemical study of five cases. Mod Pathol 2012;25:993-9.
51. Thomas de Montpreville V, Mansuet-Lupo A, Le Naoures C, et al. Micronodular thymic carcinoma with lymphoid hyperplasia: relevance of immunohistochemistry with a small panel of antibodies for diagnosis-a RYTHMIC study. Virchows Arch 2021;479:741-6.
52. Yagi H, Nakaguro M, Ito M, et al. Difference in the distribution of tumor-infiltrating CD8+ T cells and FOXP3+ T cells between micronodular thymoma with lymphoid stroma and micronodular thymic carcinoma with lymphoid stroma. Pathol Int 2021;71:453-62.
53. Thomas-de-Montpréville V, Chalabreysse L, Hofman V, et al. Micronodular thymic epithelial tumors with lymphoid hyperplasia and mimicking lesions. Histol Histopathol 2025;40:1-10.
54. Liu PP, Su YC, Niu Y, et al. Comparative clinicopathological and immunohistochemical study of micronodular thymoma and micronodular thymic carcinoma with lymphoid stroma. J Clin Pathol 2021;75:702-5.
55. Suster S, Moran CA. Primary thymic epithelial neoplasms showing combined features of thymoma and thymic carcinoma. A clinicopathologic study of 22 cases. Am J Surg Pathol 1996;20:1469-80.
56. Marx A, Chan JKC, Chalabreysse L, et al. The 2021 WHO Classification of Tumors of the Thymus and Mediastinum: What Is New in Thymic Epithelial, Germ Cell, and Mesenchymal Tumors? J Thorac Oncol 2022;17:200-13.
57. Roden AC, Ahmad U, Cardillo G, et al. Thymic Carcinomas-A Concise Multidisciplinary Update on Recent Developments From the Thymic Carcinoma Working Group of the International Thymic Malignancy Interest Group. J Thorac Oncol 2022;17:637-50.
58. von der Thüsen J. Thymic epithelial tumours: histopathological classification and differential diagnosis. Histopathology 2024;84:196-215.
59. Tomaru U, Yamada Y, Ishizu A, et al. Proteasome subunit β5t expression in cervical ectopic thymoma. J Clin Pathol 2012;65:858-9.
60. Yamada Y, Tomaru U, Ishizu A, et al. Expression of proteasome subunit β5t in thymic epithelial tumors. Am J Surg Pathol 2011;35:1296-304.
61. Hayashi A, Fumon T, Miki Y, et al. The evaluation of immunohistochemical markers and thymic cortical microenvironmental cells in distinguishing thymic carcinoma from type b3 thymoma or lung squamous cell carcinoma. J Clin Exp Hematop 2013;53:9-19.

doi: 10.21037/med-24-50
Cite this article as: Yamada Y. Factors distinguishing thymomas from thymic squamous cell carcinoma: a proposal for diagnosis emphasizing the immunophenotype. Mediastinum 2025;9:25.

Review Article

Pathogenesis of thymoma-associated myasthenia gravis: a narrative review

Tatsusada Okuno[1], Naoshi Koizumi[1], Yoshiaki Yasumizu[2,3,4]

[1]Department of Neurology, Graduate School of Medicine, University of Osaka, Suita, Osaka, Japan; [2]Department of Neurology, Yale School of Medicine, New Haven, CT, USA; [3]Department of Immunobiology, Yale School of Medicine, New Haven, CT, USA; [4]Department of Experimental Immunology, Immunology Frontier Research Center, University of Osaka, Suita, Osaka, Japan

Contributions: (I) Conception and design: T Okuno; (II) Administrative support: T Okuno; (III) Provision of study materials or patients: All authors; (IV) Collection and assembly of data: N Koizumi; (V) Data analysis and interpretation: Y Yasumizu, N Koizumi; (VI) Manuscript writing: All authors; (VII) Final approval of manuscript: All authors.

Correspondence to: Tatsusada Okuno, MD, PhD. Department of Neurology, Graduate School of Medicine, University of Osaka, 2-15 Yamadaoka, Suita, Osaka 565-0871, Japan. Email: okuno@neurol.med.osaka-u.ac.jp.

Background and Objective: Patients with thymomas often develop autoimmune neuromuscular diseases, including myasthenia gravis (MG). Autoantigen expression in thymomas plays an important role in disease pathogenesis. Since thymomas are mainly composed of the cortex, with few medullae, MG may be caused by immature thymoma-derived T cells that fail to undergo negative selection and have not yet acquired sufficient self-tolerance. However, due to the complexity and diversity of thymoma cell populations, a comprehensive understanding of the mechanisms underlying its association with MG has yet to be achieved. The purpose of this article is to provide an overview of the normal thymus function and the pathogenesis of thymoma associated with MG and other autoimmune diseases, with the aim to highlight newly identified mechanisms that may offer novel insights into their development.

Methods: To address the lack of information regarding the MG-thymoma association, we applied a bioinformatics approach to thymomas.

Key Content and Findings: By analyzing bulk RNA-sequencing (RNA-seq) and single-cell RNA-seq (scRNA-seq) data from thymomas, we identified neuromuscular medullary thymic epithelial cells (nmTECs) as neuromuscular antigen-expressing cell populations. Medullary structures, although much smaller than those of the normal thymus, are present in thymomas with MG and MG-susceptible genes are clustered. We observed spatial nmTEC colocalization and an immune niche, inferring an interaction and suggesting a pathological role of nmTECs in MG.

Conclusions: After providing an up-to-date overview of normal thymus function, along with data and hypotheses regarding the association between thymoma and MG, we present bioinformatic findings regarding the thymoma.

Keywords: Thymoma-associated myasthenia gravis (TAMG); neuro muscular medullary thymic epithelial cells (nmTECs); medullary structure; single-cell RNA-sequencing (scRNA-seq); spatial transcriptome

Received: 01 May 2025; Accepted: 22 September 2025; Published online: 26 September 2025.

doi: 10.21037/med-25-28

View this article at: https://dx.doi.org/10.21037/med-25-28

Introduction

Normal thymus function

T cell development in the normal thymus

The thymus, an organ in which T cells differentiate and mature, enables immune cells to defend against infection while avoiding autoimmunity. The cellular mechanisms of immune tolerance in the thymus involve thymic epithelial cells (TECs), dendritic cells (DCs), and B cells. The thymus structure comprises the cortex, medulla, and perivascular spaces (PVSs) (1). Bone marrow-derived T cell progenitors mature within the thymus and differentiate into $CD4^+$ single-positive (SP) or $CD8^+$ SP T cells, which subsequently exit to the periphery. Key events that occur during intrathymic T cell differentiation include the following:

(I) Generation of thymocytes expressing a wide variety of T cell receptors (TCRs) by rearrangement of the TCR genes within the thymic cortex;
(II) Positive selection in the cortex, achieved by inducing apoptosis of T cells that fail to recognize the self-major histocompatibility complex (self-MHC), thereby selecting T cells capable of recognizing self-antigens;
(III) Chemokine-mediated migration of thymocytes from the cortex to the medulla;
(IV) Negative selection in the medulla, eliminating T cells expressing TCRs that strongly recognize self-antigens;
(V) The appearance of $CD8^+$ and $CD4^+$ SP thymocytes.

In essence, the thymus uses a purposeful mechanism that initially produces T cells with an extensive repertoire of TCRs beneficial to the host defense, before eliminating those with potentially autoreactive TCRs (negative selection). Errors in these processes result in autoreactive T cells, ultimately leading to the development of autoimmune diseases.

Tissue-restricted self-antigens (TRAs) in the thymus

The expression of TRAs by medullary TECs (mTECs) is an important mechanism for eliminating autoantigen reactive T cells in the thymus. Autoimmune regulator (AIRE), a transcriptional modulator mainly expressed in mTECs, is the most well-known molecule involved in this process (1). In mTECs, AIRE is part of a multimeric complex that includes proteins related to nuclear transport, chromatin binding/structure, transcription, and pre-messenger RNA processing (2). AIRE induces "promiscuous gene expression" of more than 3,000 TRAs (1,3). The mechanism by which AIRE promotes tissue TRA expression has been elucidated in terms of the DNA and chromatin structure (4). Researchers used Assay for Transposase-Accessible Chromatin using sequencing (ATAC-seq) analysis to identify Z-DNA motifs (left-handed double-helical DNA structures) and transcription factors nuclear factor erythroid 2-musculoaponeurotic fibrosarcoma oncogene homolog (NFE2-MAF) binding sites which play important roles in selecting AIRE target genes (5). In addition to AIRE, approximately 400 other TRAs are regulated by forebrain embryonic zinc finger-like protein 2 (Fezf2) (6), whereas approximately 1,000 TRAs are co-regulated by Fezf2 and AIRE or Fezf2 and chromodomain helicase DNA-binding protein 4 (Chd4) (1,7,8). Recent multi-omics studies have revealed TRA-related mechanisms. The fine classification and spatial proximity of post-AIRE mTECs have been reported (9,10). For example, neuroendocrine cells have been identified and located in close proximity to Hassall's corpuscles (9,10). Single-cell ATAC-seq has revealed that post AIRE mTECs possess diverse chromatin accessibility states. These cells, termed "mimetic cells", exhibit characteristics of peripheral tissues such as the skin, lung, liver, intestinal cells, and neuroendocrine cells (11,12), and can induce immune tolerance.

Histologic thymoma classification and its T cell differentiation potential

Histologic thymoma classification

A thymoma is a tumor composed of TECs and lymphocytes. Thymoma local extension and metastasis is generally described using the Masaoka-Koga Staging system. The recently introduced tumor, lymph nodes, metastasis (TNM) staging system is being used in parallel with the Masaoka-Koga system (13). Additionally, the histopathological classification follows the World Health Organization (WHO) system, which categorizes thymomas into types A, AB, B1, B2, and B3 based on epithelial cell characteristics and lymphocyte proportions.

T cell differentiation potential of thymoma

Most lymphocytes in thymomas are $CD4^+CD8^+$ double-positive (DP) T cells, whereas TCRαβ-positive $CD4^+$ SP and $CD8^+$ SP cells have also been identified in patients with thymomas. Tumor epithelial cells in thymomas have functions similar to those of normal TECs and induce the differentiation of bone marrow-derived T cell progenitors into $CD4^+$ SP and $CD8^+$ SP cells (14,15).

Thymoma and autoimmune diseases

Prevalence of autoimmune diseases associated with thymoma

Thymomas are frequently associated with myasthenia gravis (MG). Indeed, approximately 10–20% of patients with MG have thymomas, and MG is the most common autoimmune disease associated with thymomas (30–44%) (16). In terms of the frequency of MG according to histologic subtype, MG is rare in patients with type A, but relatively more common in those with type B2, accounting for 24–71% of cases. Type B1 and B3 account for 7–70% and 25–65% of cases, respectively (15,17). Thymomas are not only associated with MG but also with pure red cell aplasia (approximately 4%), Isaac's syndrome (approximately 3%), systemic lupus erythematosus (approximately 2%), hypo-γ-globulinemia, myositis, stiff-person syndrome, rippling muscle disease, Morvan's syndrome, dermatomyositis, encephalitis, Hashimoto's thyroiditis, Graves' disease, Cushing's syndrome, Addison's disease, type 1 diabetes, paraneoplastic pemphigus, colitis, hepatitis, rheumatoid arthritis, and Sjögren's syndrome (16,18,19).

Pathogenic mechanisms of autoimmune diseases associated with thymoma

Common tumor-related paraneoplastic autoimmune diseases, such as Lambert-Eaton Myasthenic syndrome associated with small cell lung carcinoma, possess autoantibodies that target autoantigens that are common to both tumor cells and target organs of autoimmunity (20). Given that the thymus was originally a tissue that expressed self-antigens, thymomas likely cause autoimmune diseases because of self-antigen expression (20,21). Indeed, thymoma-associated MG (TAMG) is sometimes accompanied by anti-striational and synaptic autoantibodies, whereas thymomas express muscle antigens such as titin and ryanodine receptors, as well as neural antigens such as gamma-aminobutyric acid (GABA) receptor and leucine-rich glioma inactivated 1 (LGI-1) protein (22,23). However, considering that autoimmune phenomena associated with thymomas occur at a notably high frequency (>50% compared to <5% in other tumors), mechanisms other than self-antigen expression within the thymoma microenvironment possibly contribute to autoimmunity induction (20). Many studies have focused on self-antigens and T cells in elucidating TAMG pathogenesis. The following sections provide an overview of these findings. We present this article in accordance with the Narrative Review reporting checklist (available at https://med.amegroups.com/article/view/10.21037/med-25-28/rc).

Methods

In this narrative review, we aimed to summarize and interpret the immunopathological mechanisms underlying TAMG, based on a selection of key published studies. We prioritized original research that contributed significantly to the understanding of self-antigen expression, T cell kinetics, and impaired negative selection in TAMG, including both classical findings and recent immunological insights.

In particular, we placed special emphasis on studies involving bioinformatic analysis. While a wide range of molecular and cellular investigations were reviewed, we focused our in-depth discussion on bulk RNA-sequencing (RNA-seq), single-cell RNA-seq (scRNA-seq), and spatial transcriptomic data obtained from our original studies of patients with TAMG. These data-driven approaches enabled us to identify novel cell populations and spatial niches that may be critical for MG onset in thymoma.

The selected studies were not systematically screened from all available literature but rather chosen based on their clinical relevance, mechanistic insight, and citation impact. Our goal was to provide a balanced and conceptually integrative view of TAMG pathogenesis, supported by both historical and state-of-the-art data (*Table 1*).

Results

Autoantigen expression

The acetylcholine receptor (AChR) is the target antigen in MG (24). In MG with thymic hyperplasia, thymic myoid cells express fetal and adult-type AChRs (25-27). However, thymomas do not contain myoid cells (28); thus, the precise nature of the target antigens in thymomas continues to be debated. Neoplastic epithelial cells express various AChR subunits but not whole receptors (29-31). Due to the lack of strong evidence that the AChR itself acts as an autoantigen in thymomas, the mechanism of molecular mimicry has also been investigated. Midsize neurofilament (NF-M) overexpression within the neoplastic epithelial cells of type B thymomas (32) and five identical, repetitive AChR-like epitopes on NF-M recognized by monoclonal anti-AChR antibody have been demonstrated (33). NF-Ms have also been found to be expressed and share epitopes with titin (32). Therefore, T cells from patients with TAMG react to NF-

Table 1 Search strategy summary

Items	Specification
Date of search	March 31, 2025
Database and other source searched	PubMed and Google Scholar
Search terms used	"Thymoma", "myasthenia gravis", "TAMG", "thymus", "autoimmune disease", "single-cell RNA-seq", "spatial transcriptome", and "T cell"
Timeframe	Up to March 31, 2025
Inclusion and exclusion criteria	All English language articles, including original full-length articles and review articles were included. Articles that did not provide information on TAMG or the thymus were excluded
Selection process	All articles selected according to the predefined inclusion and exclusion criteria were independently reviewed by all authors. Consensus was reached after discussion based on these criteria

RNA-seq, RNA-sequencing; TAMG, thymoma-associated myasthenia gravis.

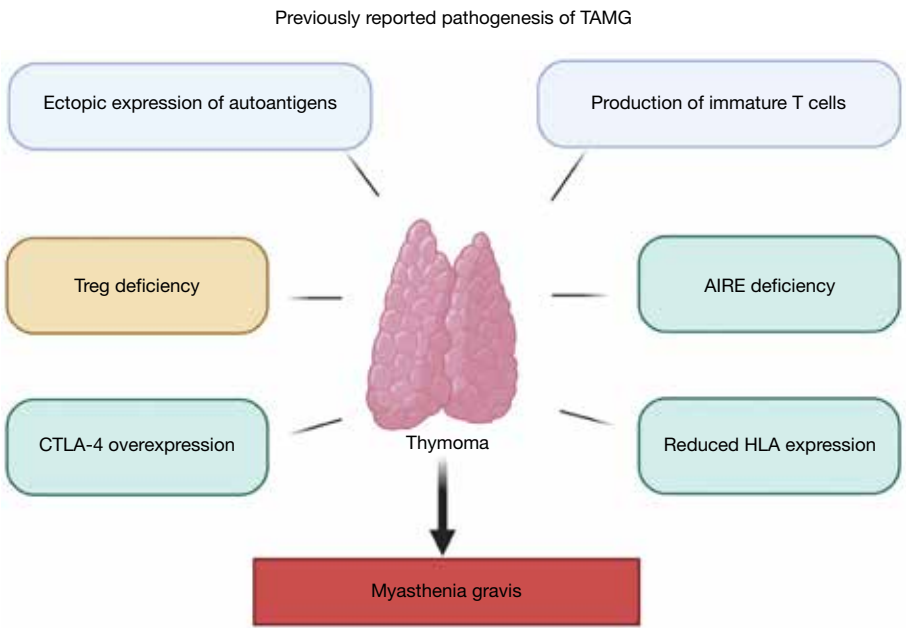

Figure 1 Previously reported pathogenesis of TAMG. Several factors have been implicated in TAMG pathogenesis, including ectopic expression of autoantigens in thymomas, immature T cell production, Treg decrease, and impaired negative selection due to AIRE deficiency, reduced HLA expression, and CTLA-4 overexpression. AIRE, autoimmune regulator; CTLA-4, cytotoxic T-lymphocyte antigen 4; HLA, human leukocyte antigen; TAMG, thymoma-associated myasthenia gravis.

Ms (33) and trigger an autoimmune response to muscular antigens, including AChR and titin (*Figure 1*) (34). Taken together, these observations indicate that, in thymomas, the mechanism of molecular mimicry may be more pivotal than the direct expression of the AChR itself. However, since the region of AChR that shares molecular homology with neurofilament is considered to be within its intracellular domain (33), intrathymic autoantigen expression alone is probably insufficient to fully explain the onset of TAMG.

Aberrant T cell kinetics in thymoma

T cell production in MG-associated thymoma

T cell kinetics have been extensively investigated in patients with TAMG. TCR excision circles (TRECs), which are circular DNA fragments formed during TCR

gene rearrangement in developing T cells within the thymus, have been examined as an indicator of recent thymic emigrants in patients with TAMG. The TREC levels in $CD4^+$ and $CD8^+$ peripheral blood lymphocytes in patients with TAMG are significantly higher than those in healthy individuals (14), indicating active thymic output and a robust generation of new T cells in patients with TAMG. Consistently, in contrast to thymomas without MG, MG-associated thymomas shed large numbers of mature $CD4^+CD45RA^+$ cells into the blood (*Figure 1*) (35). Moreover, thymic carcinomas (type C) that do not exhibit thymocyte proliferation rarely develop into MG (36). Collectively, these data indicate that robust T cell production from thymomas increases the likelihood of developing MG.

Dysregulated helper T cell differentiation in TAMG

The aberrant differentiation of effector helper T cells has been reported in patients with TAMG. Indeed, in these patients, the proportion of T follicular helper (TFH) cells ($CD4^+CXCR5^+$ T cells), which facilitate antibody production from B cells, was significantly higher than that in healthy controls and patients with thymomas without MG (37). In addition, the expression levels of TFH cell surface markers, such as C-X-C chemokine receptor type 5 (CXCR5), programmed cell death protein 1 (PD-1), inducible costimulatory molecule (ICOS), and the transcription factor B-cell lymphoma 6 protein (Bcl-6), were significantly elevated in thymomas from patients with MG compared to both control groups and patients with thymomas without MG. These molecules correlate with TFH cell functions and are involved in the pathogenesis of autoimmune diseases (38). Another study confirmed increased interleukin (IL)-21 and IL-4 production in TAMG, along with an increased proportion of peripheral helper T (Tph) cells in peripheral blood. In addition, increased ICOS expression and higher T helper type 17 (Th17) cells frequency were observed in both patients with TAMG and those with thymomas without MG (39). We performed scRNA-seq analysis of peripheral $CD4^+$ T cells from patients with autoimmune disease and demonstrated through meta-analysis that Th17 and T helper type 1 (Th1) cells are characteristic of MG (40). Regarding regulatory T cells (Tregs), the promotion of intratumoral $CD4^+CD25^+FoxP3^+$ Tregs in thymocytes was found to be reduced in thymomas [TAMG (+) and TAMG (–)] compared to normal thymus (*Figure 1*) (41,42). Taken together, these data indicate that patients with TAMG have dysregulated Th cell differentiation, which leads to autoantibody production.

Negative selection

Accumulating evidence suggests that negative selection is dysregulated in MG-associated thymomas. Although thymomas express a variety of autoantigens, AIRE expression is reduced in thymoma (43,44). Since both MG (+) and MG (–) thymomas show deficiencies in AIRE, AIRE deficiency alone is clearly insufficient to elicit MG (20). However, AIRE deficiency may impair negative selection, potentially contributing to MG development (*Figure 1*) (45,46). MHC class II molecules play an important role in the negative selection of thymocytes by presenting peptides. Many studies have reported that thymomas exhibit low levels of MHC class II molecules (1), whereas TECs exhibit MHC haploinsufficiency (1). These abnormalities may disrupt proper T cell development (*Figure 1*) (1,47-49). Genetic abnormalities that alter T cell activation have been reported in TAMG. Some patients with TAMG have gain-of-function mutations in cytotoxic T-lymphocyte antigen 4 (CTLA4) and protein tyrosine phosphatase non-receptor type 22 (PTNP22), suggesting their involvement in disease development (50-52). Signaling through CTLA4 and PTPN22 is generally immunosuppressive and prevents autoimmune diseases; however, in the thymus, it increases the risk of autoimmunity by inhibiting negative selection (*Figure 1*).

Working hypothesis on TAMG development and ongoing issues

Several hypotheses have been proposed to explain the mechanism of TAMG development. Based on findings regarding the loss of self-tolerance in TAMG, Shelly *et al.* posited 'The immature T cell theory' hypothesis, which states that, in thymoma, thymocytes are immature and develop MG because they do not have sufficient self-tolerance (53). Marx *et al.* integrated findings from thymoma and peripheral immunity data in TAMG and proposed a pathway from thymoma to the onset of MG. According to their hypothesis, naïve effector T cells that fail to acquire self-tolerance are exported from thymomas without undergoing appropriate negative selection (20). When these T cells encounter relevant epitopes presented by antigen-presenting cells outside the thymus, they become activated, potentially triggering autoantibody production through B cell stimulation.

These hypotheses have been derived from studies focusing

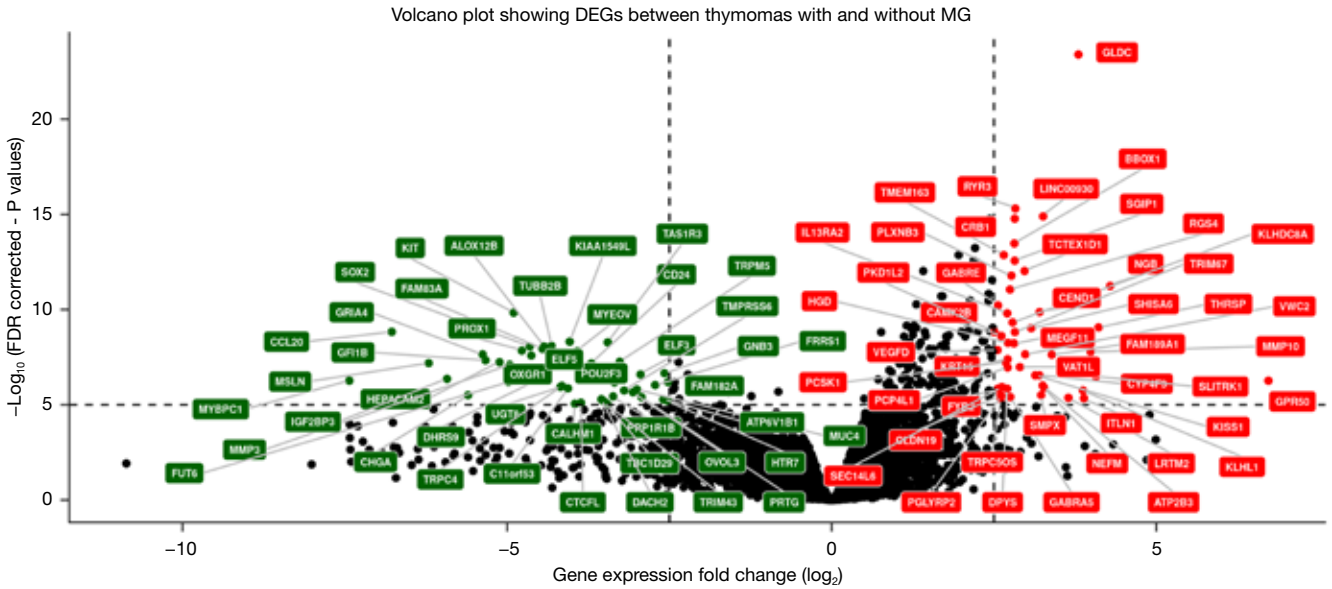

Figure 2 Gene expression signature of MG-associated thymoma identified using bulk RNA-seq. Volcano plot displaying DEGs between thymomas with and without MG based on bulk RNA-seq analysis of open data source. Red and green dots indicate significantly upregulated and downregulated genes in MG, respectively (FDR corrected P<1e−5 and |$\log_2$fold change| >2.5). Black dots represent genes that did not show significant differential expression. Representative MG-related genes including NF-M, RYR3, and GABRA5 were among the upregulated genes (56). DEG, differentially expressed gene; FDR, false discovery rate; GABA, gamma-aminobutyric acid; GABRA5, GABA receptor 5; MG, myasthenia gravis; NF-M, midsize neurofilament; RNA-seq, RNA-sequencing; RYR3, ryanodine receptor 3.

on specific molecules, cells, or signaling pathways involved in TAMG. However, they are largely based on targeted observations and do not necessarily represent an unbiased sampling of the highly heterogeneous cellular composition within thymomas. As such, it remains possible that key cellular players or pathogenic mechanisms have been overlooked.

To comprehensively elucidate the pathogenesis of TAMG, high-resolution, data-driven, and unbiased approaches are needed to capture the full complexity of the thymoma microenvironment. scRNA-seq is essential for a thorough understanding of the mechanisms underlying thymoma development (54,55). These techniques have the potential to provide an unbiased analysis and landscape of the complex process involved in MG pathogenesis in thymoma. Here, we attempted to introduce our recent data regarding TAMG by using a bioinformatic approach.

Application of bioinformatic analysis for MG-associated thymoma

scRNA-seq for thymoma: neuromuscular mTEC (nmTEC) identification using multi-omics analysis

Initially, we re-analyzed publicly available thymoma datasets, particularly focusing on The Cancer Genome Atlas (TCGA) dataset, which includes bulk RNA-seq data from 116 thymoma cases annotated with MG status and histologic classifications. By comparing the gene expression profiles of MG-associated and non-MG-associated thymomas, we identified MG-specific differentially expressed genes, including ryanodine receptors, GABA receptors, glycine receptors, and neurofilaments (*Figure 2*). These proteins have previously been implicated as target antigens in thymoma-associated autoimmune neuromuscular diseases (18,56).

To identify specific cell populations expressing MG-related molecules, we performed scRNA-seq on thymoma and peripheral blood mononuclear cell samples obtained from four patients with TAMG (*Figure 3A*). This analysis revealed a previously uncharacterized TEC subset that was distinct from known subsets (*Figure 3A*). Although this novel cell subset did not express AIRE, immunohistochemical analysis confirmed specific expression of neuromuscular antigens such as neurofilaments and GABA receptors at the protein level (*Figure 3B*). We termed this novel cell population "nmTECs" (*Figure 3A*) (56).

Gene set enrichment analysis (GSEA) suggested that

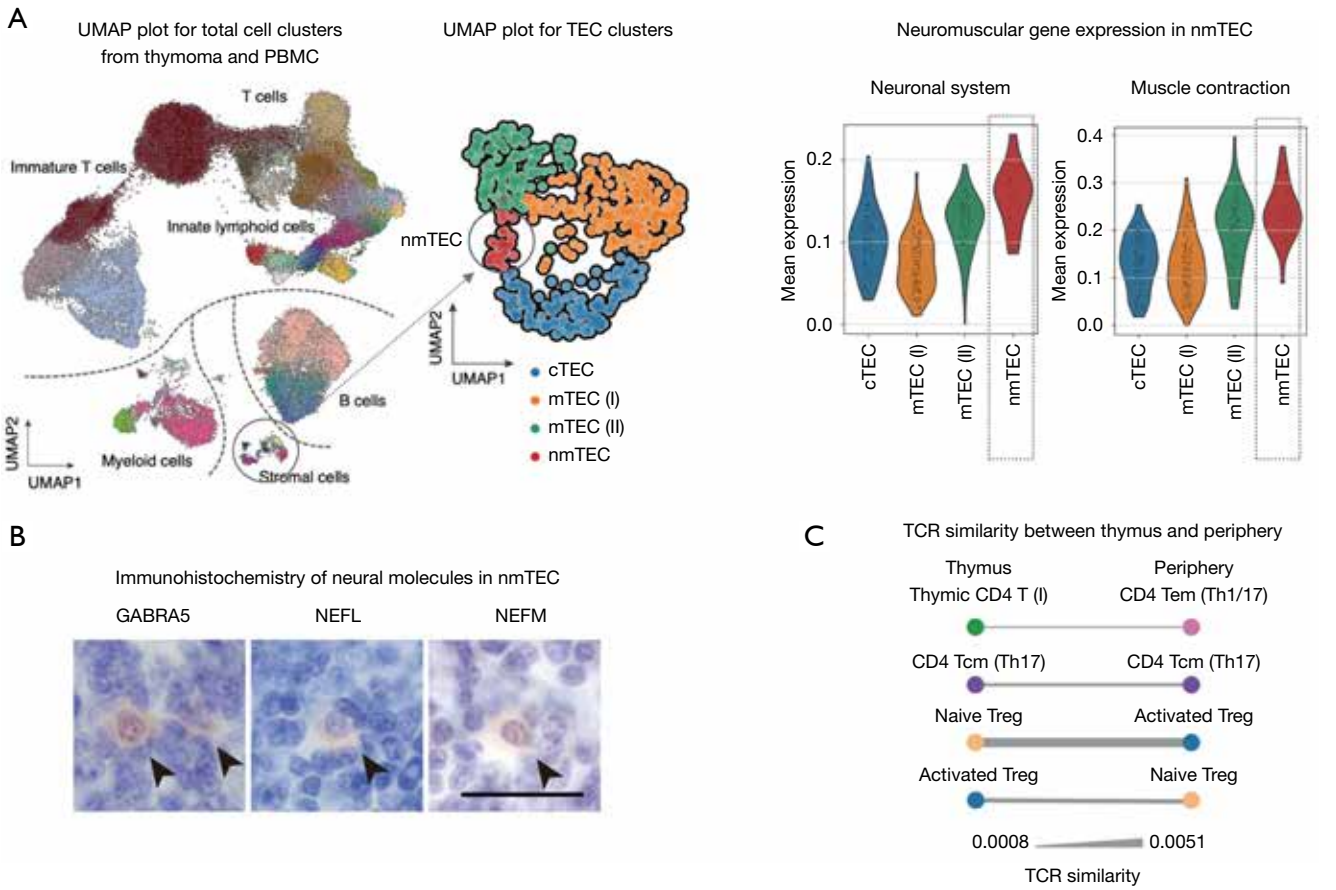

Figure 3 scRNA-seq analysis revealed that MG-specific molecules are neuromuscular antigens expressed in nmTECs. (A) UMAP plot (left) showing the distribution of 65,935 cells obtained from thymoma tissue and PBMCs of four anti-AChR antibody-positive patients, identifying 49 transcriptionally distinct clusters, including T cells, B cells, innate lymphoid cells, myeloid cells, stromal cells, and TECs. UMAP plot (middle) shows subclustering of TECs including a novel cluster of nmTECs. Violin plots (right) depict the mean expression levels of REACTOME pathway gene sets related to the neuronal (left) and muscular (right) system across TEC subsets. nmTECs exhibited unique upregulation of neuromuscular gene programs compared to other TEC populations. (B) Immunostaining confirmed that neuromuscular antigens such as NF and GABA receptor are present at the protein level in thymoma. Scale bar: 20 μm. The black arrows indicate the stained regions. (C) TCR similarity between peripheral blood and thymoma. The thickness of edges represents TCR similarity. This figure was reproduced from Yasumizu *et al.* (56). AChR, acetylcholine receptor; cTECs, cortical TECs; GABA, gamma-aminobutyric acid; GABRA5, GABA receptor 5; MG, myasthenia gravis; mTECs, medullary TECs; NEFL, neurofilament light chain; NEFM, neurofilament medium chain; NF, neurofilament; nmTECs, neuromuscular medullary TECs; PBMCs, peripheral blood mononuclear cells; RNA-seq, RNA-sequencing; scRNA-seq, single-cell RNA-seq; Tcm, central memory T cells; TCR, T cell receptor; TECs, thymic epithelial cells; Tem, effector memory T cells; Th1, T helper type 1; Th17, T helper type 17; Treg, regulatory T cell; UMAP, Uniform Manifold Approximation and Projection.

nmTECs are actively involved in antigen processing and presentation through both MHC class I and II pathways, indicating that they play a significant role in the induction of TAMG and other thymoma-associated autoimmune neuromuscular diseases (56). Furthermore, nmTECs showed strong interactions with lymphocytes, monocytes, and DCs, highlighting their potential key role in MG pathogenesis (56). In addition, C-X-C motif chemokine ligand 12 (CXCL12), a chemokine critical for angiogenesis and lymphocyte recruitment, was highly expressed in nmTECs, whereas its receptor C-X-C chemokine receptor type 4 (CXCR4) was identified in thymic B cells, TFH

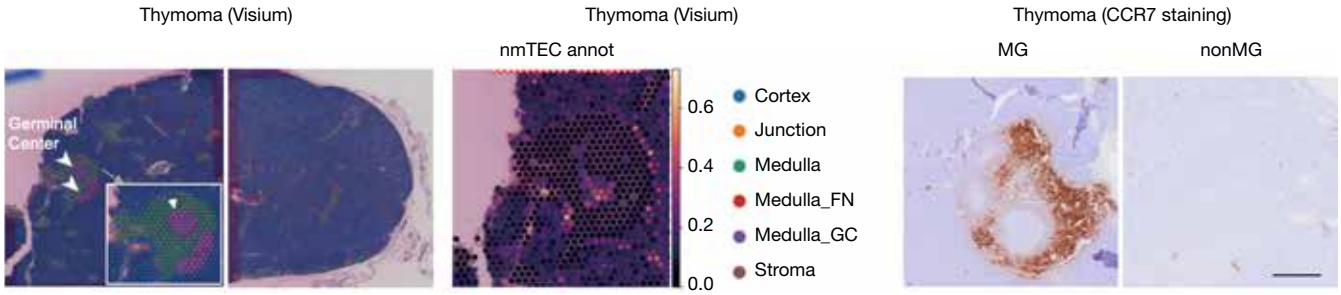

Figure 4 Spatial transcriptomic profiling and Immunostaining of thymomas with or without MG. FFPE sections from thymomas were analyzed using the CytAssist Visium spatial transcriptomics platform and immunostaining. The left and middle are Visium-based spatial transcriptome maps annotated by Leiden clustering and spatial domain classification, and the right shows immunostaining for CCR7. Spots are colored according to tissue regions: cortex (blue), junction (orange), medulla (green), medulla_FN (medulla-specific clusters characterized by FN1 expression) (red), medulla_GC (purple), and stroma (brown). Thymomas are primarily composed of cortical regions with reduced medullary areas. MG-associated thymomas (anti-AChR antibody positive) show relatively enlarged medullary regions located at the periphery and contain ectopic GC-like structures (arrowheads). Spatial domain annotation and nmTEC prediction indicate that nmTECs are enriched at the boundary between cortex and medulla. This figure was reproduced from Yasumizu *et al.* (57). Immunostaining for CCR7, a medullary marker, revealed that MG-associated type B1 thymomas had significantly larger medullae than those without MG. Scale bar: 500 μm. AChR, acetylcholine receptor; CCR7, C-C chemokine receptor type 7; FFPE, formalin-fixed, paraffin-embedded; FN, fibronectin; GC, germinal center; MG, myasthenia gravis; nmTECs, neuromuscular medullary TECs; TECs, thymic epithelial cells.

cells, and Tregs (56). These findings suggest that nmTECs contribute to distinct thymoma microenvironment formation that promotes immune cell recruitment and activation within tumors (56).

We also observed TFH cells and germinal center (GC) B cells within thymomas, along with evidence of B cell activation and differentiation of naive B cells into GC B, memory B, and plasma cells (56). Interestingly, when we analyzed TCR similarity between the thymus and the periphery for each cluster, we found that T cells, including Tregs, displayed high levels of TCR similarity (*Figure 3C*).

These findings suggest that antigen presentation by nmTECs, modulated by extrathymomal $CD4^+$ T cells, may initiate an immune response within the thymoma that ultimately leads to autoantibody production. Thus, nmTECs appear to not only present antigens but also to actively shape a microenvironment that facilitates lymphocyte recruitment and antibody production within thymomas (56).

Spatial transcriptomics for thymoma: localization and associated niche of nmTECs

To visualize the autoimmune responses in the TAMG, we used spatial transcriptome analysis on paraffin-embedded thymoma sections, which allowed for the collection of spatially resolved messenger RNA expression data. This approach facilitated clustering of the cortical, medullary, and border regions, validating the distinct structural organization observed in the thymic tissue. Comparative analyses revealed structural differences between the normal thymus, MG-associated thymoma, and non-MG thymomas. In the normal thymus, the cortex is located peripherally and surrounds a large central medulla. However, in type B1 MG-associated thymomas, the medullary region was enlarged and located peripherally compared to non-MG thymomas (*Figure 4*). C-C chemokine receptor type 7 (CCR7) staining, a medullary marker, confirmed that the medullary regions were enlarged in MG-associated type B1 thymomas compared to non-MG thymomas (*Figure 4*). These observations led us to hypothesize that disruption of the corticomedullary architecture and significant medullary expansion are critical for autoimmune responses. The medulla harbors disease susceptibility genes, as identified by genome-wide association studies, suggesting that it is a key site for autoimmune activation in MG (57).

Finally, we investigated the spatial localization of nmTECs. These cells were identified at the corticomedullary junction, a region that is abundant in DP ($CD4^+CD8^+$) T cells (*Figure 4*) (57). Chemokine expression patterns in thymomas closely resemble those in the normal thymus (57), suggesting that DP cells may be activated by neuromuscular antigens and subsequently migrate to the medulla. The

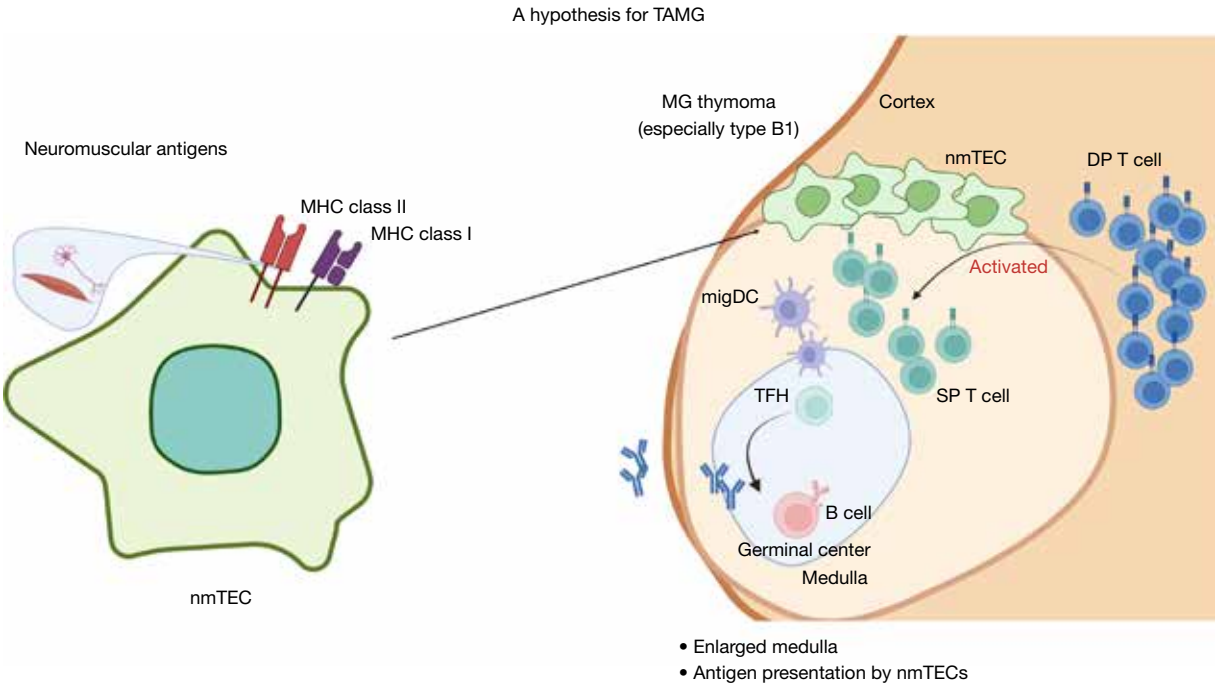

Figure 5 Graphical abstract. This schematic summarizes the spatial immunopathology of MG-associated thymoma. In seropositive cases, the medullary region is relatively enlarged and structurally remodeled. At the cortico-medullary junction, nmTECs expressing neuromuscular autoantigens are enriched and may contribute to the development of autoreactive T cells. Ectopic lymphoid structures are observed in the medulla, where TFH, dendric, and B cells interact, potentially driving autoantibody production. DP, double-positive; MG, myasthenia gravis; MHC, major histocompatibility complex; nmTECs, neuromuscular medullary TECs; SP, single-positive; TAMG, thymoma-associated myasthenia gravis; TECs, thymic epithelial cells; TFH, T follicular helper.

adjacent areas contained antigen-presenting DCs, effector T cells, including TFH and antibody-producing B cells. These findings suggest that the cascade from antigen presentation to autoantibody production is initiated in the medulla adjacent to nmTECs (*Figure 5*) (57).

Conclusions

By integrating bulk RNA-seq, scRNA-seq, spatial transcriptome analysis, pathological information, and clinical information related to thymomas, we found that TECs expressing neuromuscular antigens and medullary structures may be involved in TAMG pathogenesis. The medullary-like structures were larger in MG-associated type B1 thymomas than in non-MG-associated B1 thymomas, suggesting that the involvement of nmTECs and adjacent medullary structures may be particularly important in type B1 TAMG development. However, there was no significant difference in the area of medullary-like structures between cases with and without MG, despite the presence of nmTECs in type B2 thymomas. Therefore, microenvironments other than medullary-like structures may contribute to MG development in type B2 thymomas, highlighting the need for further studies to identify them.

Bioinformatic methods have the potential to comprehensively capture the thymoma microenvironment, which cannot be analyzed by conventional pathological examination or flow cytometry. Given that such research approaches are conducted in combination with conventional pathological examination and immune cell analysis, new discoveries will be made.

Acknowledgments

Figure 3 is reproduced from the article "Myasthenia gravis-specific aberrant neuromuscular gene expression by medullary thymic epithelial cells in thymoma" by Yasuimizu *et al.*, published in *Nature Communications* [2022], licensed under a Creative Commons Attribution 4.0 International

Footnote

Provenance and Peer Review: This article was commissioned by the Guest Editor (Malgorzata Szolkowska) for "The Series Dedicated to the 14th International Thymic Malignancy Interest Group Annual Meeting (ITMIG 2024)" published in *Mediastinum*. The article has undergone external peer review.

Reporting Checklist: The authors have completed the Narrative Review reporting checklist. Available at https://med.amegroups.com/article/view/10.21037/med-25-28/rc

Peer Review File: Available at https://med.amegroups.com/article/view/10.21037/med-25-28/prf

Funding: This work was supported by JSPS KAKENHI (Nos. 23K27517 and 25H01863 to T.O.) and by AMED (No. 23gm1810003h0002 to A.K.).

Conflicts of Interest: All authors have completed the ICMJE uniform disclosure form (available at https://med.amegroups.com/article/view/10.21037/med-25-28/coif). "The Series Dedicated to the 14th International Thymic Malignancy Interest Group Annual Meeting (ITMIG 2024)" was commissioned by the editorial office without any funding or sponsorship. T.O. reported supports from JSPS KAKENHI (Nos. 23K27517 and 25H01863), and AMED (No. 23gm1810003h0002). The authors have no other conflicts of interest to declare.

Ethical Statement: The authors are accountable for all aspects of the work in ensuring that questions related to the accuracy or integrity of any part of the work are appropriately investigated and resolved.

References

1. Marx A, Yamada Y, Simon-Keller K, et al. Thymus and autoimmunity. Semin Immunopathol 2021;43:45-64.
2. Abramson J, Giraud M, Benoist C, et al. Aire's partners in the molecular control of immunological tolerance. Cell 2010;140:123-35.
3. Derbinski J, Schulte A, Kyewski B, et al. Promiscuous gene expression in medullary thymic epithelial cells mirrors the peripheral self. Nat Immunol 2001;2:1032-9.
4. Matsumoto M, Yoshida H, Tsuneyama K, et al. Revisiting Aire and tissue-restricted antigens at single-cell resolution. Front Immunol 2023;14:1176450.
5. Fang Y, Bansal K, Mostafavi S, et al. AIRE relies on Z-DNA to flag gene targets for thymic T cell tolerization. Nature 2024;628:400-7.
6. Kadouri N, Nevo S, Goldfarb Y, et al. Thymic epithelial cell heterogeneity: TEC by TEC. Nat Rev Immunol 2020;20:239-53.
7. Tomofuji Y, Takaba H, Suzuki HI, et al. Chd4 choreographs self-antigen expression for central immune tolerance. Nat Immunol 2020;21:892-901.
8. Takaba H, Morishita Y, Tomofuji Y, et al. Fezf2 Orchestrates a Thymic Program of Self-Antigen Expression for Immune Tolerance. Cell 2015;163:975-87.
9. Yayon N, Kedlian VR, Boehme L, et al. A spatial human thymus cell atlas mapped to a continuous tissue axis. Nature 2024;635:708-18.
10. Bautista JL, Cramer NT, Miller CN, et al. Single-cell transcriptional profiling of human thymic stroma uncovers novel cellular heterogeneity in the thymic medulla. Nat Commun 2021;12:1096.
11. Michelson DA, Hase K, Kaisho T, et al. Thymic epithelial cells co-opt lineage-defining transcription factors to eliminate autoreactive T cells. Cell 2022;185:2542-2558.e18.
12. Givony T, Leshkowitz D, Del Castillo D, et al. Thymic mimetic cells function beyond self-tolerance. Nature 2023;622:164-72.
13. Detterbeck FC, Nicholson AG, Kondo K, et al. The Masaoka-Koga stage classification for thymic malignancies: clarification and definition of terms. J Thorac Oncol

2011;6:S1710-6.
14. Buckley C, Douek D, Newsom-Davis J, et al. Mature, long-lived CD4+ and CD8+ T cells are generated by the thymoma in myasthenia gravis. Ann Neurol 2001;50:64-72.
15. Okumura M, Fujii Y, Shiono H, et al. Immunological function of thymoma and pathogenesis of paraneoplastic myasthenia gravis. Gen Thorac Cardiovasc Surg 2008;56:143-50.
16. Marx A, Willcox N, Leite MI, et al. Thymoma and paraneoplastic myasthenia gravis. Autoimmunity 2010;43:413-27.
17. Marx A, Ströbel P, Weis CA. The pathology of the thymus in myasthenia gravis. Mediastinum 2018;2:66.
18. Zekeridou A, McKeon A, Lennon VA. Frequency of Synaptic Autoantibody Accompaniments and Neurological Manifestations of Thymoma. JAMA Neurol 2016;73:853-9.
19. Blum TG, Misch D, Kollmeier J, et al. Autoimmune disorders and paraneoplastic syndromes in thymoma. J Thorac Dis 2020;12:7571-90.
20. Marx A, Porubsky S, Belharazem D, et al. Thymoma related myasthenia gravis in humans and potential animal models. Exp Neurol 2015;270:55-65.
21. Wolff AS, Kärner J, Owe JF, et al. Clinical and serologic parallels to APS-I in patients with thymomas and autoantigen transcripts in their tumors. J Immunol 2014;193:3880-90.
22. Romi F, Bø L, Skeie GO, et al. Titin and ryanodine receptor epitopes are expressed in cortical thymoma along with costimulatory molecules. J Neuroimmunol 2002;128:82-9.
23. Simabukuro MM, Petit-Pedrol M, Castro LH, et al. GABAA receptor and LGI1 antibody encephalitis in a patient with thymoma. Neurol Neuroimmunol Neuroinflamm 2015;2:e73.
24. Marx A, Kirchner T, Hoppe F, et al. Proteins with epitopes of the acetylcholine receptor in epithelial cell cultures of thymomas in myasthenia gravis. Am J Pathol 1989;134:865-77.
25. Curnow J, Corlett L, Willcox N, et al. Presentation by myoblasts of an epitope from endogenous acetylcholine receptor indicates a potential role in the spreading of the immune response. J Neuroimmunol 2001;115:127-34.
26. Geuder KI, Marx A, Witzemann V, et al. Pathogenetic significance of fetal-type acetylcholine receptors on thymic myoid cells in myasthenia gravis. Dev Immunol 1992;2:69-75.
27. Schluep M, Willcox N, Vincent A, et al. Acetylcholine receptors in human thymic myoid cells in situ: an immunohistological study. Ann Neurol 1987;22:212-22.
28. Kirchner T, Hoppe F, Müller-Hermelink HK, et al. Acetylcholine receptor epitopes on epithelial cells of thymoma in myasthenia gravis. Lancet 1987;1:218.
29. Wilisch A, Gutsche S, Hoffacker V, et al. Association of acetylcholine receptor alpha-subunit gene expression in mixed thymoma with myasthenia gravis. Neurology 1999;52:1460-6.
30. Maclennan CA, Vincent A, Marx A, et al. Preferential expression of AChR epsilon-subunit in thymomas from patients with myasthenia gravis. J Neuroimmunol 2008;201-202:28-32.
31. Marx A, Pfister F, Schalke B, et al. The different roles of the thymus in the pathogenesis of the various myasthenia gravis subtypes. Autoimmun Rev 2013;12:875-84.
32. Marx A, Wilisch A, Schultz A, et al. Expression of neurofilaments and of a titin epitope in thymic epithelial tumors. Implications for the pathogenesis of myasthenia gravis. Am J Pathol 1996;148:1839-50.
33. Schultz A, Hoffacker V, Wilisch A, et al. Neurofilament is an autoantigenic determinant in myasthenia gravis. Ann Neurol 1999;46:167-75.
34. Sommer N, Willcox N, Harcourt GC, et al. Myasthenic thymus and thymoma are selectively enriched in acetylcholine receptor-reactive T cells. Ann Neurol 1990;28:312-9.
35. Ströbel P, Helmreich M, Menioudakis G, et al. Paraneoplastic myasthenia gravis correlates with generation of mature naive CD4(+) T cells in thymomas. Blood 2002;100:159-66.
36. Radovich M, Pickering CR, Felau I, et al. The Integrated Genomic Landscape of Thymic Epithelial Tumors. Cancer Cell 2018;33:244-258.e10.
37. Zhang M, Zhou Y, Guo J, et al. Thymic TFH cells involved in the pathogenesis of myasthenia gravis with thymoma. Exp Neurol 2014;254:200-5.
38. Song Y, Zhou L, Miao F, et al. Increased frequency of thymic T follicular helper cells in myasthenia gravis patients with thymoma. J Thorac Dis 2016;8:314-22.
39. Cebi M, Cakar A, Erdogdu E, et al. Thymoma patients with or without myasthenia gravis have increased Th17 cells, IL-17 production and ICOS expression. J Neuroimmunol 2023;381:578129.
40. Yasumizu Y, Takeuchi D, Morimoto R, et al. Single-cell transcriptome landscape of circulating CD4+ T cell populations in autoimmune diseases. Cell Genom. 2024;4:100473.

41. Scarpino S, Di Napoli A, Stoppacciaro A, et al. Expression of autoimmune regulator gene (AIRE) and T regulatory cells in human thymomas. Clin Exp Immunol 2007;149:504-12.
42. Ströbel P, Rosenwald A, Beyersdorf N, et al. Selective loss of regulatory T cells in thymomas. Ann Neurol 2004;56:901-4.
43. Ströbel P, Murumägi A, Klein R, et al. Deficiency of the autoimmune regulator AIRE in thymomas is insufficient to elicit autoimmune polyendocrinopathy syndrome type 1 (APS-1). J Pathol 2007;211:563-71.
44. Marx A, Hohenberger P, Hoffmann H, et al. The autoimmune regulator AIRE in thymoma biology: autoimmunity and beyond. J Thorac Oncol 2010;5:S266-72.
45. Sohn SJ, Thompson J, Winoto A. Apoptosis during negative selection of autoreactive thymocytes. Curr Opin Immunol 2007;19:510-5.
46. Ashby KM, Hogquist KA. A guide to thymic selection of T cells. Nat Rev Immunol 2024;24:103-17.
47. Inoue M, Okumura M, Miyoshi S, et al. Impaired expression of MHC class II molecules in response to interferon-gamma (IFN-gamma) on human thymoma neoplastic epithelial cells. Clin Exp Immunol 1999;117:1-7.
48. Ströbel P, Chuang WY, Chuvpilo S, et al. Common cellular and diverse genetic basis of thymoma-associated myasthenia gravis: role of MHC class II and AIRE genes and genetic polymorphisms. Ann N Y Acad Sci 2008;1132:143-56.
49. Zettl A, Ströbel P, Wagner K, et al. Recurrent genetic aberrations in thymoma and thymic carcinoma. Am J Pathol 2000;157:257-66.
50. Zheng K, Zhang J, Zhang P, et al. PTPN22 and CTLA-4 gene polymorphisms in resected thymomas and thymus for myasthenia gravis. Thorac Cancer 2012;3:307-12.
51. Chuang WY, Ströbel P, Belharazem D, et al. The PTPN22gain-of-function+1858T(+) genotypes correlate with low IL-2 expression in thymomas and predispose to myasthenia gravis. Genes Immun 2009;10:667-72.
52. Chuang WY, Ströbel P, Gold R, et al. A CTLA4high genotype is associated with myasthenia gravis in thymoma patients. Ann Neurol 2005;58:644-8.
53. Shelly S, Agmon-Levin N, Altman A, et al. Thymoma and autoimmunity. Cell Mol Immunol 2011;8:199-202.
54. Nabel CS, Ackman JB, Hung YP, et al. Single-Cell Sequencing Illuminates Thymic Development: An Updated Framework for Understanding Thymic Epithelial Tumors. Oncologist 2024;29:473-83.
55. Park JE, Botting RA, Domínguez Conde C, et al. A cell atlas of human thymic development defines T cell repertoire formation. Science 2020;367:eaay3224.
56. Yasumizu Y, Ohkura N, Murata H, et al. Myasthenia gravis-specific aberrant neuromuscular gene expression by medullary thymic epithelial cells in thymoma. Nat Commun 2022;13:4230.
57. Yasumizu Y, Kinoshita M, Zhang MJ, et al. Spatial transcriptomics elucidates medulla niche supporting germinal center response in myasthenia gravis-associated thymoma. Cell Rep 2024;43:114677.

doi: 10.21037/med-25-28
Cite this article as: Okuno T, Koizumi N, Yasumizu Y. Pathogenesis of thymoma-associated myasthenia gravis: a narrative review. Mediastinum 2025;9:26.

Review Article

Artificial intelligence for diagnosis and prognosis of thymic epithelial tumors: a systematic review

Anna Salut Esteve Domínguez[1]^, Marlou Dimmers[2], Ties A. Mulders[3], Daphne Dumoulin[2]^, Dirk De Ruysscher[4,5]^, Stephanie Peeters[4]^, Jan von der Thüsen[1]^, Farhan Akram[1]^

[1]Department of Pathology and Clinical Bioinformatics, Erasmus Medical Center, Rotterdam, The Netherlands; [2]Department of Respiratory Medicine, Erasmus Medical Center, Rotterdam, The Netherlands; [3]Department of Radiology and Nuclear Medicine, Erasmus Medical Center, Rotterdam, The Netherlands; [4]Department of Radiation Oncology (Maastro), GROW Research Institute for Oncology and Reproduction, Maastricht University Medical Centre+, Maastricht, The Netherlands; [5]Department of Radiotherapy, Erasmus MC Cancer Institute, Rotterdam, The Netherlands

Contributions: (I) Conception and design: AS Esteve Domínguez, J von der Thüsen, F Akram; (II) Administrative support: S Peeters, J von der Thüsen, F Akram; (III) Provision of study materials or patients: AS Esteve Domínguez, M Dimmers; (IV) Collection and assembly of data: AS Esteve Domínguez, M Dimmers, TA Mulders; (V) Data analysis and interpretation: AS Esteve Domínguez, M Dimmers, F Akram; (VI) Manuscript writing: All authors; (VII) Final approval of manuscript: All authors.

Correspondence to: Farhan Akram, PhD. Department of Pathology and Clinical Bioinformatics, Erasmus Medical Center, Dr. Molewaterplein 40, Rotterdam, GD 3015, The Netherlands. Email: f.akram@erasmusmc.nl.

Background: Thymic epithelial tumors (TETs) are rare, but they are the most common tumors in the anterior mediastinum. The use of artificial intelligence (AI) in the medical field is rapidly advancing. Especially in a rare disease such as TET, AI can help to improve existing care and foster new innovations. However, there are many different AI models with various implications. This systematic review aims to give an overview of recent studies on AI applications for the diagnosis and prognosis of TETs.

Methods: In this systematic review, six electronic databases were searched for research papers with the keywords “thymoma”, “thymic epithelial tumors”, “thymic carcinoma”, “artificial intelligence”, “machine learning” and “deep learning”. The screening was performed by two reviewers and conflicts were resolved by a third reviewer.

Results: After removal of duplicates, 582 articles were included. Of these, 65 articles were eligible for inclusion after screening. AI models are used mainly for distinguishing between different mediastinal tumor types (n=21), risk stratification (n=26), surgical planning (n=7) and for assisting in subtyping (n=4). For prognostic purposes, AI is used for predicting clinical outcome as well as the chance of metastasis or prognosis (n=7). Models using combined clinical and radiomics data performed better than models with a single type of data. Some of the AI models outperformed physicians or successfully supported physicians in their workflow.

Conclusions: Many AI models have been studied in the context of the diagnosis and prognosis of TETs. Even though results are promising, external validation is often lacking, and sample sizes are small. Therefore, most models are not yet ready for clinical implementation. Further research on AI models with larger datasets and external validation is necessary, with careful consideration of the risk of data leakage.

Keywords: Thymic epithelial tumors (TETs); artificial intelligence (AI); diagnosis; prognosis

Received: 05 June 2025; Accepted: 10 September 2025; Published online: 26 September 2025.
doi: 10.21037/med-25-34
View this article at: https://dx.doi.org/10.21037/med-25-34

^ ORCID: Anna Salut Esteve Domínguez, 0000-0001-5409-5410; Daphne Dumoulin, 0000-0001-5578-7902; Dirk De Ruysscher, 0000-0002-1214-3557; Stephanie Peeters, 0000-0003-0128-3121; Jan von der Thüsen, 0000-0001-9699-4860; Farhan Akram, 0000-0003-4109-2645.

Introduction

Thymic epithelial tumors (TETs)

TETs are rare neoplasms of the thymus gland, yet represent the most common primary tumors of the prevascular mediastinum, with an incidence of 0.23–0.3 per 100,000 persons annually (1,2). The main subtypes include thymomas, thymic carcinomas (TCs), and thymic neuroendocrine tumors (NETs) (3). Diagnosis of TETs is rapidly evolving. The World Health Organization (WHO) established a TET classification system in 1999 (4), with subsequent refinements aimed at reducing interobserver variability (5-8).

Diagnostic workflow

TETs may present with clinical symptoms such as cough, chest pain, and dyspnea, or with paraneoplastic syndromes (e.g., myasthenia gravis), but are frequently asymptomatic and discovered incidentally on chest imaging (9). When a mediastinal mass is found, radiologic imaging distinguishes malignant lesions from benign conditions like thymic hyperplasia (10). Contrast-enhanced computed tomography (CT) scans provide details on tumor characteristics and local spread; magnetic resonance imaging (MRI) can further aid in differentiating benign from malignant thymic lesions, particularly for cystic lesions (11). Positron emission tomography with fluorodeoxyglucose (FDG-PET) assesses metabolic activity and aids evaluation of tumor aggressiveness (11,12).

Despite being highly informative, radiological tests often cannot provide a definitive diagnosis because imaging features frequently overlap between tumor types and non-thymic lesions. Therefore, histopathological analysis through needle biopsy, mediastinoscopy, or surgical resection is essential for diagnosis, classification, and biological assessment (13).

Histological subtyping

Following tissue sampling, subtyping per WHO classification is critical. Thymomas are categorized as A, AB, B1, B2, or B3 (*Figure 1*), based on epithelial cell morphology and lymphocyte proportions (13). TC is a separate, more aggressive subtype, spanning well-differentiated to poorly-differentiated categories (1,14-17).

Subtyping plays a vital role in guiding treatment decisions (10). Type A, AB and B1 thymomas are generally indolent, whereas types B2, B3 and TC are associated with more aggressive clinical courses and higher rates of invasion and recurrence (18). Histology also guides staging, as more aggressive histologies correlate with higher Masaoka-Koga or traditional tumor-nodes-metastasis (TNM) stages (19,20). Furthermore, it guides decisions regarding adjuvant therapies and postoperative surveillance. Therefore, expert pathological assessment remains essential (10).

However, subtyping remains subjective, with significant interobserver variability, notably for subtypes B1 and B2 (4,21). These challenges underscore the potential value of AI in improving diagnostic consistency.

Preoperative diagnosis

For suspected TET cases, a detailed and accurate preoperative diagnostic evaluation is essential for selecting the optimal treatment. This evaluation aims to distinguish benign (non-cancerous) growths from malignant neoplasms, which are cancerous growths that can invade nearby tissues and spread. It is also important to determine whether the tumor originates from the thymus gland or another mediastinal structure. Furthermore, classifying patients by tumor type and risk level, such as low-risk (A, AB, B1) or high-risk (B2, B3, TC), is critical for accurate staging and guiding subsequent treatment. This is especially important because thymomas and TCs are distinct tumors that require different management approaches (10,22).

Highlight box

Key findings

- Artificial intelligence (AI) models for thymic epithelial tumors (TETs) mainly target diagnosis (tumor type, risk stratification, surgical planning, subtyping) and prognosis (outcome, metastasis prediction), with risk stratification most studied.
- Combining clinical and radiomics data boosts performance; some AI tools outperform or support physicians effectively.

What is known and what is new?

- TETs are rare but the most common anterior mediastinal tumors; AI shows promise in rare disease imaging.
- About 65 studies focus on AI for TET diagnosis and prognosis, highlighting the benefits of multi-modal data integration.
- Challenges include small sample sizes, lack of external validation, and risks of data leakage.

What is the implication, and what should change now?

- Larger datasets and rigorous external validation are crucial for clinical adoption.
- Standardization and preventing data leakage must be prioritized to ensure reliable, explainable, generalizable AI models for TET care.

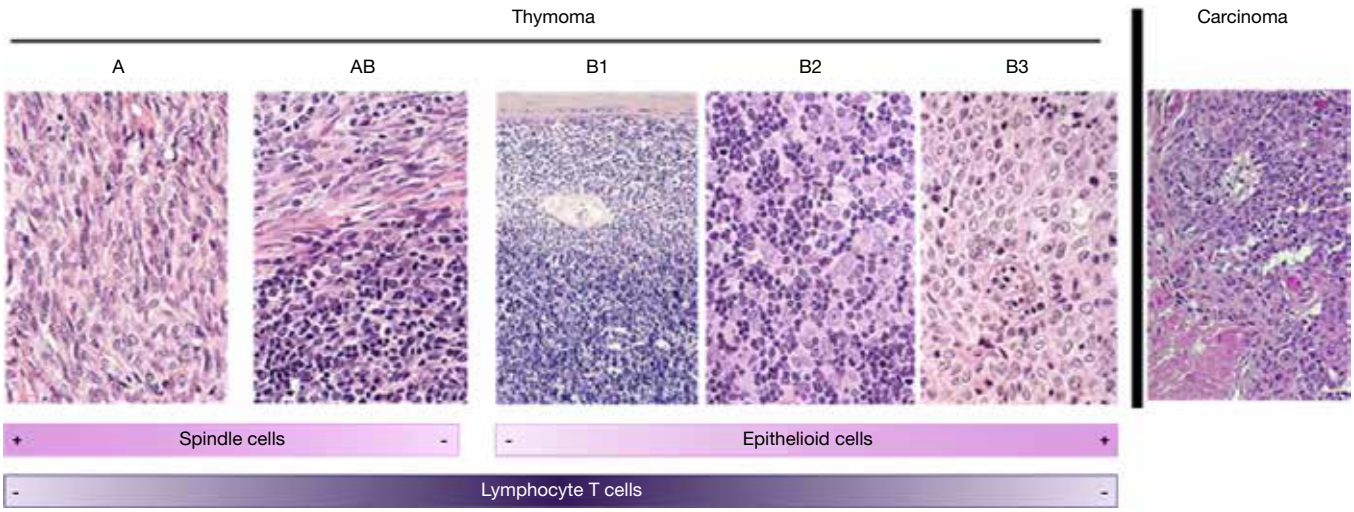

Figure 1 Different subsets of TETs, classified according to the WHO classification (H&E, magnification 10×). TET, thymic epithelial tumor; WHO, World Health Organization.

Artificial intelligence (AI) in medicine

AI is now integral to healthcare, excelling at analyzing large datasets for pattern recognition, prediction, and decision support, and driving innovation in diagnostics and patient management across multiple domains.

AI methodologies

Machine learning (ML)

ML utilizes large datasets to uncover complex relationships and classify or predict outcomes without explicit rules. Techniques include support vector machines (SVM), random forests (RF), and gradient boosting (GB).

Deep learning (DL)

A subset of ML based on artificial neural networks (ANNs), particularly convolutional neural networks (CNNs), which excel at image recognition and classification, making them especially useful in radiology and pathology.

Types of data

In general, AI models in medicine utilize:

(I) Clinical data: a detailed list of information about patients, including details such as age, medical history, laboratory tests, and treatment outcomes.

(II) Pathology data: it includes whole slide images of tissue samples, details of the staining procedure, and molecular analysis results.

(III) Radiomics data: focuses on extracting quantitative features like texture, shape, and intensity from medical images.

(IV) Omics data: provides molecular-level insights into diseases, aiding biomarker discovery and the development of targeted therapies.

Types of clinical goal

(I) Diagnostic support: AI models improve neoplasm detection and characterization through modalities such as CT and MRI. Integrating clinical, radiomics, and pathology data enhances diagnostic precision and informs personalized treatment.

(II) Outcome prediction: models predict disease progression, response, recurrence risk, and survival, supporting individualized therapeutic strategies.

AI for TET diagnosis and prognosis

Given the diagnostic challenges of TETs, including radiologic ambiguity, heterogeneity, and limited risk stratification, AI is well-positioned to:

(I) Enhance preoperative risk and stage assessment using radiologic data;

(II) Detect tumor invasiveness and metastatic potential;

(III) Predict prognosis, including recurrence, survival, and treatment response;

(IV) Reduce variability in histopathologic classification;

(V) Integrate multimodal data for personalized management.

AI-enhanced diagnostic and prognostic pathways support earlier intervention, more precise treatment selection, and

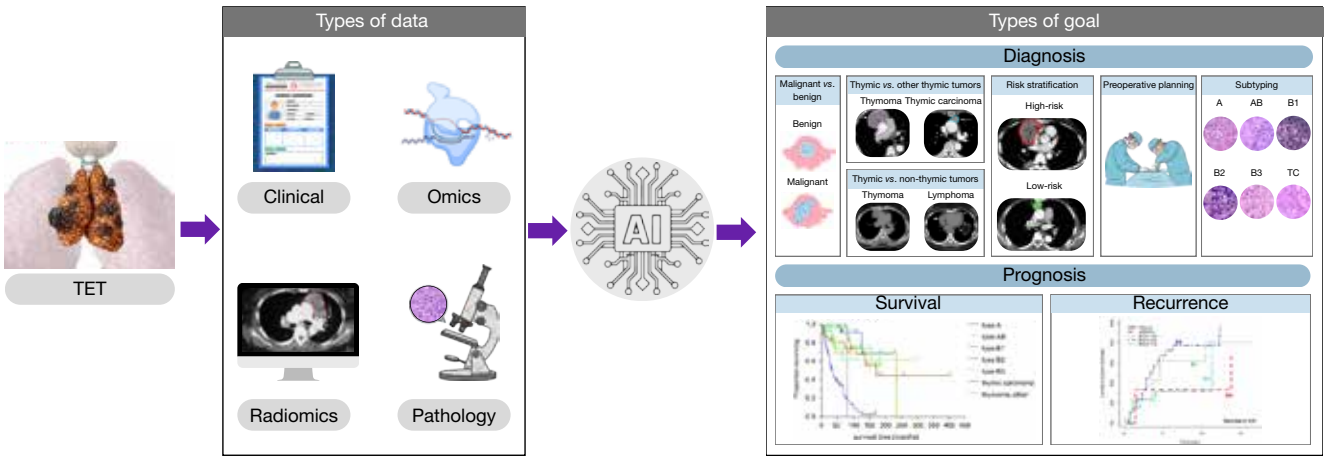

Figure 2 Pipeline illustrating TET analysis using clinical, radiology, pathology, omics, or combined multi-omics data. It includes diagnosis (tumor type, risk stratification, surgical planning, subtyping) and prognosis (recurrence, survival). TET, thymic epithelial tumor.

better overall patient outcomes and quality of life. *Figure 2* illustrates the overall framework used for analyzing TETs, incorporating clinical, radiological, pathological, omics, and integrated multi-omics data for diagnosis and prognosis.

Objectives of the systematic review

With significant advances in oncology diagnostics and prognostics, this review assesses the current state-of-the-art AI applications in TET diagnosis and prognosis. The review is guided by questions addressing: to guide this systematic review, the following key research questions were formulated.

(I) AI methodologies and diagnostic accuracy (ACC):
  (i) Which AI methods (DL, ML, radiomics) are used for TET diagnosis?
  (ii) How have AI-based risk tools influenced preoperative decisions, treatment planning and prognostic counseling?
  (iii) How does AI performance compare to traditional clinical and expert methods?

(II) Prognostic and predictive modeling: how accurately do AI models predict clinical outcomes such as stage, invasiveness, recurrence, metastasis, and survival?

(III) Methodological limitations and challenges:
  (i) What challenges (dataset limitations, overfitting, lack of validation, interpretability) exist in current AI models?
  (ii) Are there performance differences across TET subtypes or imaging modalities?

(IV) Clinical integration and future directions:
  (i) What steps are needed for clinical adoption (validation, regulatory approval, workflow integration)?
  (ii) How might explainable AI (XAI) and multimodal data fusion increase clinical utility and acceptance?

We present this article in accordance with the PRISMA reporting checklist (available at https://med.amegroups.com/article/view/10.21037/med-25-34/rc).

Methods

Literature review

First, the study was registered in PROSPERO (CRD420251015861). Second, we defined the reviewers for the screening step. A.S.E.D., M.D. and T.A.M. were involved in the review. A comprehensive search strategy was developed and applied across six major databases: Medline (Ovid), Embase (Embase.com), Web of Science, Cochrane Central Register of Controlled Trials, Cumulative Index to Nursing and Allied Health Literature (CINAHL) Plus, and Google Scholar (via Publish or Perish). There were no date restrictions, allowing for the inclusion of all relevant literature up to March 2025.

Eligibility criteria and study selection

Search queries combined controlled vocabulary and free-text terms focused on TETs (e.g., "thymoma",

"thymic carcinoma", "thymic epithelial tumor") and AI methodologies (e.g., "artificial intelligence", "machine learning", "deep learning"). Duplicate entries were removed, resulting in 582 unique studies. Detailed information regarding search terminology for each database and corresponding search research results is provided in Appendix 1. Studies applying AI to TETs for diagnostic or prognostic purposes were included. The following exclusion criteria were applied:

(I) Studies not focused on TETs;
(II) Studies not employing AI methods;
(III) Studies unrelated to diagnosis or prognosis applications;
(IV) Abstract-only studies;
(V) Not a peer-reviewed research article;
(VI) Non-English language articles;
(VII) Studies not conducted on human subjects.

Data extraction

Screening was conducted using Rayyan software (23) by A.S.E.D., M.D. and T.A.M. First, titles and abstracts were screened by A.S.E.D. and M.D.; subsequently, full-text reviews were conducted independently by A.S.E.D. and M.D. Discrepancies were resolved through discussion with a third reviewer T.A.M.

Following the completion of the screening process, A.S.E.D. proceeded to extract data using the following variables: DOI, title, publication year, study aim (with focus on AI and TETs), diagnostic or prognostic objective, type and source of dataset, data availability, dataset link, dataset modality, staining type, sample type, number of samples, methods, AI technique (e.g., ML, DL), model type (e.g., supervised), and outcomes [e.g., area under the curve (AUC), ACC]. Limitations, findings, and contributions were also collected to prepare for the discussion.

Data synthesis

Due to substantial differences in AI applications, study designs, algorithms, patient cohorts, evaluation methods, and reported metrics, we chose a narrative synthesis over meta-analysis. This approach allows a more flexible and descriptive review of each study. It is particularly suitable for diagnostic ACC studies where patient groups and test conditions often vary, introducing heterogeneity and potential bias. Meta-analysis is generally discouraged in such cases. We also did not assess bias formally, as many studies provided insufficient methodological detail. In addition, there is no accepted reference standard for AI-based analysis of TETs.

Results

Literature search

The Preferred Reporting Items for Systematic Reviews and meta-analysis (PRISMA) flow diagram (*Figure 3*) illustrates the systematic search for studies on the use of TETs and AI for diagnosis and prognosis. The initial search yielded 998 records across the six databases mentioned above. After removing 416 duplicates, 582 unique records were screened by A.S.E.D. and M.D. A total of 132 full-text articles were assessed. According to the eligibility criteria, 54 studies were excluded, and 23 records resulted in disagreement between A.S.E.D. and M.D. T.A.M. selected 10 from these conflicting records. As a result, a total of 65 studies were selected for the final analysis.

Applications of AI methods for diagnosis

This section focuses on research studies utilizing AI for diagnosis. We have divided these studies into two categories: preoperative assessment and subtyping, according to the articles reviewed.

Preoperative assessment

The studies addressed significant diagnostic challenges, including the differentiation of benign from malignant lesions, the distinction between thymomas and other types of thymic or non-thymic tumors, risk stratification, and supporting surgical planning.

Malignant or benign

Ma *et al.* (24) designed a radiomics-based model using CT images of 100 patients (54 with benign lesions, 46 with malignant lesions). For feature extraction, the Least Absolute Shrinkage and Selection Operator (LASSO) algorithm was used. After feature selection, a Logistic Regression (LR) model was used for classification. The model achieved an ACC of 0.82 on the test set.

Mayoral *et al.* (25) analyzed 239 patients with 25 visual CT features and 101 radiomic features. They aimed to classify benign *vs.* malignant lesions, and thymoma *vs.* TC using three SVM models: one with conventional, one with radiomic, and one with combined features. The combined model performed best with an AUC of 0.71 for benign *vs.*

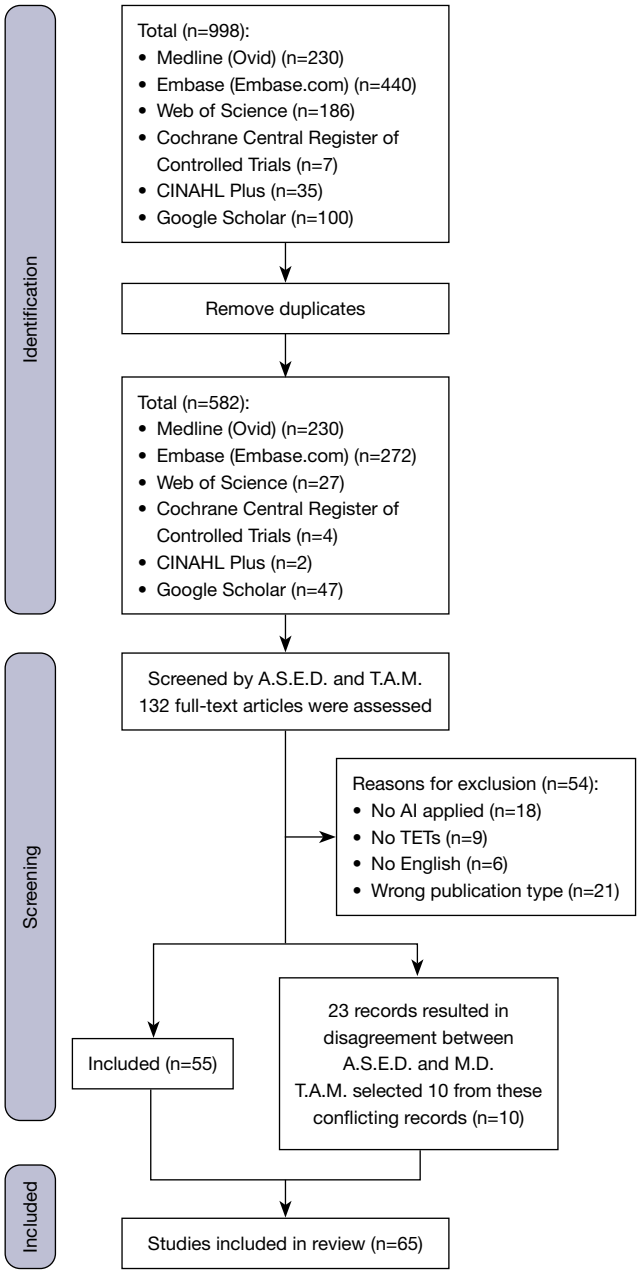

Figure 3 Flowchart of the study according to the PRISMA statement. AI, artificial intelligence; CINAHL, Cumulative Index to Nursing and Allied Health Literature; PRISMA, Preferred Reporting Items for Systematic Reviews and meta-analysis; TET, thymic epithelial tumor.

malignant, and 0.81 for thymoma *vs.* TC.

Thymomas vs. other thymic tumors

Thymic cysts are rare, typically benign lesions that require no intervention, whereas TETs are primarily treated with surgical removal. Differentiating between the two on imaging can be challenging, which is clinically important. Recent studies have explored the application of AI to improve diagnostic ACC using radiomics and DL on contrast-enhanced CT scans.

Yang *et al.* (26,27) conducted multicenter studies using deep transfer learning (DTL) and clinical-radiomics models to distinguish thymomas from thymic cysts. Their models, those based on three-dimensional (3D) ResNet50 and Densenet169, demonstrated high diagnostic performance (AUCs up to 0.99), with XAI methods such as Shapley Additive Explanations (SHAP) and Gradient-weighted Class Activation Mapping (Grad-CAM) used to enhance interpretability.

Zhao *et al.* (28) used radiomics and LR to differentiate TETs from cysts (AUC of 1.0) and for risk stratification of TETs (AUC of 0.76). Similarly, Wang *et al.* (29) applied an XGBoost model to separate mediastinal cysts from tumors in 592 patients, outperforming radiologists with an AUC of 0.97. Liu *et al.* (30) achieved comparable ACC (AUC of 0.94) using LR to distinguish anterior mediastinal cysts from B1/B2 thymomas.

Zhang *et al.* (31) created a CT-based radiomics nomogram combining LASSO-selected features with CT data to differentiate thymic cysts from TETs in 190 patients. The model achieved an AUC of 0.94, outperforming both the CT-only model (AUC of 0.85) and radiologist assessments, thereby demonstrating superior diagnostic ACC.

Differentiating thymoma from TC is critical due to their divergent tumor behavior and treatment strategies. Dai *et al.* (32) developed a simplified RF model using key CT features, achieving an AUC of 0.96. Ohira *et al.* (33) used radiomics and LASSO to reach an AUC of 0.88, while Tian *et al.* (34) applied radiomic feature selection and RF modeling, achieving an AUC of 0.90.

Thymic tumors vs. non-thymic tumors

Accurate differentiation between thymic tumors and non-thymic prevascular mediastinal masses, particularly lymphomas, remains challenging due to overlapping imaging features. Recent developments in AI, radiomics, and molecular profiling have provided promising tools to enhance diagnostic precision and guide treatment strategies.

Several studies have focused on distinguishing TETs from mediastinal lymphomas. Li *et al.* (35) developed a PET/CT-based radiomics model incorporating clinical variables [age, lactate dehydrogenase (LDH), SUV_{avg}] via an RF algorithm, achieving strong performance (AUC of 0.95 in training and 0.91 in internal validation). Xia *et al.* (36)

used an ensemble ML approach combining contrast-enhanced CT radiomics and clinical data across two centers, yielding AUCs of 0.85–0.86 and boosting the performance of junior radiologists.

Addressing cases without defining clinical markers like myasthenia gravis or calcification, Huang *et al.* (37) implemented a radiomics-driven LR model, achieving high training ACC (AUC of 0.99), but its external validation was less robust (AUC of 0.80). Lin *et al.* (38) introduced dynamic contrast-enhanced MRI and decision trees, achieving 72.6% overall ACC for multiclass classification, with even stronger performance in binary tasks (e.g., Hodgkin *vs.* non-Hodgkin lymphoma).

Kirienko *et al.* (39) found clinical features to outperform non-contrast CT radiomics alone (AUC of 0.98), but adding radiomics provided complementary value. A molecular diagnostic approach by Latiri *et al.* (40) used DNA methylation profiling to distinguish T-lymphoblastic lymphoma from lymphocyte-rich thymoma, achieving perfect validation separation using six gene promoters in an ML model.

Dong *et al.* (41) differentiated mass-like thymic hyperplasia from low-risk thymoma using a radiomics nomogram (AUC of 0.90), while Agar *et al.* (42) applied transformer-based DL on CT, achieving near-perfect thymoma classification.

Comparative approaches underscore the potential of radiomics. Chang *et al.* (43) evaluated 376 patients in a multicenter study, comparing radiomics-based LightGBM models with 3D CNNs for TET classification. LightGBM outperformed CNNs with an AUC of 0.95. He *et al.* (44) developed radiomics, clinico-radiologic, and combined models using contrast-enhanced CT to differentiate TET from lymphoma; the radiomics model achieved an AUC of 0.96 and ACC of 0.90, outperforming traditional methods.

Shang *et al.* (45) applied radiomics-based ML to differentiate anterior mediastinal cysts from thymomas and stratify thymomas by risk. Their models achieved AUCs of 0.92 and 0.81, respectively.

Risk stratification

Risk stratification is central to the management of TETs, and among AI applications in this domain, it remains the most thoroughly investigated. Numerous studies have investigated a range of ML and DL techniques to classify TETs by WHO histology, clinical stage, and aggressiveness, using CT, MRI, and PET-based imaging, often in combination with clinical data.

Zhang *et al.* (46) achieved excellent results using a decision tree with CT radiomics and semantic features, with AUCs of 0.96 (stage) and 0.86 (WHO subtype) in a multicenter cohort. Similarly, Yoshida *et al.* (47) used a modified visual geometry group 16 (VGG16) CNN on CT images (AUC of 0.69); radiologists improved with AI support, although the improvement was not statistically significant.

Liu *et al.* (48) developed increasingly sophisticated models: a radiomics-based SVM with transfer learning (AUC of 0.95), followed by a 3D DL pipeline combining nnU-Net and ResNet50 (AUC of 0.89, sensitivity of 1.00), outperforming simpler models. Zhou *et al.* (49) and Chen *et al.* (50) combined handcrafted and deep features in radiomics nomograms; Chen's transformer-enhanced model had the strongest external validation (AUCs of 0.85–0.87).

Other CT-based studies highlighted the value of multiphasic imaging. Liu *et al.* (51) combined non-enhanced CT (NECT), arterial phase CT (AECT), and venous phase CT (VECT) phase features (AUC of 0.94), and Feng *et al.* (52) used NECT with SVM (AUC 0.84), although sensitivity for TC detection remained limited. PET/CT studies such as Ozkan *et al.* (53) and Nakajo *et al.* (54) paired PET radiomics with DL, achieving AUCs of 0.83 and 0.94, demonstrating strong discrimination for carcinoma.

MRI-based approaches have also been effective. Xiao *et al.* (55) developed a logistic regression nomogram using MRI radiomics, apparent diffusion coefficient (ADC), and morphology (AUC of 0.88), consistent with earlier SVM results from Xiao *et al.* (56).

Other efforts focused on model interpretability or staging. Blüthgen *et al.* (57) applied RFs with SHAP to predict WHO subtype and TNM stage (AUCs 0.88, 0.84) and Moon *et al.* (58) used an end-to-end 3D DL pipeline for staging (ResNet50, AUC 0.81).

Additional radiomics-based CT studies by Yu *et al.* (59), Ren *et al.* (60), Hu *et al.* (61), and Shen *et al.* (62) confirmed the feasibility of LR and RF classifiers, typically achieving AUCs ranging from 0.84 to 0.87, with improved performance when combined with clinical staging variables.

Several radiomics studies have advanced risk stratification in TETs using CT-based modeling. Chen *et al.* (63) developed a nomogram integrating eight LASSO-selected radiomic features and CT traits with AUCs of 0.89 for the training set and 0.86 for the validation set. Dong *et al.* (64) combined contrast-enhanced CT (CECT) radiomics with clinical factors (yielding a validation AUC of 0.87).

Liang *et al.* (65) used multiphasic CT (NECT, AECT, VECT) in a stacked ensemble model across 131 cases,

incorporating phase-difference features and demographics. Their model achieved AUCs of 0.95 for the training set and 0.90 for the validation set, emphasizing phase heterogeneity. Similarly, Liu *et al.* (66) classified TETs into low/high-risk and carcinoma groups using radiomics-clinical fusion, reaching AUCs of 0.88–0.94 and demonstrating superior performance compared to radiologists.

Liu *et al.* (67) incorporated habitat-based and peritumoral features, derived via k-means clustering, with clinical data in 140 thymoma patients. Using XGBoost, the model achieved an AUC of 0.81 and an ACC of 0.77, emphasizing the prognostic value of the tumor microenvironment.

Liufu *et al.* (68) showed that multiphasic CECT-based radiomics, combined with radiological features, achieved high diagnostic ACC with AUCs of 0.99 for the training set and 0.94 for the validation set in distinguishing high- from low-risk TETs. Kayi Cangir *et al.* (69) identified four key CT radiomics features and found that the K-nearest neighbors (KNN) and LR models reached AUCs of 0.94 in the validation set, supporting their use in preoperative risk assessment. Wang *et al.* (70) used texture-based radiomics from NECT and CECT images to predict the TET risk and stage, achieving AUCs up to 0.87, with CECT models outperforming radiologists (P=0.03). Similarly, Sui *et al.* (71) applied LASSO to derive radiomics signatures, reporting AUCs of 0.83 and 0.86 for risk and stage prediction, respectively, also surpassing radiologist performance (ACCs of 0.87 *vs.* 0.78).

Preoperative planning

Recent work has increasingly used AI to predict surgical complexity in TETs, focusing on resectability and vascular involvement to guide operative planning.

Li *et al.* (72) developed a CT-based radiomics model focused on the superior vena cava and left innominate vein. Using non-contrast CT scans of 204 patients, they extracted over 2,600 features that were filtered by LASSO and SVM. Their combined two-dimensional (2D)/3D model outperformed expert radiologists with AUCs up to 0.99.

Similarly, Onozato *et al.* (73) applied XGBoost to preoperative CT data from 212 patients across three institutions to predict concurrent resections. Their model achieved AUCs of 0.80 (training) and 0.82 (validation), with lung and pericardium submodels performing well (AUCs of 0.81 and 0.92).

DL models have also enhanced staging and segmentation. Yang *et al.* (74) introduced a 3D DenseNet to classify Masaoka-Koga stage I *vs.* II using CECT in 174 cases, achieving an AUC of 0.77 and identifying tumor enhancement as the key predictor.

Araujo-Filho *et al.* (75) built a CT-based radiomics model using elastic-net LR in 243 patients to predict incomplete resections (R1/R2) and advanced-stage disease (III/IV), reaching AUCs of 0.80 and 0.71, respectively. Texture metrics from the gray-level co-occurrence matrix, run-length matrix, and size zero matrix emerged as key discriminators.

Tumor segmentation, critical for surgical and radiologic workflow, has benefited from advanced DL architectures. Li *et al.* (76) introduced DSC-Net, a CNN with dense residual connections and pseudo-color CT preprocessing, trained on 310 patients. It outperformed U-Net variants, achieving 92.96% ACC, 87.86% intersection over union (IoU), and a boundary F1 score of 0.91.

Li *et al.* (77) further developed TA-Net, a hybrid Transformer-CNN model incorporating self-attention and attention gates, yielding a Dice score of 89.92%, an IoU of 83.80%, and 92.49% ACC. In 2023, Li *et al.* (78) proposed MG-Net, which extended this with global-enhanced convolution, spatial attention, and adaptive fusion to segment across WHO subtypes. Trained on the same cohort, the model achieved Dice of 91.57%, excelling in AB subtypes (Dice of 93.84%) and underperforming slightly in B3 (Dice of 88.19%). For a more detailed comparison of TET diagnosis (on retrospective) studies, please refer to *Table 1*.

Subtyping

Four recent studies developed AI models to subtype TETs from histopathological images. Recent advances in AI have enabled increasingly accurate thymoma subtyping using both histopathological and radiological data.

Wang *et al.* (79) introduced a weakly supervised, interpretable model for classifying thymoma using whole-slide images (WSIs). Leveraging attention-based multi-instance learning, the model classified 222 slides into five WHO subtypes (A, AB, B1, B2, B3), achieving an AUC of 0.94 and ACC of 0.72. Category heatmap visualization revealed subtype heterogeneity, and cell-level analyses confirmed biologically relevant features.

Lv *et al.* (80) explored hyperspectral imaging for thymoma typing, combining spectral data with a Res2Net-48 CNN. They converted spectral signatures from 180 tissue samples into Gramian angular field images and classified six subtypes (A, AB, B1, B2, B3, TC) with an ACC of 95%.

Zhang *et al.* (81) developed a vision transformer model, MC-ViT, using 323 WSIs to subtype eight TET classes—including mixed B1 + B2 and B2 + B3. The model used multi-scale patches (10×, 20×, 40×) and dual branches: local

Table 1 Studies related to preoperative assessment using AI

Cites	Aim of the study	Type of data	Data availability	Type of samples used	No. of samples	AI method	Models	Results (AUC, ACC, ...)	XAI	Centers
Ma *et al.* (24)	Malignant or benign	Radiology and clinical data	In-house	CT	100	Supervised ML	LASSO + LR	ACC 0.82 (test); AUC 0.75 (test)	None	1
Mayoral *et al.* (25)	Malignant or benign and thymoma *vs.* other thymic tumors	Radiology	In-house	CT	239	Supervised ML	LR	AUC 0.72 (test); AUC 0.81 (test)	None	1
Yang *et al.* (26)	Thymoma *vs.* other thymic tumors	Radiology	In-house	CT	345	Supervised DL	3D ResNet50	AUC 0.94(internal test); AUC 0.94, 0.91 (external test)	Grad-CAM, SHAP	3
Yang *et al.* (27)	Thymoma *vs.* other thymic tumors	Radiology and clinical data	In-house	CT + clinical (age and gender)	264	Supervised DL and ML	Densenet169	AUC 0.96 (Densenet169); AUC 0.95 (Combined)	None	2
Tian *et al.* (34)	Thymoma *vs.* other thymic tumors and PFS	Radiology	In-house	CT	124	Supervised ML	RF	Thymoma *vs.* other: AUC 0.89 Stage: AUC 0.77	None	1
Zhao *et al.* (28)	Thymoma *vs.* other thymic tumors and risk	Radiology	In-house	CT	36	Supervised ML	LASSO + LR	Thymoma *vs.* other: AUC 1 Risk: AUC 0.76	None	1
Dai *et al.* (32)	Thymoma *vs.* other thymic tumors	Radiology and clinical data	In-house	CT + clinical (sex, age, clinical presentation and myasthenia gravis)	137	Supervised ML	RF	AUC 0.96 (test); ACC 0.96 (test)	None	2
Wang *et al.* (29)	Thymoma *vs.* other thymic tumors	Radiology	In-house	CT	592	Supervised ML	XGBoost	AUC 0.972 (internal), 0.910 (external)	SHAP	2
Liu *et al.*(30)	Thymoma *vs.* other thymic tumors	Radiology and clinical data	In-house	CT + clinical (age, gender, primary site, lesion size)	188	Supervised ML	LASSO + LR	AUC of 0.941 in the training set and 0.938 in the test set	None	1
Zhang *et al.* (31)	Thymoma *vs.* other thymic tumors	Radiology and clinical data	In-house	CT + clinical (gender, age, and myasthenia gravis)	190	Supervised ML	LASSO + multivariate LR	ACC 0.95 (model); ACC 0.64 (radiologist) on validation	None	1
Ohira *et al.* (33)	Thymoma *vs.* other thymic tumors	Radiology	In-house	CT	61	Supervised ML	LASSO + LR	AUC 0.88 (validation)	None	1
Li *et al.* (35)	Thymic tumors *vs.* non-thymic tumors	Radiology and clinical data	In-house	PET/CT + clinical (age, gender, lactate dehydrogenase level, pathological results, presence of myasthenia gravis symptoms, and B symptoms)	255	Supervised ML	RF	AUC 0.95 (train), 0.91 (internal test). SN 0.8 and SP 0.78 (external test)	None	1
Agar *et al.* (42)	Thymic tumors *vs.* non-thymic tumors	Radiology	In-house	CT	298	Supervised DL and ML	Transformers + SVM	ACC 1 (test); ACC 0.99 (validation)	None	1
Xia *et al.* (36)	Thymic tumors *vs.* non-thymic tumors	Radiology and clinical data	In-house	CT + clinical (age, symptoms, LDH and lymphocyte count)	189	Supervised ML	Ensemble classifier (SVM, LR, Bayes)	AUC: 0.75 (radiomics); AUC: 0.85 (clinico-radiomics) The human-machine hybrid models improved on test: AUC from 0.76 to 0.87 (reader 1); AUC from 0.70 to 0.86 (reader 2); AUC from 0.60 to 0.84 (reader 3)	None	2
Latiri *et al.* (40)	Thymic tumors *vs.* non-thymic tumors	Omics data	In-house	DNA methylation	102	Supervised ML	Extra trees regressor	MACROD2 can accurately distinguish T-LBL from TdT + T-cell-rich thymoma	None	1
Huang *et al.* (37)	Thymic tumors *vs.* non-thymic tumors	Radiology	In-house	CT	114	Supervised ML	LR	AUC 0.99 (train); AUC 0.80 (external test)	None	3
Dong *et al.* (41)	Thymic tumors *vs.* non-thymic tumors	Radiology and clinical data	In-house	CT	135	Supervised ML	LASSO + LR	AUC 0.90 (combined) on validation	None	1
Lin *et al.*(38)	Thymic tumors *vs.* non-thymic tumors	Radiology and clinical data	In-house	MRI + clinical (age)	62	Supervised ML	DT	ACC 0.73	None	1
Chang *et al.* (43)	Thymic tumors *vs.* non-thymic tumors	Radiology and clinical data	In-house	CT + clinical (age, sex, myasthenia gravis)	376	Supervised DL and ML	3D CNN + LightGBM + Extra tree	AUC 0.95 (ML); AUC 0.93 (DL)	None	1
Kirienko *et al.* (39)	Thymic tumors *vs.* non-thymic tumors	Radiology and clinical data	In-house	CT + clinical (age, sex, presence of B symptoms, lymphadenopathies, autoimmune disorders, white blood cell counts)	108	Supervised ML	LDA	AUC 0.84 (radiomics); AUC 0.98 (clinical); AUC 0.95 (combined)	None	1

Table 1 (*continued*)

Table 1 (*continued*)

Cites	Aim of the study	Type of data	Data availability	Type of samples used	No. of samples	AI method	Models	Results (AUC, ACC, ...)	XAI	Centers
He *et al.* (44)	Thymic tumors *vs.* non-thymic tumors	Radiology and clinical data	In-house	CT + clinical (age, gender)	242	Supervised ML	Multivariable LR	AUC 0.84 (clinico-radiologic); AUC 0.96 (radiomics); AUC 0.96 (combined) validation	None	1
Zhang *et al.* (46)	Risk stratification	Radiology and clinical data	In-house	CT + clinical (age, gender, patient-reported symptoms)	187	Supervised ML	LR	AUC 0.96 (test) (stage); AUC 0.86 (test) (risk)	None	3
Yoshida *et al.* (47)	Risk stratification	Radiology	In-house	CT	159	Supervised DL	VGG16	ACC 0.71 (AI model); ACC 0.62–0.69 (radiologist); ACC 0.68–0.70 (radiologist + AI model)	None	1
Liu *et al.* (48)	Risk stratification	Radiology	In-house	PCT	147	Supervised DL + ML	3D ResNet50 + MLP classifier	AUC 0.99 (training); AUC 0.89 (test)	None	1
Liu *et al.* (51)	Risk stratification	Radiology and clinical data	In-house	CT + clinical (gender, age, and symptoms)	150	Supervised ML	SVM	AUC 0.99 (test); AUC 0.95 (training)	None	1
Zhou *et al.* (49)	Risk stratification	Radiology	In-house	CT	734	Supervised DL and ML	ResNet50 + LASSO	AUC 0.97 (external)	None	3
Chen *et al.* (50)	Risk stratification	Radiology and clinical data	In-house	CT + clinical (gender and age)	257	Supervised DL	Transformers	AUC 0.87 (internal validation); AUC 0.85 (external validation)	None	3
Liufu *et al.* (68)	Risk stratification	Radiology	In-house	CT	305	Supervised ML	Multivariate LR	AUC 0.99 (training); AUC 0.94 (validation)	None	1
Feng *et al.* (52)	Risk stratification	Radiology and clinical data	In-house	CT + clinical (gender, age, clinical symptoms, and smoking status)	509	Supervised ML	SVM	AUC 0.84 (validation); AUC 0.84 (test)	None	1
Ozkan *et al.* (53)	Risk stratification	Radiology and clinical data	In-house	PET-CT + clinical (Gender and age, Myasthenia gravis status, Serum levels of LDH, ALP, CRP, Hb, white blood cell count, lymphocyte count, and platelet counts)	27	Supervised ML	LR, MLP	AUC 0.88	None	1
Blüthgen *et al.* (57)	Risk stratification	Radiology	In-house	CT	62	Supervised ML	RF	Risk: AUC 0.88 (test) Stage: AUC 0.84 (test) MG: AUC 0.64 (test)	SHAP	1
Xiao *et al.* (55)	Risk stratification	Radiology and clinical data	In-house	MRI + clinical (age, gender, presence of myasthenia gravis, symptom presentation, maximal tumor diameter, estimated tumor volume, and tumor shape)	182	Supervised ML	LASSO + multivariate LR	AUC 0.95 (training); 0.88 (test)	None	1
Kayi Cangir *et al.* (69)	Risk stratification	Radiology and clinical data	In-house	CT + clinical (age, gender, smoking status, clinical presentation, myasthenia gravis, previous malignancy, laboratory values, type of treatment)	83	Supervised ML	LASSO + ML: XGBoost, RF, DT	AUC 0.998-1 (XGBoost, RF, and DT) on training	None	1
Hu *et al.* (61)	Risk stratification	Radiology	In-house	CT	155	Supervised ML	LASSO + RF	AUC 0.87 (RF)	None	1
Wang *et al.* (70)	Risk stratification	Radiology	In-house	CT	199	Supervised ML	LASSO + LR	Risk: AUC 0.80 (NECT); AUC 0.83 (CECT) Stage: ACC 0.82 (NECT); ACC 0.87 (CECT); ACC 0.78 (radiologists)	None	1
Xiao *et al.* (56)	Risk stratification	Radiology and clinical data	In-house	MRI + clinical (age, sex, presence of myasthenia gravis, and symptoms)	189	Supervised ML	SVM	Risk: AUC 0.88 (training); AUC 0.77 (test) Staging: AUC 0.95 (training); AUC 0.91 (test) Nomogram: AUC 0.97 (training); AUC 0.96 (test)	None	1
Moon *et al.* (58)	Risk stratification	Radiology	In-house	CT	125	Supervised DL	3D U-Net++	Segmentation: Dice 0.95 (3D U-Net++) Risk: AUC 0.91 (validation); AUC 0.81 (test)	Grad-CAM	2
Sui *et al.* (71)	Risk stratification	Radiology	In-house	CT	298	Supervised ML	LASSO + LR	AUC 0.77 (UECT) (validation); AUC 0.73 (CECT) (validation)	None	2
Nakajo *et al.* (54)	Risk stratification	Radiology	In-house	PET-CT	79	Supervised DL and ML	CNN + LR	AUC 0.90 (LR)	None	1

Table 1 (*continued*)

Table 1 (*continued*)

Cites	Aim of the study	Type of data	Data availability	Type of samples used	No. of samples	AI method	Models	Results (AUC, ACC, ...)	XAI	Centers
Shen *et al.* (62)	Risk stratification	Radiology and clinical data	In-house	CT + clinical (age, gender, presence of myasthenia gravis, chest pain, respiratory symptoms and TNM staging)	136	Supervised ML	LASSO + LR	AUC 0.84 (training); AUC 0.79 (external test)	None	2
Liu *et al.* (67)	Risk stratification	Radiology and clinical data	In-house	TC + clinical (age, gender, chest pain, and other symptoms like cough and myasthenia gravis)	140	Supervised ML	eXtreme Gradient Boosting (XGBoost)	AUC 0.81 (test)	SHAP	1
Dong *et al.* (64)	Risk stratification	Radiology and clinical data	In-house	CT + clinical (age, sex, myasthenia gravis, maximum tumor diameter, calcification, boundary, and pleural effusion)	110	Supervised ML	LASSO + LR	AUC 0.82 (radiomics); AUC 0.87 (combined) on validation	None	1
Chen *et al.* (63)	Risk stratification	Radiology	In-house	CT	179	Supervised ML	LASSO + multivariate LR	AUC 0.75 (radiomics); AUC 0.83 (combined) on external test	None	2
Liang *et al.* (65)	Risk stratification	Radiology and clinical data	In-house	CT + clinical (age and sex)	131	Supervised ML	LASSO + XGBoost	AUC 0.97 (radiomics); AUC 0.98 (combined) on validation	None	1
Shang *et al.* (45)	Thymoma *vs.* other thymic tumors and risk stratification	Radiology and clinical data	In-house	CT + clinical (age, sex, and symptoms such as myasthenia gravis, chest pain, and respiratory symptoms)	201	Supervised ML	Thymoma *vs.* other thymic tumors: SVM + gradient boosting decision tree (GBDT)	Thymoma *vs.* other thymic tumors: AUC 0.88 (radiomics); AUC 0.92 (combined)	None	3
							Risk: Gaussian NB + GBDT (radiomics); DT + KNN (combined)	Risk: AUC 0.75 (radiomics); AUC 0.78 (combined) on external test		
Liu *et al.* (66)	Risk stratification	Radiology and clinical data	In-house	CT + clinical (age, gender and symptoms)	190	Supervised ML	GBDT + LR	NECT-based clinical radiomics model: AUC 0.770 (low-risk); AUC 0.69 (high-risk); AUC 0.78 (TC); ACC 0.57 on validation	None	1
Ren *et al.* (60)	Risk stratification	Radiology and clinical data	In-house	CT + clinical (gender, age, and symptoms)	172	Supervised ML	LASSO + LR	AUC 0.66 (model 1); AUC 0.82 (model 2); AUC 0.86 (model 3); AUC 0.94 (model 4) on validation	None	1
Yu *et al.* (59)	Risk stratification	Radiology	In-house	CT	164	Supervised ML	LASSO + LR	ACC 0.72 (training); ACC 0.62 (internal test)	None	1
Li *et al.* (72)	Surgery planning	Radiology	In-house	CT	204	Supervised	LASSO + SVM	AUC 0.99 (nomogram); AUC 0.78 (radiologist) on test	None	1
Yang *et al.* (74)	Surgery planning	Radiology	In-house	CT	174	Supervised DL	3D-DenseNet	AUC 0.77	None	1
Araujo-Filho *et al.* (75)	Surgery planning	Radiology	In-house	CT	243	Supervised ML	LR	AUC 0.80 (incomplete resections); AUC 0.70 (advanced stage tumors) on test	None	1
Onozato *et al.* (73)	Surgery planning	Radiology	In-house	CT	212	Supervised ML	GB + XGB	AUC 0.82 (validation)	None	3
Li *et al.* (76)	Surgery planning	Radiology	In-house	CT	310	Supervised DL	CNN (DSC-Net)	ACC 0.93 (test); IoU 0.88 (test)	None	1
Li *et al.* (77)	Surgery planning	Radiology	In-house	CT	310	Supervised DL	CNN + transformer (TA-Net)	ACC 0.92 (test); IoU 0.90 (test)	None	1
Li *et al.* (78)	Surgery planning	Radiology	In-house	CT	310	Supervised DL	CNN (MG-Net)	ACC 0.94 (test); IoU 0.86 (test)	Grad-CAM	1

3D, three-dimensional; ACC, accuracy; AI, artificial intelligence; ALP, alkaline phosphatase; AUC, area under curve; CECT, contrast-enhanced computed tomography; CNN, convolutional neural network; CRP, C-reactive protein; CT, computed tomography; DL, deep learning; DT, decision trees; GB, gradient boosting; GBDT, gradient boost decision tree; Grad-CAM, gradient-weighted class activation mapping; Hb, hemoglobin; IoU, intersection over union; KNN, K-nearest neighbors; LASSO, Least Absolute Shrinkage and Selection Operator; LDA, linear discriminant analysis; LDH, lactate dehydrogenase; LR, Logistic Regression; ML, machine learning; MLP, multi-layer perceptron; NECT, non-enhanced computed tomography; PET, positron emission tomography; RF, random forest; SHAP, shapley additive explanations; SN, sensitivity; SP, specificity; SVM, support vector machine; T-LBL, T-lymphoblastic lymphoma; TNM, tumor node metastasis; UECT, unenhanced computed tomography; VGG16, visual geometry group 16; XAI, explainable AI; XGB, extreme gradient boosting.

Table 2 Studies related to subtyping using AI

Cites	Aim of the study	Type of data	Data availability	Type of samples used	No. of samples	AI method	Models	Results (AUC, ACC, ...)	XAI	Centers
Wang *et al.* (79)	A, AB, B1, B2, B3	Pathology	In-house	WSIs	222	Semi supervised DL	ResNet50	AUC 0.92 (internal test)	Category heatmap	1
Lv *et al.* (80)	A, AB, B1, B2, B3, and TC	Pathology	In-house	Patches	180	Supervised DL	Res2Net-48	AUC 0.96 (internal test)	None	1
Zhang *et al.* (81)	A, AB, B1, B1+B2, B2, B2+B3, B3, and TC	Pathology	In-house	WSIs	323	Supervised DL	Transformer	AUC 0.923 (Pathological information); AUC 0.96 (Subtyping)	None	1
Zhang *et al.* (82)	A, AB, B1, B1+B2, B2, B2+B3, B3, and TC	Radiology and pathology	In-house	WSIs	126 (850 CT + 895 WSI)	Semi supervised DL	ResNet-18/34 (MHD-Net)	AUC: 0.66 (radiology); AUC: 0.74 (pathology) on test	None	1

ACC, accuracy; AI, artificial intelligence; AUC, area under curve; CT, computed tomography; DL, deep learning; WSIs, whole-slide images; XAI, explainable AI.

feature extraction (CAST) and subtype prediction (WT). MC-ViT achieved an ACC of 95% and an F1-score of 0.94; CAST alone achieved an F1-score of 0.94. Expanding to multimodal learning, Zhang *et al.* (82) proposed MHD-Net, trained on paired CT and pathology but deployable with CT alone, achieving an ACC of 89.89% on 126 patients. For a more detailed comparison of the TET subtyping studies, please refer to *Table 2*.

Applications of AI methods for prognosis

Survival

Tian *et al.* (34) performed a retrospective study using radiomic features from preoperative CT scans of 124 TET patients to predict risk-group type, TNM stage, and survival outcomes. Using 851 extracted features, RF and random survival forest (RSF) models were built. The model achieved survival prediction AUCs of 0.94 [overall survival (OS)] and 0.81 [progression-free survival (PFS)] when combining radiomic and clinical data. High-risk patients exhibited significantly worse survival outcomes.

Kim *et al.* (83) used Lunit SCOPE IO, a CNN-based AI tool, to analyze haematoxylin and eosin (H&E) WSIs from 35 unresectable thymic tumor cases and measure tumor-infiltrating lymphocytes (TILs). TILs increased post-neoadjuvant therapy. Patients with higher intratumoral TILs had improved survival as well as lower recurrence rates. Patients with TIL levels >10% had a 5-year survival rate of 73.8%. Desert immune phenotypes were linked to poor response (OR of 0.04).

Yang *et al.* (84) developed an 11-gene prognostic model based on immune microenvironment profiles from 121 thymoma patients in The Cancer Genome Atlas (TCGA). Two immunotypes with distinct immune cell patterns and survival outcomes were identified. The model, including genes like *CD1C* and *CELF5*, showed high prognostic power (AUC of 0.93) and was validated using Gene Expression Omnibus (GEO) data. High-risk scores were linked to worse survival, higher tumor mutation burden, increased stemness, and distinct immune cell infiltration. *CD1C* overexpression was confirmed by immunohistochemistry.

Zhang *et al.* (85) used clustering, gene set variation analysis (GSVA), and ML to study metabolic reprogramming in thymoma by integrating RNA sequencing (RNA-seq) and metabolomic data from 121 TCGA patients and 10 tissue samples. The lacto/neolacto-series pathway correlated with progression. An RF model and SHAP scores identified B3GNT5 as a potential prognostic biomarker.

Han *et al.* (86) developed a DL model based on a quasi-3D U-Net to segment TETs in 18F-FDG PET/CT scans from 186 patients. Automated parameters [SUV_{max}, metabolic tumor volume (MTV), total lesion glycolysis (TLG)] showed high agreement with manual values [concordance correlation coefficient (CCC) >0.92]. SUV_{max} was found to be an independent prognostic factor. Segmentation achieved a mean Dice score of 0.83.

Recurrence

Zhang *et al.* (85) analyzed proteomic data from 30 TET samples, identifying HNRNPA2B1 as a marker associated to poor survival and recurrence, and suggested ergotamine as a drug target. Su *et al.* (87) used RNA-seq from 114 TCGA patients to develop a 4-long noncoding (lnc) RNAs classifier via LASSO Cox regression, which demonstrated superior performance compared to clinical staging with AUCs of 0.80 (3-year) and 0.79 (5-year). Both highlight molecular models' value in predicting TET recurrence. For more detailed comparison of TET prognostic studies, please refer to *Table 3*.

Discussion

AI is rapidly transforming healthcare. In medicine, its impact is especially profound for diseases that are both rare and highly variable (89). TETs are difficult to diagnose accurately. Our findings show that AI enhances diagnostic precision and speed, supporting timely, personalized care and helping patients receive optimal treatment.

AI applications in TETs are diverse, aiding diagnosis, prognosis, and treatment planning. In radiology, AI supports tumor classification, risk stratification, and surgical planning. In pathology, DL helps identify subtypes beyond human perception. Prognostically, AI predicts outcomes like metastasis and recurrence. This systematic review of 65 studies highlights AI's growing role in enhancing diagnostic ACC and prognostic assessment in TETs, demonstrating its clinical relevance and potential impact.

The comparison between human radiologists and AI models has been a significant focus in recent research. Studies (29,70) have developed a top-performing model that provided valuable feedback to radiologists, helping them understand the logic behind radiomics textures. This feedback mechanism enhances the interpretability and clinical utility of AI tools. Similarly, Zhang *et al.* (31)'s radiomics nomogram method achieved higher ACC than conventional CT models and radiologist judgments, consistently yielding higher AUC values. In risk stratification, Yoshida *et al.* (47) developed a CT-based DL model to differentiate low- and high-risk thymomas. It achieved 71.3% ACC, outperforming radiologists (whose ACC ranged from 61.9% to 70.0%). Xia *et al.* (36)'s clinico-radiomics model improved TET-lymphoma differentiation, especially for less experienced radiologists by reducing diagnostic bias.

Subjectivity and interobserver variability are major challenges in both radiology and pathology, and remain significant barriers in subtyping efforts. To reduce bias, Wang *et al.* (79) used a consensus-labeled dataset. The issue of subjectivity in radiological assessment has been highlighted by several studies. Ohira *et al.* (33) demonstrated that radiomics features outperformed radiologists in diagnostic ACC. Chen *et al.* (63) identified drawbacks including inter-reader variability and poor repeatability. Shang *et al.* (45) noted that CT interpretations are influenced by radiologists' experience, which limits their ability to distinguish mediastinal cysts from thymomas.

A solution to the subjectivity in radiological assessment is the use of automatic segmentation. Several researchers have identified this as an important application area. Wang *et al.* (29) suggested using DL methods with computer vision to train an automated model for lesion regions of interest (ROI) delineation, enabling clinical translation. Li *et al.* (77) proposed a hybrid CNN-transformer architecture, TA-Net, for effective thymoma segmentation on chest CT, achieving superior performance and consistent delineation to assist radiologists. Several studies have demonstrated that automated segmentation reduces intra-observer variations (47,86). Liu *et al.* (48) used a 3D segmentation model on radiomics data, which outperformed 2D segmentation, demonstrating the advantages of three-dimensional approaches in capturing the complex spatial characteristics of tumors.

Multi-approach methodologies have shown promising results in improving diagnostic ACC. Lin *et al.* (38) built ML models for predicting pathological subtypes of prevascular mediastinal tumors using clinical and MRI data, achieving varying sensitivity rates for detecting different tumor types. Liu *et al.* (48) developed a DL model combining segmentation and risk stratification to improve diagnostic consistency. Moon *et al.* (58) proposed a deep-learning framework for automatic segmentation and classification of high-risk TET cases, while Mayoral *et al.* (25) focused on predicting pathologic diagnoses of anterior mediastinal masses using ML models based on CT conventional and radiomic features. Their research showed that the best diagnostic performance was achieved by

Table 3 Studies related to prognosis using AI

Cites	Aim of the study	Type of data	Data availability	Type of samples used	No. of samples	AI method	Models	Results (AUC, ACC, ...)	XAI	Centers
Tian *et al.* (34)	Thymoma *vs.* other thymic tumors and PFS	Radiology and clinical data	In-house	CT + clinical (age, sex, myasthenia gravis, multiple primary malignant tumors, and biopsy status)	124	Supervised ML	RF, RSF	Thymoma *vs.* thymic carcinoma: AUC 0.90 Stage: 898 (WHO); AUC 0.78 (TNM) Survival: iAUC 0.92 (OS); iAUC 0.79 (PFS)	None	1
Kim *et al.* (83)	Neoadjuvant therapy response and OS and DFS	Pathology	In-house	Patch	35	Supervised DL	Lunit SCOPE IO tool (CNN)	High intratumoral TIL (iTIL >147/mm^2): better survival; OS 45 months; DFS 12 months High stromal TIL (sTIL >232.1/mm^2): OS 62 months; DFS 28 months	None	1
Yang *et al.* (84)	Survival outcomes	Omics	TCGA and GEO	RNA-Seq	121 (TCGA) + 36 (GEO)	Unsupervised and supervised ML	LASSO + Cox regression analysis	An immune subtypes: immunotype A was associated with better survival (Kaplan-Meier, P<0.05) Prognostic model (high-low risk): AUC 0.93 (GSE29695 set)	None	TCGA + GEO
Zhou *et al.* (88)	Identify prognostic biomarkers and therapeutic targets for recurrent TET	Omics	In-house	Proteomic	30	Supervised ML	SVM-RFE	Kaplan-Meier plot: low expression of HNRNPA2B1 correlated significantly with poor survival	None	1
Su *et al.* (87)	RFS	Omics and clinical data	TCGA	RNA-seq + clinical (age, sex, height, weight, race, initial sample weight, tumor site, mutation count, WHO histological types, and Masaoka staging)	114	Supervised ML	LASSO + Cox proportional hazards regression	AUC 0.80 (3-year RFS); AUC 0.79 (5-year RFS)	None	1
Zhang *et al.* (85)	DFS	Omics	TCGA	RNA-seq	121	Supervised ML	RF	IHC and transcriptomics determined the high expression of B3GNT5, which was associated with poorer disease-free survival (HR =0.33, P<0.05).	SHAP	1
Han *et al.* (86)	Segmentation-disease recurrence, and survival	Radiology	In-house	PET/CT	186	Supervised DL	Segmentation: quasi-3D U-net + LR Survival: Cox proportional hazards	Segmentation: AUC 0.95 (SUV_{max}); AUC 0.85 (MTV); AUC 0.87 (TLG) Survival: SUV_{max} emerged as an independently significant prognostic factor	None	1

ACC, accuracy; AI, artificial intelligence; AUC, area under the curve; CNN, convolutional neural network; CT, computed tomography; DFS, disease-free survival; DL, deep learning; GEO, gene expression omnibus; HR, hazard ratio; iAUC, integrated area under the curve; IHC, immunohistochemistry; iTIL, intratumoral tumor-infiltrating lymphocyte; LASSO, Least Absolute Shrinkage and Selection Operator; LR, Logistic Regression; ML, machine learning; MTV, metabolic tumor volume; OS, overall survival; PET/CT, positron emission tomography/computed tomography; PFS, progression-free survival; RF, random forest; RFE, recursive feature elimination; RFS, recurrence-free survival; RNA-seq, RNA sequencing; RSF, random survival forest; sTIL, stromal tumor-infiltrating lymphocyte; SUV, standardised uptake value; SVM, support vector machine; TCGA, The Cancer Genome Atlas; TET, thymic epithelial tumor; TIL, tumor-infiltrating lymphocyte; TLG, total lesion glycolysis; TNM, tumor node metastasis; WHO, World Health Organization; XAI, explainable AI.

integrating both conventional and radiomic features within the predictive frameworks. Shang *et al.* (45) addressed two core challenges: isolating thymic cysts from thymomas and stratifying thymomas by risk. Han *et al.* (86) presented a two-stage DL model based on automatic segmentation of thymic tumors and recurrence prediction.

The integration of multimodal data improves diagnostic ACC. Zhang *et al.* (82) developed MHD-Net, a memory-aware hetero-model distillation network that transfers multimodal knowledge using only radiology data. Its spatial fusion module enhances radiology-pathology feature fusion, while the typing memory module stores pathology features to boost cross-modal learning. Liu *et al.* (30) explored CT-based radiomics for diagnosing anterior mediastinal cysts as well as type B1 and B2 thymomas, finding that a combined model using enhanced CT and clinical factors shows potential for differential diagnosis. Other CT radiomics studies (55,59-62) confirmed ML models' feasibility for classifying prevascular mediastinal lesions and showed improved performance with the addition of clinical staging data.

External validation was commonly performed across numerous studies and showed promising results (26,27,29,36,37,46,49,50,62,73) (*Table 1*). Robust external validation is essential to ensure AI models generalize well, enhancing reproducibility and enabling reliable clinical implementation across diverse patient populations and healthcare settings.

XAI techniques have been increasingly incorporated to make AI processes more transparent (26,29,57,58,72). Used techniques such as SHAP and Grad-CAM analyses to provide insights into how their models make decisions, enhancing trust and understanding among clinical users.

These advancements in AI applications for TETs diagnosis and prognosis represent significant progress in addressing the challenges associated with these rare and heterogeneous tumors. By applying various AI techniques, from radiomics to DL and multimodal approaches, researchers are developing tools that can assist clinicians in making more accurate and early diagnoses, ultimately leading to better patient outcomes through personalized treatment strategies.

Limitations and future work

Most reviewed studies share common limitations. Many are retrospective and single-center, which limits the generalizability of their findings. A major challenge is the lack of external validation, which hinders the assessment of model robustness. Manual segmentation, which is frequently used, is prone to observer bias. Additionally, small sample sizes and the absence of standardized imaging protocols or inconsistent use across different scanners further limit model reliability. The interpretability of DL models remains limited, affecting clinical trust.

In subtyping studies, data leakage is a critical concern. WSIs or image patches from the same patient are often split across training, validation, and test sets. This leads models to learn patient-specific features rather than disease-related patterns, artificially inflating performance and reducing generalizability. Such practices compromise the true evaluation of model effectiveness and highlight the need for more rigorous data handling and validation strategies in future research. To support clinical adoption, future efforts must be directed toward filling these gaps:

(I) Conduct prospective, multicenter studies to capture diverse clinical populations and improve model relevance;
(II) Use standardized imaging protocols to reduce variability and bias, ensuring consistent, reliable results across centers;
(III) Secure diagnosis agreement from at least three experts to enhance ACC and reliability;
(IV) Perform external validation on independent datasets to evaluate real-world model performance;
(V) Replace manual ROI segmentation with validated automated methods to minimize user bias and improve reproducibility;
(VI) Integrate multimodal data such as radiomics, clinical, histopathological, and molecular information to enable more comprehensive feature extraction;
(VII) Incorporate XAI techniques to enhance model transparency and clinical trust.
(VIII) Test models across different scanners and protocols to ensure cross-device robustness;
(IX) Utilize federated learning to train models across institutions without data sharing, preserving privacy while boosting generalizability;
(X) Develop foundational models trained on large, diverse datasets, then fine-tune for specific tasks, improving training efficiency and adaptability;
(XI) Expand the focus to include prognosis prediction, thereby enhancing clinical utility beyond diagnosis and subtyping.

Conclusions

Most preoperative studies integrate clinical and radiomic

data to distinguish benign from malignant thymic tumors or differentiate thymomas from other tumor types. They also aim to stratify patients by risk. Feature reduction techniques, such as LASSO or deep reductions using CNNs, are commonly used. Final classifications typically rely on statistical models or ML classifiers. While the applications of DL methods for classification remain limited, such approaches are gradually emerging. Other studies support surgical planning by applying DL for tumor segmentation, followed by staging classification. Classifiers trained on segmentation outputs can estimate tumor stage and predict resectability.

Subtyping efforts primarily use H&E WSIs, which are preprocessed into small image patches for CNN input. However, many studies fail to avoid data leakage, often including patches from the same patient in both training and test sets—compromising reliability. Radiomics-based subtyping is rare and lacks strong predictive features.

Prognostic modeling remains less developed, with limited literature and a scarcity of external validation. Some models use omics data with ML to predict survival or recurrence, though they often exclude imaging and histology, thereby reducing clinical relevance.

To enhance trust in AI, newer studies increasingly compare model performance with clinical experts. There is also growing use of XAI techniques like SHAP and Grad-CAM to interpret model decisions and reduce black-box concerns.

Risk stratification is the most common application across all goals, guiding preoperative planning and supporting personalized care. However, most models still require more thorough external validation and greater multimodal integration to ensure clinical utility.

Acknowledgments

The authors thanks to the reviewers for their contributions and Wichor Bramer from the Erasmus MC Medical Library for developing the search strategies.

Footnote

Provenance and Peer Review: This article was commissioned by the Guest Editor (Malgorzata Szolkowska) for "The Series Dedicated to the 14th International Thymic Malignancy Interest Group Annual Meeting (ITMIG 2024)" published in *Mediastinum*. The article has undergone external peer review.

Reporting Checklist: The authors have completed the PRISMA reporting checklist. Available at https://med.amegroups.com/article/view/10.21037/med-25-34/rc

Peer Review File: Available at https://med.amegroups.com/article/view/10.21037/med-25-34/prf

Funding: This work was supported by Hanarth Fonds grant 2022 (PI: Stephanie Peeters).

Conflicts of Interest: All authors have completed the ICMJE uniform disclosure form (available at https://med.amegroups.com/article/view/10.21037/med-25-34/coif). "The Series Dedicated to the 14th International Thymic Malignancy Interest Group Annual Meeting (ITMIG 2024)" was commissioned by the editorial office without any funding or sponsorship. J.v.d.T. serves as an unpaid editorial board member of *Mediastinum* from May 2024 to December 2025. D.D. reported consulting fees from MSD, Amgen, Roche, BMS, Astra Zeneca, and Pfizer. D.D.R. reported grants or contracts from various entities, indicating institutional financial interests without personal financial gain from organizations such as AstraZeneca, BMS, Beigene, Philips, Olink, and Eli Lilly, where his involvement includes research grants, support, and advisory board participation. S.P. reported Hanarth grant financed the INTHYM project, on AI for histopathological classification and recurrence prediction of TET. The authors have no other conflicts of interest to declare.

Ethical Statement: The authors are accountable for all aspects of the work in ensuring that questions related to the accuracy or integrity of any part of the work are appropriately investigated and resolved.

References

1. International Agency for Research on Cancer, World

Health Organization, International Academy of Pathology. Thoracic tumours. 5th ed. IARC; 2021.
2. Hsu CH, Chan JK, Yin CH, et al. Trends in the incidence of thymoma, thymic carcinoma, and thymic neuroendocrine tumor in the United States. PLoS One 2019;14:e0227197.
3. Travis WD, Brambilla E, Burke AP, et al. Introduction to The 2015 World Health Organization Classification of Tumors of the Lung, Pleura, Thymus, and Heart. J Thorac Oncol 2015;10:1240-2.
4. Wolf JL, van Nederveen F, Blaauwgeers H, et al. Interobserver variation in the classification of thymic lesions including biopsies and resection specimens in an international digital microscopy panel. Histopathology 2020;77:734-41.
5. Roden AC, Yi ES, Jenkins SM, et al. Reproducibility of 3 histologic classifications and 3 staging systems for thymic epithelial neoplasms and its effect on prognosis. Am J Surg Pathol 2015;39:427-41.
6. Oselin K, Girard N, Lepik K, et al. Pathological discrepancies in the diagnosis of thymic epithelial tumors: the Tallinn-Lyon experience. J Thorac Dis 2019;11:456-64.
7. Verghese ET, den Bakker MA, Campbell A, et al. Interobserver variation in the classification of thymic tumours--a multicentre study using the WHO classification system. Histopathology 2008;53:218-23.
8. Dawson A, Ibrahim NB, Gibbs AR. Observer variation in the histopathological classification of thymoma: correlation with prognosis. J Clin Pathol 1994;47:519-23.
9. Yoon SH, Choi SH, Kang CH, et al. Incidental Anterior Mediastinal Nodular Lesions on Chest CT in Asymptomatic Subjects. J Thorac Oncol 2018;13:359-66.
10. Girard N, Ruffini E, Marx A, et al. Thymic epithelial tumours: ESMO Clinical Practice Guidelines for diagnosis, treatment and follow-up. Ann Oncol 2015;26 Suppl 5:v40-55.
11. Li HR, Gao J, Jin C, et al. Comparison between CT and MRI in the Diagnostic Accuracy of Thymic Masses. J Cancer 2019;10:3208-13.
12. Strollo DC, Rosado-de-Christenson ML. Tumors of the thymus. J Thorac Imaging 1999;14:152-71.
13. von der Thüsen J. Thymic epithelial tumours: histopathological classification and differential diagnosis. Histopathology 2024;84:196-215.
14. Alqaidy D. Thymoma: An Overview. Diagnostics (Basel) 2023;13:2982.
15. Suster S, Moran CA. Thymic carcinoma: spectrum of differentiation and histologic types. Pathology 1998;30:111-22.
16. Suster S, Moran CA. Histologic classification of thymoma: the World Health Organization and beyond. Hematol Oncol Clin North Am 2008;22:381-92.
17. Suster S, Moran CA. Thymoma, atypical thymoma, and thymic carcinoma. A novel conceptual approach to the classification of thymic epithelial neoplasms. Am J Clin Pathol 1999;111:826-33.
18. Weis CA, Yao X, Deng Y, et al. The impact of thymoma histotype on prognosis in a worldwide database. J Thorac Oncol 2015;10:367-72.
19. Detterbeck FC, Nicholson AG, Kondo K, et al. The Masaoka-Koga stage classification for thymic malignancies: clarification and definition of terms. J Thorac Oncol 2011;6:S1710-6.
20. Tosi D, Damarco F, Franzi S, et al. Outcomes of extended surgical resections for locally advanced thymic malignancies: a narrative review. Gland Surg 2022;11:611-21.
21. Molina TJ, Bluthgen MV, Chalabreysse L, et al. Impact of expert pathologic review of thymic epithelial tumours on diagnosis and management in a real-life setting: A RYTHMIC study. Eur J Cancer 2021;143:158-67.
22. Drevet G, Collaud S, Tronc F, et al. Optimal management of thymic malignancies: current perspectives. Cancer Manag Res 2019;11:6803-14.
23. Ouzzani M, Hammady H, Fedorowicz Z, et al. Rayyan-a web and mobile app for systematic reviews. Syst Rev 2016;5:210.
24. Ma Y, Liu L, Liu J, et al. Prediction of benign and malignant thymic tumors based on radiomics features. In: 2019 IEEE International Conference on Mechatronics and Automation (ICMA). IEEE; 2019.
25. Mayoral M, Pagano AM, Araujo-Filho JAB, et al. Conventional and radiomic features to predict pathology in the preoperative assessment of anterior mediastinal masses. Lung Cancer 2023;178:206-12.
26. Yang Y, Cheng J, Chen L, et al. Application of machine learning for the differentiation of thymomas and thymic cysts using deep transfer learning: A multi-center comparison of diagnostic performance based on different dimensional models. Thorac Cancer 2024;15:2235-47.
27. Yang Y, Cheng J, Peng Z, et al. Development and Validation of Contrast-Enhanced CT-Based Deep Transfer Learning and Combined Clinical-Radiomics Model to Discriminate Thymomas and Thymic Cysts: A Multicenter Study. Acad Radiol 2024;31:1615-28.
28. Zhao W, Ozawa Y, Hara M, et al. Computed tomography radiomic feature analysis of thymic epithelial tumors:

Differentiation of thymic epithelial tumors from thymic cysts and prediction of histological subtypes. Jpn J Radiol 2024;42:367-73.
29. Wang X, You X, Zhang L, et al. A radiomics model combined with XGBoost may improve the accuracy of distinguishing between mediastinal cysts and tumors: a multicenter validation analysis. Ann Transl Med 2021;9:1737.
30. Liu L, Lu F, Pang P, et al. Can computed tomography-based radiomics potentially discriminate between anterior mediastinal cysts and type B1 and B2 thymomas? Biomed Eng Online 2020;19:89.
31. Zhang C, Yang Q, Lin F, et al. CT-Based Radiomics Nomogram for Differentiation of Anterior Mediastinal Thymic Cyst From Thymic Epithelial Tumor. Front Oncol 2021;11:744021.
32. Dai H, Huang Y, Xiao G, et al. Predictive Features of Thymic Carcinoma and High-Risk Thymomas Using Random Forest Analysis. J Comput Assist Tomogr 2020;44:857-64.
33. Ohira R, Yanagawa M, Suzuki Y, et al. CT-based radiomics analysis for differentiation between thymoma and thymic carcinoma. J Thorac Dis 2022;14:1342-52.
34. Tian D, Yan HJ, Shiiya H, et al. Machine learning-based radiomic computed tomography phenotyping of thymic epithelial tumors: Predicting pathological and survival outcomes. J Thorac Cardiovasc Surg 2023;165:502-516.e9.
35. Li J, Cui N, Jiang Z, et al. Differentiating thymic epithelial tumors from mediastinal lymphomas: preoperative nomograms based on PET/CT radiomic features to minimize unnecessary anterior mediastinal surgery. J Cancer Res Clin Oncol 2023;149:14101-12.
36. Xia H, Yu J, Nie K, et al. CT radiomics and human-machine hybrid system for differentiating mediastinal lymphomas from thymic epithelial tumors. Cancer Imaging 2024;24:163.
37. Huang X, Wang X, Liu Y, et al. Contrast-enhanced CT-based radiomics differentiate anterior mediastinum lymphoma from thymoma without myasthenia gravis and calcification. Clin Radiol 2024;79:e500-10.
38. Lin CY, Yen YT, Huang LT, et al. An MRI-Based Clinical-Perfusion Model Predicts Pathological Subtypes of Prevascular Mediastinal Tumors. Diagnostics (Basel) 2022;12:889.
39. Kirienko M, Ninatti G, Cozzi L, et al. Computed tomography (CT)-derived radiomic features differentiate prevascular mediastinum masses as thymic neoplasms versus lymphomas. Radiol Med 2020;125:951-60.
40. Latiri M, Belhocine M, Smith C, et al. DNA methylation as a new tool for the differential diagnosis between T-LBL and lymphocyte-rich thymoma. J Pathol 2024;264:284-92.
41. Dong W, Xiong S, Wang X, et al. Development and validation of a contrast-enhanced CT-based radiomics nomogram for differentiating mass-like thymic hyperplasia and low-risk thymoma. J Cancer Res Clin Oncol 2023;149:14901-10.
42. Agar M, Aydin S, Cakmak M, et al. Detection of Thymoma Disease Using mRMR Feature Selection and Transformer Models. Diagnostics (Basel) 2024;14:2169.
43. Chang CC, Tang EK, Wei YF, et al. Clinical radiomics-based machine learning versus three-dimension convolutional neural network analysis for differentiation of thymic epithelial tumors from other prevascular mediastinal tumors on chest computed tomography scan. Front Oncol 2023;13:1105100.
44. He W, Xia C, Chen X, et al. Computed Tomography-Based Radiomics for Differentiation of Thymic Epithelial Tumors and Lymphomas in Anterior Mediastinum. Front Oncol 2022;12:869982.
45. Shang L, Wang F, Gao Y, et al. Machine-learning classifiers based on non-enhanced computed tomography radiomics to differentiate anterior mediastinal cysts from thymomas and low-risk from high-risk thymomas: A multi-center study. Front Oncol 2022;12:1043163.
46. Zhang L, Xu Z, Feng Y, et al. Risk stratification of thymic epithelial tumors based on peritumor CT radiomics and semantic features. Insights Imaging 2024;15:253.
47. Yoshida Y, Yanagawa M, Sato Y, et al. Differential diagnosis between low-risk and high-risk thymoma: Comparison of diagnostic performance of radiologists with and without deep learning model. Acta Radiol Open 2024;13:20584601241288509.
48. Liu W, Wang W, Guo R, et al. Deep learning for risk stratification of thymoma pathological subtypes based on preoperative CT images. BMC Cancer 2024;24:651.
49. Zhou H, Bai HX, Jiao Z, et al. Deep learning-based radiomic nomogram to predict risk categorization of thymic epithelial tumors: A multicenter study. Eur J Radiol 2023;168:111136.
50. Chen X, Feng B, Xu K, et al. Development and validation of a deep learning radiomics nomogram for preoperatively differentiating thymic epithelial tumor histologic subtypes. Eur Radiol 2023;33:6804-16.
51. Liu W, Wang W, Zhang H, et al. Development and Validation of Multi-Omics Thymoma Risk Classification Model Based on Transfer Learning. J Digit Imaging

2023;36:2015-24.
52. Feng XL, Wang SZ, Chen HH, et al. Optimizing the radiomics-machine-learning model based on non-contrast enhanced CT for the simplified risk categorization of thymic epithelial tumors: A large cohort retrospective study. Lung Cancer 2022;166:150-60.
53. Ozkan E, Orhan K, Soydal C, et al. Combined clinical and specific positron emission tomography/computed tomography-based radiomic features and machine-learning model in prediction of thymoma risk groups. Nucl Med Commun 2022;43:529-39.
54. Nakajo M, Takeda A, Katsuki A, et al. The efficacy of (18)F-FDG-PET-based radiomic and deep-learning features using a machine-learning approach to predict the pathological risk subtypes of thymic epithelial tumors. Br J Radiol 2022;95:20211050.
55. Xiao G, Hu YC, Ren JL, et al. MR imaging of thymomas: a combined radiomics nomogram to predict histologic subtypes. Eur Radiol 2021;31:447-57.
56. Xiao G, Rong WC, Hu YC, et al. MRI Radiomics Analysis for Predicting the Pathologic Classification and TNM Staging of Thymic Epithelial Tumors: A Pilot Study. AJR Am J Roentgenol 2020;214:328-40.
57. Blüthgen C, Patella M, Euler A, et al. Computed tomography radiomics for the prediction of thymic epithelial tumor histology, TNM stage and myasthenia gravis. PLoS One 2021;16:e0261401.
58. Moon YS, Park B, Park J, et al. Identification and risk classification of thymic epithelial tumors using 3D computed tomography images and deep learning models. Biomed Signal Process Control 2024;95:106473.
59. Yu C, Li T, Yang X, et al. Contrast-enhanced CT-based radiomics model for differentiating risk subgroups of thymic epithelial tumors. BMC Med Imaging 2022;22:37.
60. Ren C, Li M, Zhang Y, et al. Development and validation of a CT-texture analysis nomogram for preoperatively differentiating thymic epithelial tumor histologic subtypes. Cancer Imaging 2020;20:86.
61. Hu J, Zhao Y, Li M, et al. Machine-learning-based computed tomography radiomic analysis for histologic subtype classification of thymic epithelial tumours. Eur J Radiol 2020;126:108929.
62. Shen Q, Shan Y, Xu W, et al. Risk stratification of thymic epithelial tumors by using a nomogram combined with radiomic features and TNM staging. Eur Radiol 2021;31:423-35.
63. Chen X, Feng B, Li C, et al. A radiomics model to predict the invasiveness of thymic epithelial tumors based on contrast-enhanced computed tomography. Oncol Rep 2020;43:1256-66.
64. Dong W, Xiong S, Lei P, et al. Application of a combined radiomics nomogram based on CE-CT in the preoperative prediction of thymomas risk categorization. Front Oncol 2022;12:944005.
65. Liang Z, Li J, Tang Y, et al. Predicting the risk category of thymoma with machine learning-based computed tomography radiomics signatures and their between-imaging phase differences. Sci Rep 2024;14:19215.
66. Liu J, Yin P, Wang S, et al. CT-Based Radiomics Signatures for Predicting the Risk Categorization of Thymic Epithelial Tumors. Front Oncol 2021;11:628534.
67. Liu W, Wang W, Guo M, et al. Tumor habitat and peritumoral region evolution-based imaging features to assess risk categorization of thymomas. Clin Radiol 2024;79:e1117-25.
68. Liufu Y, Wen Y, Wu W, et al. Radiomics Analysis of Multiphasic Computed Tomography Images for Distinguishing High-Risk Thymic Epithelial Tumors From Low-Risk Thymic Epithelial Tumors. J Comput Assist Tomogr 2023;47:220-8.
69. Kayi Cangir A, Orhan K, Kahya Y, et al. CT imaging-based machine learning model: a potential modality for predicting low-risk and high-risk groups of thymoma: "Impact of surgical modality choice". World J Surg Oncol 2021;19:147.
70. Wang X, Sun W, Liang H, et al. Radiomics Signatures of Computed Tomography Imaging for Predicting Risk Categorization and Clinical Stage of Thymomas. Biomed Res Int 2019;2019:3616852.
71. Sui H, Liu L, Li X, et al. CT-based radiomics features analysis for predicting the risk of anterior mediastinal lesions. J Thorac Dis 2019;11:1809-18.
72. Li Z, Wang F, Zhang H, et al. The predictive value of a computed tomography-based radiomics model for the surgical separability of thymic epithelial tumors from the superior vena cava and the left innominate vein. Quant Imaging Med Surg 2023;13:5622-40.
73. Onozato Y, Suzuki H, Matsumoto H, et al. Machine learning models from computed tomography to diagnose thymic epithelial tumors requiring combined resection. J Thorac Dis 2024;16:4935-46.
74. Yang L, Cai W, Yang X, et al. Development of a deep learning model for classifying thymoma as Masaoka-Koga stage I or II via preoperative CT images. Ann Transl Med 2020;8:287.
75. Araujo-Filho JAB, Mayoral M, Zheng J, et al. CT

Radiomic Features for Predicting Resectability and TNM Staging in Thymic Epithelial Tumors. Ann Thorac Surg 2022;113:957-65.
76. Li J, Sun W, Feng X, et al. A dense connection encoding–decoding convolutional neural network structure for semantic segmentation of thymoma. Neurocomputing 2021;451:1-11.
77. Li J, Sun W, Feng X, et al. A hybrid network integrated convolution and Transformer for thymoma segmentation. Intell Med 2023;03:164-72.
78. Li J, Sun W, von Deneen KM, et al. MG-Net: Multi-level global-aware network for thymoma segmentation. Comput Biol Med 2023;155:106635.
79. Wang C, Du X, Yan X, et al. Weakly supervised learning in thymoma histopathology classification: an interpretable approach. Front Med (Lausanne) 2024;11:1501875.
80. Lv Q, Liang K, Tian C, et al. Unveiling Thymoma Typing Through Hyperspectral Imaging and Deep Learning. J Biophotonics 2024;17:e202400325.
81. Zhang H, Chen H, Qin J, et al. MC-ViT: Multi-path cross-scale vision transformer for thymoma histopathology whole slide image typing. Front Oncol 2022;12:925903.
82. Zhang H, Liu J, Liu W, et al. MHD-Net: Memory-Aware Hetero-Modal Distillation Network for Thymic Epithelial Tumor Typing With Missing Pathology Modality. IEEE J Biomed Health Inform 2024;28:3003-14.
83. Kim DH, Lim Y, Kim S, et al. Artificial intelligence-powered spatial analysis of tumor-infiltrating lymphocytes as a biomarker in locally advanced unresectable thymic epithelial neoplasm: A single-center, retrospective, longitudinal cohort study. Thorac Cancer 2023;14:3001-11.
84. Yang Y, Xie L, Li C, et al. Prognostic Model of Eleven Genes Based on the Immune Microenvironment in Patients With Thymoma. Front Genet 2022;13:668696.
85. Zhang X, Zeng B, Zhu H, et al. Role of glycosphingolipid biosynthesis coregulators in malignant progression of thymoma. Int J Biol Sci 2023;19:4442-56.
86. Han S, Oh JS, Kim YI, et al. Fully Automatic Quantitative Measurement of 18F-FDG PET/CT in Thymic Epithelial Tumors Using a Convolutional Neural Network. Clin Nucl Med 2022;47:590-8.
87. Su Y, Chen Y, Tian Z, et al. lncRNAs classifier to accurately predict the recurrence of thymic epithelial tumors. Thorac Cancer 2020;11:1773-83.
88. Zhou Z, Lu Y, Gu Z, et al. HNRNPA2B1 as a potential therapeutic target for thymic epithelial tumor recurrence: An integrative network analysis. Comput Biol Med 2023;155:106665.
89. Wojtara M, Rana E, Rahman T, et al. Artificial intelligence in rare disease diagnosis and treatment. Clin Transl Sci 2023;16:2106-11.

doi: 10.21037/med-25-34
Cite this article as: Esteve Domínguez AS, Dimmers M, Mulders TA, Dumoulin D, De Ruysscher D, Peeters S, von der Thüsen J, Akram F. Artificial intelligence for diagnosis and prognosis of thymic epithelial tumors: a systematic review. Mediastinum 2025;9:27.

Supplementary

Appendix 1 Search results on Mach 2025, with detailed use of search terms in each database.
20250213 Anna Salut Esteve Domínguez
Thymic Epithelial Tumours medical imaging AI

Database searched	Platform	Years of coverage	Records	Records after duplicates removed
Medline ALL	Ovid	1946–Present	230	230
Embase	Embase.com	1971–Present	440	272
Web of Science Core Collection*	Web of Knowledge	1975–Present	186	27
Cochrane Central Register of Controlled Trial	Wiley	1992–Present	7	4
CINAHL Plus	EBSCO	1982–Present	35	2
Additional Search Engines: Google Scholar**			100	47
Total			998	582

*Science Citation Index Expanded (1975-present); Social Sciences Citation Index (1975–present); Arts & Humanities Citation Index (1975–present) ; Conference Proceedings Citation Index-Science (1990–present); Conference Proceedings Citation Index-Social Science & Humanities (1990–present); Emerging Sources Citation Index (2005-present). **Google Scholar was searched via "Publish or Perish" to download the results in EndNote. No other database limits were used than those specified in the search strategies.

Medline 230

(exp Thymus Neoplasms / OR (thymoma* OR ((thymus* OR thymic) ADJ6 (carcin* OR neoplas* OR cancer* OR tumo*))).ab,ti,kw.) AND (exp Artificial Intelligence/ OR exp Machine Learning/ OR * Algorithms/ OR * Automation/ OR ((Algorithms/ OR Automation/) AND (exp Classification/ OR exp Diagnosis/ OR Image Processing, Computer-Assisted / OR exp Diagnostic Imaging/ OR Nomograms/ OR Prognosis/ OR Immunohistochemistry/)) OR Prediction Algorithms/ OR Machine Learning Algorithms/ OR Predictive Learning Models/ OR Classification Algorithms/ OR ((artificial* ADJ3 intelligen*) OR ((machine OR deep OR predict*) ADJ learning) OR ((automat* OR algorithm* OR model*) ADJ3 (classific* OR categori* OR sybtyp* OR predict* OR prognos* OR metasta* OR relaps* OR surviv* OR recur* OR diagnos* OR medical-imag* OR image-analy* OR ct OR tomogra* OR radiolog* OR radiomic* OR mri OR magnet*-resonan* OR perfusion* OR histolog* OR histopatholog* OR histochem* OR immunohistochem* OR nomogra* OR clinical-feature* OR clinical-data* OR clinical-character*)) OR ((CT or nomogram* OR imag* OR mri) ADJ6 (predict* OR classif* OR categori*) ADJ6 (prognos* OR relaps* OR surviv* OR recur*)) OR ((digital* OR machine) ADJ3 (radiolog* OR radiomic* OR histolog* OR histopatholog* OR histochem* OR immunohistochem*)) OR (neural* ADJ3 network*) OR Feature-select* OR Data-mining*).ab,ti,kw. OR (classifier* OR automat* OR algorithm*).ti.) NOT (exp animals/ NOT humans/)

Embase 440

('thymic neoplasm'/exp OR (thymoma* OR ((thymus* OR thymic) NEAR/6 (carcin* OR neoplas* OR cancer* OR tumo*))):ab,ti,kw) AND ('artificial intelligence'/exp OR 'machine learning'/exp OR algorithm/mj OR automation/mj OR ((algorithm/de OR automation/de) AND (classification/exp OR diagnosis/exp OR 'diagnostic value'/exp OR 'image analysis'/exp OR 'cancer prognosis'/de OR 'cancer survival'/de OR 'cancer recurrence'/de OR 'diagnostic imaging'/exp OR nomogram/de OR prediction/de OR prognosis/de OR immunohistochemistry/exp OR 'diagnostic accuracy'/exp OR 'clinical feature'/exp)) OR 'predictive model'/exp OR ((artificial* NEAR/3 intelligen*) OR ((machine OR deep OR predict*) NEXT/1 learning) OR ((automat* OR algorithm* OR model*) NEAR/3 (classific* OR categori* OR sybtyp* OR predict* OR prognos* OR metasta* OR relaps* OR surviv* OR recur* OR diagnos* OR medical-imag* OR image-analy* OR ct OR tomogra* OR radiolog* OR radiomic* OR mri OR magnet*-resonan* OR perfusion* OR histolog* OR histopatholog* OR histochem* OR immunohistochem* OR nomogra* OR clinical-feature* OR clinical-data* OR clinical-character*)) OR ((CT or nomogram* OR imag* OR mri) NEAR/6 (predict* OR classif* OR categori*) NEAR/6 (prognos* OR relaps* OR surviv* OR recur*)) OR ((digital* OR machine) NEAR/3 (radiolog* OR radiomic* OR histolog* OR histopatholog* OR histochem* OR immunohistochem*)) OR (neural* NEAR/3 network*) OR Feature-select* OR Data-mining*):ab,ti,kw OR (classifier* OR automat* OR algorithm*):ti) NOT ([animals]/lim NOT [humans]/lim)

https://dx.doi.org/10.21037/med-25-34

Web of science 186

(TS=(thymoma* OR ((thymus* OR thymic) NEAR/5 (carcin* OR neoplas* OR cancer* OR tumo*)))) AND (TS=((artificial* NEAR/2 intelligen*) OR ((machine OR deep OR predict*) NEAR/1 learning) OR ((automat* OR algorithm* OR model*) NEAR/2 (classific* OR categori* OR sybtyp* OR predict* OR prognos* OR metasta* OR relaps* OR surviv* OR recur* OR diagnos* OR medical-imag* OR image-analy* OR ct OR tomogra* OR radiolog* OR radiomic* OR mri OR magnet*-resonan* OR perfusion* OR histolog* OR histopatholog* OR histochem* OR immunohistochem* OR nomogra* OR clinical-feature* OR clinical-data* OR clinical-character*)) OR ((CT or nomogram* OR imag* OR mri) NEAR/5 (predict* OR classif* OR categori*) NEAR/5 (prognos* OR relaps* OR surviv* OR recur*)) OR ((digital* OR machine) NEAR/2 (radiolog* OR radiomic* OR histolog* OR histopatholog* OR histochem* OR immunohistochem*)) OR (neural* NEAR/2 network*) OR Feature-select* OR Data-mining*) OR TI=(classifier* OR automat* OR algorithm*)) NOT DT=(Meeting Abstract OR Meeting Summary) AND LA=(English)

Cochrane 7

((thymoma* OR ((thymus* OR thymic) NEAR/6 (carcin* OR neoplas* OR cancer* OR tumo*))):ab,ti,kw) AND (((artificial* NEAR/3 intelligen*) OR ((machine OR deep OR predict*) NEXT/1 learning) OR ((automat* OR algorithm* OR model*) NEAR/3 (classific* OR categori* OR sybtyp* OR predict* OR prognos* OR metasta* OR relaps* OR surviv* OR recur* OR diagnos* OR medical-imag* OR image-analy* OR ct OR tomogra* OR radiolog* OR radiomic* OR mri OR magnet* NEXT resonan* OR perfusion* OR histolog* OR histopatholog* OR histochem* OR immunohistochem* OR nomogra* OR clinical-feature* OR clinical-data* OR clinical-character*)) OR ((CT or nomogram* OR imag* OR mri) NEAR/6 (predict* OR classif* OR categori*) NEAR/6 (prognos* OR relaps* OR surviv* OR recur*)) OR ((digital* OR machine) NEAR/3 (radiolog* OR radiomic* OR histolog* OR histopatholog* OR histochem* OR immunohistochem*)) OR (neural* NEAR/3 network*) OR Feature-select* OR Data-mining*):ab,ti,kw OR (classifier* OR automat* OR algorithm*):ti)

("conference abstract":kw OR Trial registry record:pt)

#1 NOT #2

CINAHL 35

(MH Thymus Neoplasms + OR TI(thymoma* OR ((thymus* OR thymic) N5 (carcin* OR neoplas* OR cancer* OR tumo*))) OR AB(thymoma* OR ((thymus* OR thymic) N5 (carcin* OR neoplas* OR cancer* OR tumo*)))) AND (MH Artificial Intelligence+ OR MH Machine Learning+ OR MM Algorithms OR MM Automation+ OR ((MH Algorithms+ OR MH Automation+) AND (MH Classification+ OR MH Diagnosis+ OR MH Image Processing, Computer-Assisted OR MH Diagnostic Imaging+ OR MH Prognosis OR MH Immunohistochemistry)) OR MH Prediction Algorithms+ OR MH Machine Learning Algorithms+ OR MH Prediction Models + OR MH Classification Algorithms+ OR TI((artificial* N2 intelligen*) OR ((machine OR deep OR predict*) N1 learning) OR ((automat* OR algorithm* OR model*) N2 (classific* OR categori* OR sybtyp* OR predict* OR prognos* OR metasta* OR relaps* OR surviv* OR recur* OR diagnos* OR medical-imag* OR image-analy* OR ct OR tomogra* OR radiolog* OR radiomic* OR mri OR magnet*-resonan* OR perfusion* OR histolog* OR histopatholog* OR histochem* OR immunohistochem* OR nomogra* OR clinical-feature* OR clinical-data* OR clinical-character*)) OR ((("CT" OR nomogram* OR imag* OR mri) N5 (predict* OR classif* OR categori*) N5 (prognos* OR relaps* OR surviv* OR recur*)) OR ((digital* OR machine) N2 (radiolog* OR radiomic* OR histolog* OR histopatholog* OR histochem* OR immunohistochem*)) OR (neural* N2 network*) OR Feature-select* OR Data-mining*) OR AB((artificial* N2 intelligen*) OR ((machine OR deep OR predict*) N1 learning) OR ((automat* OR algorithm* OR model*) N2 (classific* OR categori* OR sybtyp* OR predict* OR prognos* OR metasta* OR relaps* OR surviv* OR recur* OR diagnos* OR medical-imag* OR image-analy* OR ct OR tomogra* OR radiolog* OR radiomic* OR mri OR magnet*-resonan* OR perfusion* OR histolog* OR histopatholog* OR histochem* OR immunohistochem* OR nomogra* OR clinical-feature* OR clinical-data* OR clinical-character*)) OR (("CT" OR nomogram* OR imag* OR mri) N5 (predict* OR classif* OR categori*) N5 (prognos* OR relaps* OR surviv* OR recur*)) OR ((digital* OR machine) N2 (radiolog* OR radiomic* OR histolog* OR histopatholog* OR histochem* OR immunohistochem*)) OR (neural* N2 network*) OR Feature-select* OR Data-mining*) OR TI(classifier* OR automat* OR algorithm*)) NOT (MH animals+ NOT MH humans)

Google scholar

thymoma | 'thymus | thymic epithelial | carcinoma | neoplasm | cancer | tumor | tumour' 'artificial intelligence' | 'machine | deep | predictive learning' | 'automated classification' | 'classification | prognostic algorithm'

https://dx.doi.org/10.21037/med-25-34

Superior vena cava resection without venous reconstruction for thymic tumors: a report of two cases

Xiuxiu Hao, Zhitao Gu, Xuefei Zhang, Ning Xu, Fenghao Yu, Haoran Liu, Teng Mao, Wentao Fang

Department of Thoracic Surgery, Shanghai Chest Hospital, School of Medicine, Shanghai Jiao Tong University, Shanghai, China

Contributions: (I) Conception and design: W Fang, T Mao, X Hao; (II) Administrative support: W Fang, T Mao; (III) Provision of study materials or patients: W Fang, T Mao, X Hao; (IV) Collection and assembly of data: X Hao, H Liu, X Zhang, N Xu, F Yu, H Liu; (V) Data analysis and interpretation: X Hao, Z Gu; (VI) Manuscript writing: All authors; (VII) Final approval of manuscript: All authors.

Correspondence to: Wentao Fang, MD; Teng Mao, MD. Department of Thoracic Surgery, Shanghai Chest Hospital, School of Medicine, Shanghai Jiao Tong University, 241 Huaihai Road West, Shanghai 200030, China. Email: vwtfang@hotmail.com; hippomao@hotmail.com.

Background: Venous reconstruction is required in patients with superior vena cava (SVC) resection to maintain sufficient blood flow to avoid severe complications such as cerebral edema. However, venous reconstruction might not be needed in selected patients with well-established collateral circulations under internal jugular vein pressure (IJVP) monitoring.

Case Description: In November 2020, a 57-year-old female patient presented with an anterior mediastinal mass after B2 thymoma resection for 8 years. A core needle biopsy suggested recurrence of B2 thymoma. The patient received sequential chemoradiotherapy (SCRT) and had a partial response. She underwent median sternotomy in April 2021. A collateral vessel from left innominate vein was found to descend along the left side of aortic arch. IJVP was 29 cmH_2O after clamping the SVC. The tumor and invaded structures were removed without SVC reconstruction and the azygos vein was reserved. The patient was discharged 8 days after surgery without obstructive symptoms. No tumor recurrence was found after a 44-month follow-up and abundant collateral circulations were found in postoperative imaging. In July 2022, a 56-year-old female patient with B2 thymoma was treated with concurrent chemoradiotherapy and additional 3-cycle chemotherapy before presenting to our hospital. The tumor invaded the SVC and the azygos vein, and there was tumor embolism inside the SVC. Thrombectomy in the SVC was attempted but was unsuccessful. But the IJVP was 25 cmH_2O after clamping the SVC and the azygos vein. Then the SVC, bilateral innominate veins, and azygos vein were resected without venous reconstruction. The patient was discharged 12 days after surgery without severe graft-related complications. After a 31-month follow-up, collateral circulations were more abundant and there was no recurrence of tumor.

Conclusions: To our knowledge, this is the first successful attempt of SVC resection alone without venous reconstruction and we reported long-term results. SVC resection alone under the safe threshold of IJVP was feasible and safe in selected patients with abundant collateral circulations. Patients could benefit from less surgical trauma and be spared of anticoagulants after surgery.

Keywords: Superior vena cava (SVC); mediastinal tumor; vascular prosthesis; venous pressure; case report

Received: 28 June 2025; Accepted: 02 September 2025; Published online: 26 September 2025.

doi: 10.21037/med-25-35

View this article at: https://dx.doi.org/10.21037/med-25-35

Introduction

When superior vena cava (SVC) is invaded by anterior mediastinal tumors such as thymic tumors, *en bloc* resection of the tumor and SVC are required for resectable diseases. Venous reconstruction is necessary if the SVC and/or bilateral innominate veins are resected to avoid severe complications such as cerebral edema (1-10). The surgical procedure is challenging and traumatic, and the use of bypass grafts necessitates lifelong anticoagulation therapy.

However, even with long-term anticoagulation therapy, the graft could be totally obstructed after unilateral reconstruction. Patients might not have obstructive symptoms while collateral circulations provide for venous flow from the head returning to the heart. And prior to surgery, abundant collateral circulations might develop when the initial innominate vein-SVC route is blocked due to tumor invasion (11). This led us to suppose that venous reconstruction may not always be necessary after SVC resection if there is adequate blood return to the heart through collateral circulations, and therefore negating the need for postoperative anticoagulation. We previously found that internal jugular vein pressure (IJVP) could be a feasible objective measurement of sufficient blood return from the head and upper limbs (1). The safety upper limit of 30 cmH_2O IJVP could safely guide reconstruction strategy, whether to do bilateral or only unilateral venous bypass. If IJVP is under 30 cmH_2O after SVC resection then venous reconstruction could be avoided in selected patients. Here, we present 2 cases of patients having SVC resection without venous reconstruction under the guidance of IJVP monitoring. We present this article in accordance with the CARE reporting checklist (available at https://med.amegroups.com/article/view/10.21037/med-25-35/rc).

Highlight box

Key findings

- This study reported two cases of superior vena cava (SVC) resection without venous reconstruction for thymic tumors.
- Using the internal jugular vein pressure (IJVP) monitoring guided strategy, SVC could be resected only without venous reconstruction in selected patients.
- The surgical procedure is less complex and anticoagulation therapy is exempted.

What is known and what is new?

- When SVC is resected, the traditional teaching is that venous reconstruction should be carried out to maintain sufficient blood returning to the heart to avoid severe complications such as cerebral edema.
- SVC resection alone under the safe threshold of 30 cmH_2O IJVP was feasible and safe in selected patients with abundant collateral circulations.

What is the implication, and what should change now?

- Well-developed collateral circulation may enable adequate venous return to the heart without resulting in cerebral edema even if the primary innominate vein-SVC route is blocked. The 30 cmH_2O threshold IJVP could be useful in selecting patients who could have SVC resection alone without venous reconstruction.

Case presentation

All procedures in this study were performed in accordance with the ethical standards of the institutional research committee and with the Declaration of Helsinki and its subsequent amendments. Written informed consent was obtained from the patients for the publication of this case report and accompanying images. A copy of the written consent is available for review by the editorial office of this journal.

Case 1

A 57-year-old female patient was admitted to Shanghai Chest Hospital in November 2020 with an anterior mediastinal mass after a B2 thymoma resection 8 years before. Chest computed tomography (CT) revealed an 84mm right anterior mass invading the right lung, bilateral innominate veins, and SVC, with tumor embolism inside the SVC (*Figure 1A*). Core needle biopsy suggested recurrence of B2 thymoma. After sequential chemoradiotherapy (SCRT), the patient had partial response (PR) and CT revealed the tumor still invaded the right lung, bilateral innominate veins, and SVC, but tumor embolism was not obvious (*Figure 1B*). The left superior intercostal vein ran down the left side of the aortic arch from the left innominate vein to the azygos vein (*Figure 1*). The azygos was not invaded by the tumor.

The patient underwent median sternotomy with preparation for SVC reconstruction in April 2021. A right internal jugular vein catheter was placed to monitor IJVP. A radial arterial line was inserted to monitor the systemic blood pressure during surgery. The mass invaded the right upper lobe, bilateral innominate veins and SVC. The enlarged left superior intercostal vein originated from left innominate vein and descended along the left lateral side of aortic arch and joined the azygos vein (*Figure 2A*). IJVP was found to be 29 cmH_2O after clamping the SVC. The tumor and the invaded structures were removed without SVC reconstruction and the azygos vein was reserved (*Figure 2B*). No obstructive complications were found postoperatively. Operation time was 167 minutes and blood loss was 1,000 mL. The patient started to ambulate on the 2nd postoperative day and was discharged 8 days after surgery. Pathological examination showed mixed thymic carcinoma with 20% thymic squamous cell carcinoma and 80% B2 thymoma. The tumor invaded pericardium, lung, SVC and bilateral innominate veins.

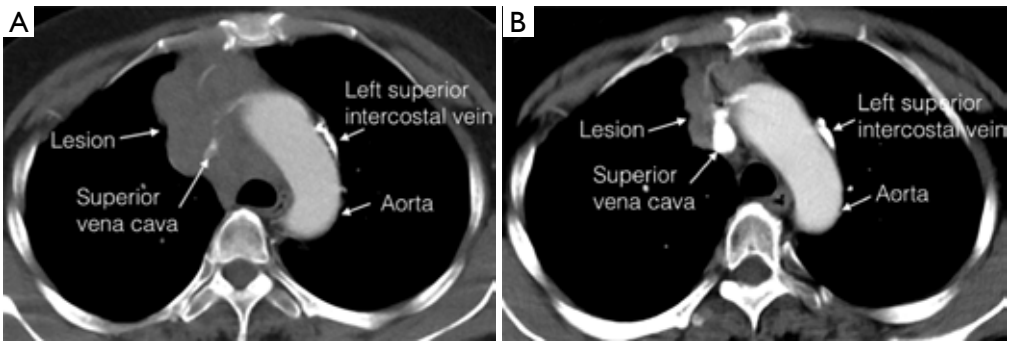

Figure 1 The preoperative chest computed tomography of case 1 patient. (A) The initial chest computed tomography of case 1 patient. (B) The chest computed tomography after sequential chemoradiotherapy of case 1 patient.

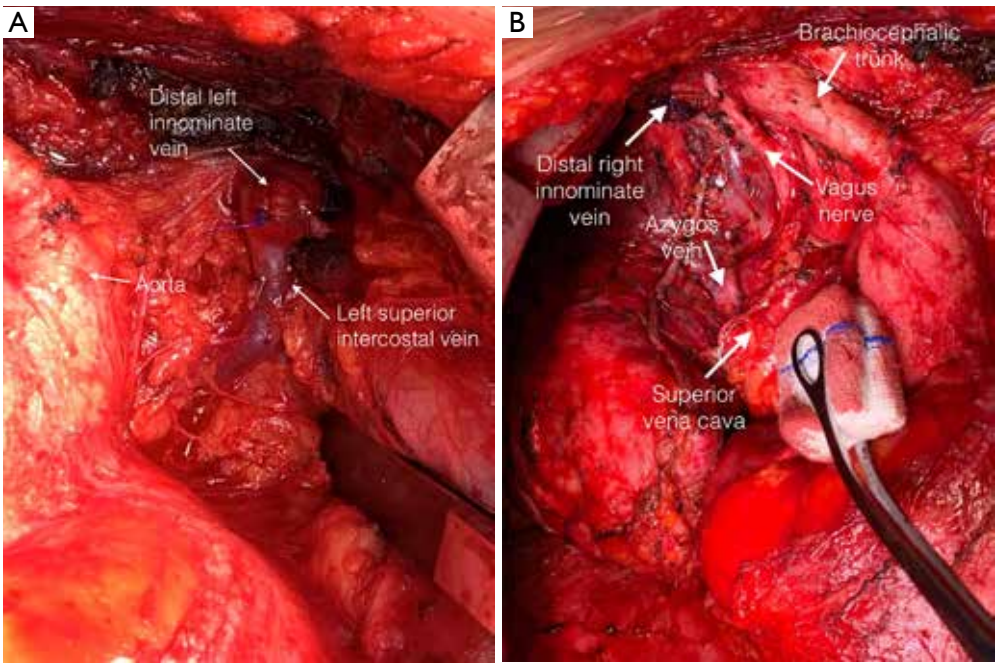

Figure 2 The intraoperative finding of case 1 patient. (A) The enlarged left superior intercostal vein originated from left innominate vein and descended along the left lateral side of aortic arch in case 1 patient. (B) The resection of superior vena cava and bilateral innominate veins without venous reconstruction and the azygos vein was reserved in case 1 patient.

No tumor recurrence was found after a 44-month follow-up and abundant collateral circulations could be seen in postoperative imaging (*Figure 3*).

Case 2

A 56-year-old female patient with facial swelling was diagnosed with B2 thymoma and received chemoradiotherapy prior to attending Shanghai Chest Hospital in July 2022. Chest CT scan revealed a 67-mm right anterior mediastinal mass invading the right lung, bilateral innominate veins, and SVC, with tumor embolism inside SVC but not invaded right atrium (*Figure 4A*). After concurrent chemoradiotherapy, the patient had PR but the tumor was still potentially unresectable, so additional 3-cycle chemotherapy was performed but with stable disease in another hospital. The chest CT scan before surgery revealed noticeable tumor shrinkage, but there was still active lesion in front of the

aorta and inside the SVC (*Figure 4B*,*4C*).

The patient underwent median sternotomy under IJVP monitoring in July 2022. The tumor invaded the SVC and azygos vein and the tumor embolism inside SVC was obvious. Thrombectomy through SVC was attempted by clamping the SVC proximally and the bilateral innominate veins distally. Unfortunately, the embolism was found to be impossible to remove completely. But IJVP was only 25 cmH_2O after clamping the SVC, innominate veins, and the azygos. Then the SVC, bilateral innominate veins and azygos vein were resected without venous reconstruction (*Figure 5*). No facial and bulbar conjunctival swelling was observed during the operation. The operation time was 245 minutes and blood loss was 600 mL. The patient did not have severe graft-related complications postoperatively and stayed in ICU for 5 days. The patient was discharged from the hospital 12 days after surgery. Pathological examination showed B3 thymoma with invasion of pericardium, lung, SVC and bilateral innominate veins.

The patient already had collateral circulations before surgery and more abundant collateral circulations could be seen after SVC resection alone without venous reconstruction (*Figure 6*). After a 31-month follow-up, there was no recurrence of tumor (*Figure 7*).

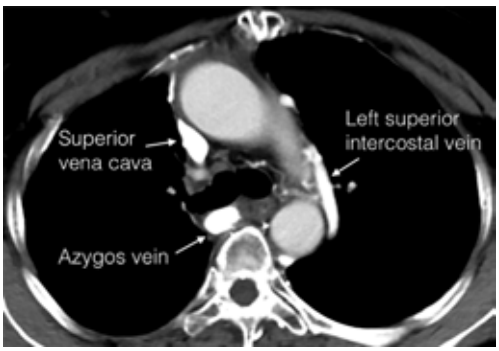

Figure 3 The chest computed tomography of case 1 patient after surgery 44 months. There was no tumor recurrence.

Discussion

We reported two cases of SVC resection alone without venous reconstruction for thymic tumors, one with the azygos vein reserved and the other with azygos vein resected. These patients recovered well without severe obstructive complications and did not require anticoagulation therapy. Long-term follow-up showed obvious collateral circulations and no tumor recurrence.

SVC receives blood return from the internal jugular veins, subclavian veins, azygos vein and smaller veins such as the internal mammary and thyroid from head, neck and upper limbs. When the SVC is resected for tumor invasion, the traditional teaching is that venous reconstruction should be followed to avoid severe or fatal complications such as cerebral edema. The surgical procedure of SVC resection and reconstruction requires continuous arterial and venous pressure measurements. Dartevelle and colleagues found that the cranial venous pressure may rise up to 40 mmHg during venous clamping, while volume expansion could maintain a subnormal arterial-venous brain gradient (2). To prevent severe graft-related complications, we used IJVP to objectively assess whether there was sufficient blood flow back to the heart in our previous study (1). We found the safety upper limit of IJVP was 30 cmH_2O and IJVP-monitoring guided surgical strategy is feasible and safe

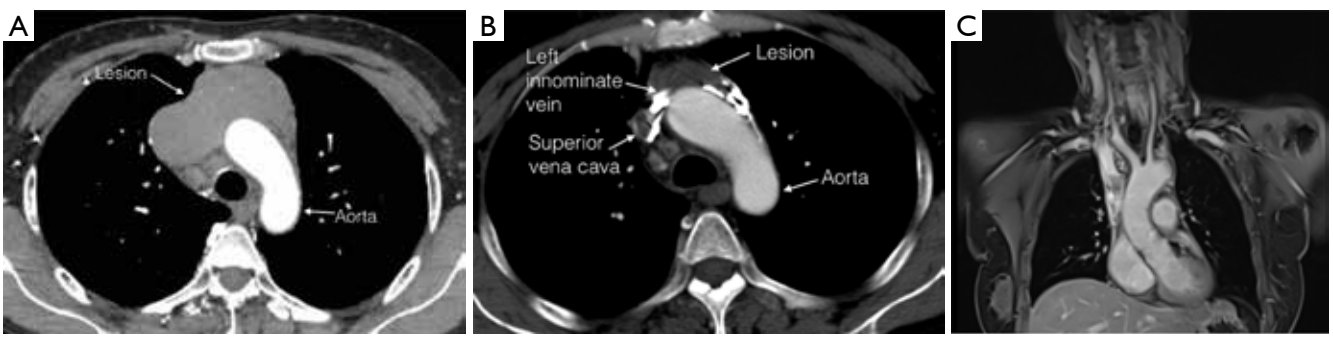

Figure 4 The preoperative chest computed tomography of case 2 patient. (A) The initial chest computed tomography of case 2 patient. (B) The chest computed tomography after concurrent chemoradiotherapy and additional 3-cycle chemotherapy of case 2 patient. (C) The chest magnetic resonance imaging after concurrent chemoradiotherapy and additional 3-cycle chemotherapy of case 2 patient.

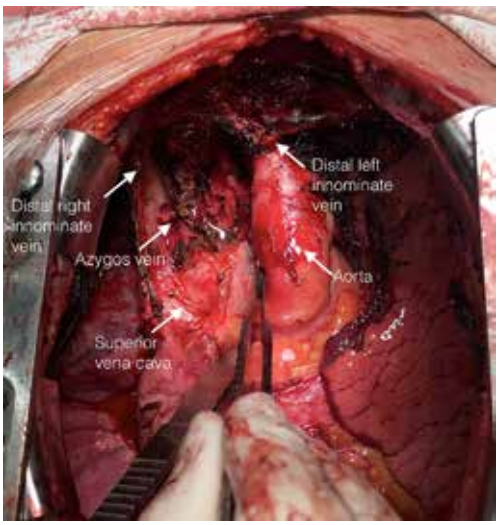

Figure 5 The resection of superior vena cava, bilateral innominate veins and azygos vein without venous reconstruction in case 2 patient.

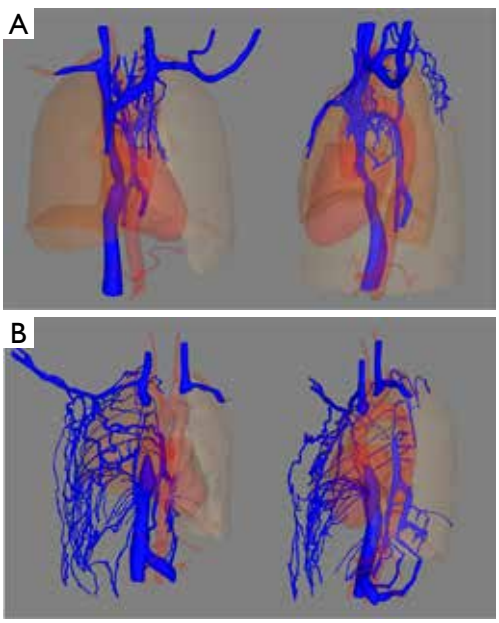

Figure 6 The three-dimensional reconstruction chest computed tomography imaging of case 2 patient. (A) Existing venous collaterals before surgery in three-dimensional reconstruction chest computed tomography imaging in case 2 patient with superior vena cava resection without venous reconstruction. (B) More abundant collaterals after surgery in three-dimensional reconstruction chest computed tomography imaging in case 2 patient with superior vena cava resection without venous reconstruction.

Figure 7 The chest computed tomography of case 2 patient after surgery 31 months. There was no tumor recurrence.

in the SVC resection and reconstruction. Therefore, we further use this safe IJVP limit to explore SVC resection alone in selected patients with abundant collateral circulations. And we routinely prepared for venous reconstruction to maintain adequate blood flow if the IJVP was above 30 cmH_2O when clamping SVC (1).

Collateral circulations may develop after chronic SVC obstruction (11). In case 1, preoperative imaging showed that the patients had an obvious collateral vein on the left side of the aortic arch originating from the left innominate vein but it was hard to know if the collateral circulations could completely compensate for the loss of the SVC-innominate vein route. So, we prepared for venous reconstruction before surgery and used intraoperative IJVP to decide whether to perform the reconstruction. We also found a thick collateral vein (left superior intercostal vein) consistent with the imaging intraoperatively (*Figure 2B*). IJVP was below 30 cmH_2O when clamping the SVC, supposing adequate blood return to the heart. Therefore, SVC and bilateral innominate veins were resected without venous reconstruction, while azygos vein were reserved. In case 2, the tumor invaded inside the SVC and azygos vein was also invaded. When clamping the SVC and azygos vein, IJVP was also below 30 cmH_2O and therefore SVC, bilateral innominate veins and azygos vein were resected without venous reconstruction. These patients recovered well postoperatively without severe obstructive complications. Long-term follow-up showed more abundant collateral circulations and no recurrence of tumor.

Postoperative anticoagulation therapy is recommended after SVC resection and reconstruction to maintain the graft patency (3,5-7). Our former experiences for patients

with SVC resection and reconstruction included continuous anti-coagulation therapy with low molecular-weight heparin in hospital and oral anticoagulant maintenance after discharge. Use of anticoagulants could result in bleeding, thrombocytopenia and nonbleeding complications such as vascular calcification, anticoagulation-related nephropathy, and osteoporosis (12,13). And patients have to take routine coagulation tests during anticoagulation therapy. Anticoagulation therapy is no longer required for patients without the use of prosthetic grafts.

Conclusions

To our knowledge, this is the first successful attempt of SVC resection alone without venous reconstruction with long-term follow-up results. SVC resection alone under IJVP monitoring was feasible and safe in selected patients. The surgical strategy could benefit patients from less surgical trauma and avoidance of anticoagulants.

Acknowledgments

None.

Footnote

Reporting Checklist: The authors have completed the CARE reporting checklist. Available at https://med.amegroups.com/article/view/10.21037/med-25-35/rc

Peer Review File: Available at https://med.amegroups.com/article/view/10.21037/med-25-35/prf

Funding: This study was supported by the National Natural Science Foundation of China (No. 82072569) and Shanghai Chest Hospital Multidisciplinary Collaborative Clinical Research Innovation Project (No. YJXT20190104).

Conflicts of Interest: All authors have completed the ICMJE uniform disclosure form (available at https://med.amegroups.com/article/view/10.21037/med-25-35/coif). W.F. serves as the Editor-in-Chief of *Mediastinum* from March 2017 to March 2027. The other authors have no conflicts of interest to declare.

Ethical Statement: The authors are accountable for all aspects of the work in ensuring that questions related to the accuracy or integrity of any part of the work are appropriately investigated and resolved. All procedures in this study were performed in accordance with the ethical standards of the institutional research committee and with the Declaration of Helsinki and its subsequent amendments. Written informed consent was obtained from the patients for the publication of this case report and accompanying images. A copy of the written consent is available for review by the editorial office of this journal.

References

1. Hao X, Gu Z, Liu H, et al. Internal jugular vein pressure monitoring guided venous reconstruction could improve perioperative safety after superior vena cava resection for mediastinal tumors: a cohort study. Int J Surg 2024;110:2730-7.
2. Dartevelle P, Macchiarini P, Chapelier A. Technique of superior vena cava resection and reconstruction. Chest Surg Clin N Am 1995;5:345-58.
3. Dartevelle PG, Chapelier AR, Pastorino U, et al. Long-term follow-up after prosthetic replacement of the superior vena cava combined with resection of mediastinal-pulmonary malignant tumors. J Thorac Cardiovasc Surg 1991;102:259-65.
4. Suzuki K, Asamura H, Watanabe S, et al. Combined resection of superior vena cava for lung carcinoma: prognostic significance of patterns of superior vena cava invasion. Ann Thorac Surg 2004;78:1184-9; discussion 1184-9.
5. Shintani Y, Ohta M, Minami M, et al. Long-term graft patency after replacement of the brachiocephalic veins combined with resection of mediastinal tumors. J Thorac Cardiovasc Surg 2005;129:809-12.
6. Spaggiari L, Leo F, Veronesi G, et al. Superior vena cava resection for lung and mediastinal malignancies: a single-center experience with 70 cases. Ann Thorac Surg 2007;83:223-9; discussion 229-30.
7. Lanuti M, De Delva PE, Gaissert HA, et al. Review of

superior vena cava resection in the management of benign disease and pulmonary or mediastinal malignancies. Ann Thorac Surg 2009;88:392-7.
8. Okereke IC, Kesler KA. Superior vena cava and innominate vein reconstruction in thoracic malignancies: single-vein reconstruction. Semin Thorac Cardiovasc Surg 2011;23:323-5.
9. McPhee A, Shaikhrezai K, Berg G. Is it safe to divide and ligate the left innominate vein in complex cardiothoracic surgeries? Interact Cardiovasc Thorac Surg 2013;17:560-3.
10. Bertolaccini L, Prisciandaro E, Galetta D, et al. Outcomes and Safety Analysis in Superior Vena Cava Resection for Extended Thymic Epithelial Tumors. Ann Thorac Surg 2021;112:271-7.
11. Marini TJ, Chughtai K, Nuffer Z, et al. Blood finds a way: pictorial review of thoracic collateral vessels. Insights Imaging 2019;10:63.
12. Piazza G, Nguyen TN, Cios D, et al. Anticoagulation-associated adverse drug events. Am J Med 2011;124:1136-42.
13. Ageno W, Donadini M. Breadth of complications of long-term oral anticoagulant care. Hematology Am Soc Hematol Educ Program 2018;2018:432-8.

doi: 10.21037/med-25-35
Cite this article as: Hao X, Gu Z, Zhang X, Xu N, Yu F, Liu H, Mao T, Fang W. Superior vena cava resection without venous reconstruction for thymic tumors: a report of two cases. Mediastinum 2025;9:28.

Case Report

Case report: awake Chamberlain mediastinotomy under hypnosis to prevent complete airway obstruction and cardiovascular collapse

Lisa Simioni[1]^, Olivia Stiennon[2], Jon Andri Lutz[1], Anna Efthymiou[3], Benoit Rouiller[1]

[1]Thoracic Unit, Department of Surgery, Cantonal Hospital of Fribourg (HFR), Villars-sur-Glâne, Switzerland; [2]Department of Anesthesiology, Cantonal Hospital of Fribourg (HFR), Villars-sur-Glâne, Switzerland; [3]Unit of Hematology, Department of Medicine, Cantonal Hospital of Fribourg (HFR), Villars-sur-Glâne, Switzerland

Contributions: Lisa Simioni, MD. Thoracic Unit, Department of Surgery, Cantonal Hospital of Fribourg (HFR), Chemin des Pensionnats 2, 1752 Villars-sur-Glâne, Switzerland. Email: lisa.simioni@hotmail.com.

Background: Large sized anterior mediastinal masses can be a challenge in thoracic surgery due to the anesthesiological risks. The management of these tumors requires a surgical biopsy to get sufficient tissue for histopathological and immunohistochemical analysis, which are essential for a precise diagnosis and target treatment.

Case Description: We report the case of a 45-year-old woman with a persistent cough and fatigue lasting 2 months. A chest computed tomography (CT) scan revealed a large anterior mediastinal mass. An initial biopsy diagnosed this patient with myeloid sarcoma. However, a further biopsy of fresh tissue was necessary to characterize the tumor to initiate targeted treatment. To avoid complete airway obstruction and cardiovascular collapse due the compression of the anterior mediastinal mass during general anesthesia, we performed a Chamberlain procedure on an awake patient using hypnosis and local anesthesia.

Conclusions: Anterior mediastinotomy according to Chamberlain approach allowed the retrieval of sufficient fresh tissue for an accurate immunohistochemical diagnosis, while avoiding more invasive and traumatic surgical approaches such as sternotomy. This approach is particularly valuable in high-risk patients where general anesthesia could exacerbate airway or cardiovascular collapse. In this context the procedure was successfully performed under local anesthesia and hypnosis in selected patients to avoid anesthesiological risks due the compression that anterior mediastinal mass can exert.

Keywords: Mediastinotomy; Chamberlain procedure; anterior mediastinal mass; hypnosis; case report

Received: 17 April 2025; Accepted: 28 July 2025; Published online: 26 September 2025.
doi: 10.21037/med-25-25
View this article at: https://dx.doi.org/10.21037/med-25-25

Introduction

Anterior mediastinal masses can have a wide range of differential diagnosis. Surgical biopsies can be necessary to get sufficient material and an anterior mediastinotomy according to Chamberlain is a widely used option (1). This approach allows access to the anterior mediastinum avoiding a sternotomy. *Figure 1* illustrates the modified Chamberlain mediastinotomy—i.e., without costotomy. This surgery is usually performed under general anesthesia and carries significant risks for the patients. The principal risks include compression of the superior vena cava leading to a cardiovascular collapse and complete airways obstruction by direct compression of the mass due to the relaxation needed for endotracheal intubation (2-4). We describe a case in which we proceeded to a surgical biopsy through an anterior mediastinotomy under hypnosis and

^ ORCID: 0009-0000-7411-827X.

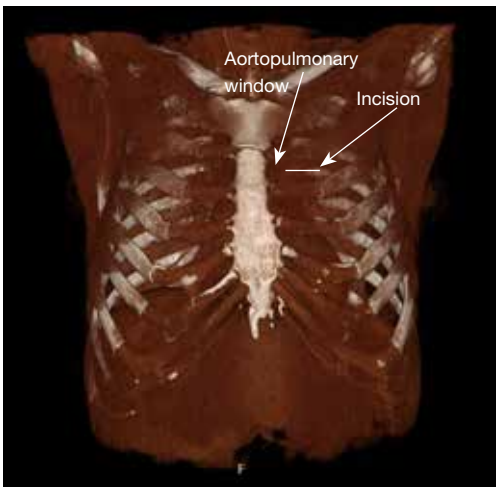

Figure 1 Image of the incision for a Chamberlain mediastinotomy. Incision at the level of the 2nd intercostal space.

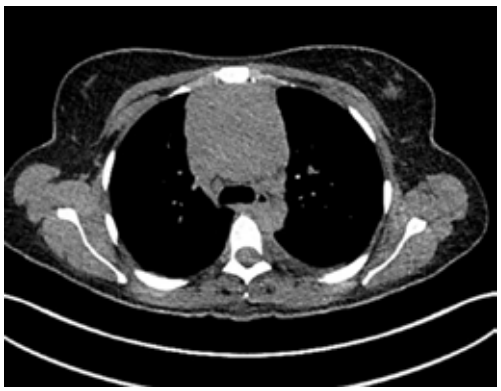

Figure 2 Image of CT scan for diagnosis of the mediastinal mass. CT, computed tomography.

Highlight box

Key findings

- Anterior mediastinotomy according to Chamberlain approach allowed the retrieval of sufficient fresh tissue for an accurate immunohistochemical diagnosis, while avoiding more invasive and traumatic surgical approaches such as sternotomy. This approach is particularly valuable in high-risk patients where general anesthesia could exacerbate airway or cardiovascular collapse. In this context the procedure was successfully performed under local anesthesia and hypnosis in selected patients to avoid anesthesiological risks due the compression that anterior mediastinal mass can exert.

What is known and what is new?

- For large anterior mediastinal masses, obtaining a biopsy with sufficient fresh tissue is essential for accurate diagnosis and target treatment. However, this procedure often carries significant anesthesiological risks of airway and cardiovascular compression during general anesthesia.
- For anterior mediastinal masses with high anesthesiological risk under general anesthesia, local anesthesia combined with hypnosis can be used as a safe and effective alternative.

What is the implication, and what should change now?

- This case demonstrates that performing anterior mediastinotomy under local anesthesia and hypnosis is a safe and effective alternative to general anesthesia for selected patients with large anterior mediastinal masses. Moving forward, surgical teams should consider adopting this approach to reduce anesthetic risks and improve patient outcomes in high-risk cases.

local anesthesia. We present this case in accordance with the CARE reporting checklist (available at https://med.amegroups.com/article/view/10.21037/med-25-25/rc).

Case presentation

A 45-year-old female presented with lower left thoracic wall pain and fatigue. Routine lab tests, including complete blood count and comprehensive metabolic panel, were unremarkable except from elevated D-dimers at 10,488 ng/mL (reference <500 ng/mL).

A thoracic computed tomography (CT) scan (*Figure 2*) revealed a large anterior-superior mediastinal mass of 80 mm × 67 mm with malignant left pleural effusion. The core biopsy was consistent with a myeloid sarcoma (MS), a rare extramedullary manifestation of acute myeloid leukemia (AML), according to World Health Organization (WHO) 2022 classification and the International Consensus Classification (ICC) 2022. The fluorine 18-labeled fluorodeoxyglucose (FDG) positron emission tomography (PET)-CT (*Figure 3*) showed increased FDG uptake by the mediastinal mass, the presence of numerous hypermetabolic lymph nodes on both sides of the diaphragm and a thickened left pleura. The bone marrow biopsy was negative for AML and a new large surgical biopsy of the mediastinal mass had to be performed for fresh tissue samples, in order to perform flow cytometry, molecular and cytogenetic analysis.

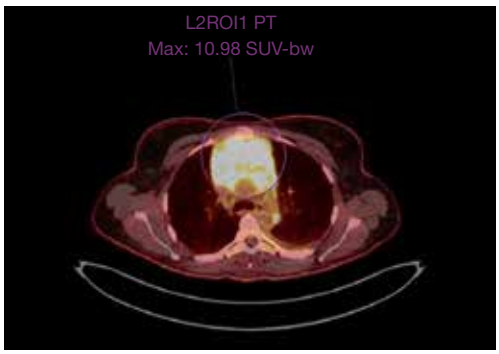

Figure 3 Image of the PET-CT scan of the mediastinal mass. CT, computed tomography; PET, positron emission tomography.

The multidisciplinary tumor board opted for an anterior mediastinotomy to collect sufficient tissue samples for the various analysis. Due to the size of the tumor, general anesthesia was associated with a very high risk of airway obstruction and vena cava compression. After thorough discussions between surgery and anesthesia teams, an alternative approach, with the employment of hypnosis paired with local anesthesia, was considered. It is worth mentioning that the patient had no prior hypnosis experience, but she was very willing to try this new technique.

The hypnotherapist visited the patient in her room. During a 20-minute session, the patient shared a positive memory and described it in detail.

In the operating room, the patient was in the supine position. A venous catheter and standard monitoring were applied to the patient. The anesthesiologist induced hypnosis using the Ericksonian technique (5). The patient was invited to focus on a point with her eyes, then to concentrate on her breathing, and finally to relive the positive memory she had chosen and described earlier. The hypnotherapist described the place, the colors, the smells, using a calm and monotonous voice. The therapist spoke throughout the entire procedure, employing techniques to dissociate the patient from the operating room. A continuous infusion of remifentanil was started with target controlled infusion (TCI) in a peripheral venous line and was modified as required. The target of our continuous infusion of remifentanil (mode TCI – target controlled infusion) was between 1 ng/mL and 3 ng/mL during the surgery. Paracetamol 1 g, ketorolac 30 mg and midazolam 0.1 mg were given before incision. The depth of sedation was monitored clinically, and the patient maintained a Ramsay Sedation Score of 2, which corresponds to an "awake, calm, and cooperative" state.

Surgeons proceeded with disinfection and draping once the patient was in state of well-being thanks to hypnosis. Local anesthesia was infiltrated through the cutaneous and subcutaneous planes and extended into the second intercostal space at the site of incision with 25 mL of lidocaïne 1% with adrenaline 1/200,000 was performed. Once the local anesthesia had taken effect, we made an incision of 5 cm at the level of the 2nd left intercostal space (*Figure 4A*, *Video 1*). This step was followed by dissection between the fibers of the pectoral muscle then by incision of the intercostal space. This allowed clear visualization of the waxy white tumor. We performed four cold blade biopsies in a square of 1 cm × 1 cm × 1 cm with a scalpel (*Figure 4B*). The biopsies were followed by careful hemostasis. During the procedure the pleural space was opened, and the resulting pneumothorax was evacuated only by aspiration before definitive skin closure (*Figure 4C*,*4D*). The surgery lasted 28 minutes.

After surgery, the patient emerges from hypnosis in operating room and she went to the recovery room. The hypnotherapist visited the patient and checked that the patient was correctly oriented in time and space. After 42 minutes, she was discharged from the recovery with a Visual Analog Scale for pain of 0/10. The postoperative chest X-ray was unremarkable. The patient was pleasantly surprised by the care and support. She evaluated her comfort of 7/10 during the procedure. Ever since, she uses hypnosis through every procedure (bone marrow biopsy, lumbar puncture, chemotherapy etc.). It is a new personal resource for the patient.

The molecular genetics of the biopsy that was conducted revealed a MS with complex karyotype and the presence of *NF1* and *PHF6* mutations, presenting a risk according to European Leukemia Net (ELN) classification. The patient opted to immediately began the induction chemotherapy with "3+7" (doxorubicine + cytarabine) and due to the high risk of relapse, will need to undergo allogeneic stem cell transplantation at first complete remission.

All procedures performed in this study were in accordance with the ethical standards of the institutional and/or national research committee(s) and with the Declaration of Helsinki and its subsequent amendments. Informed consent was obtained from the patient for publication of this case report and accompanying images and video documented in her medical record. A copy of the written consent is available for review by the editorial office of this journal.

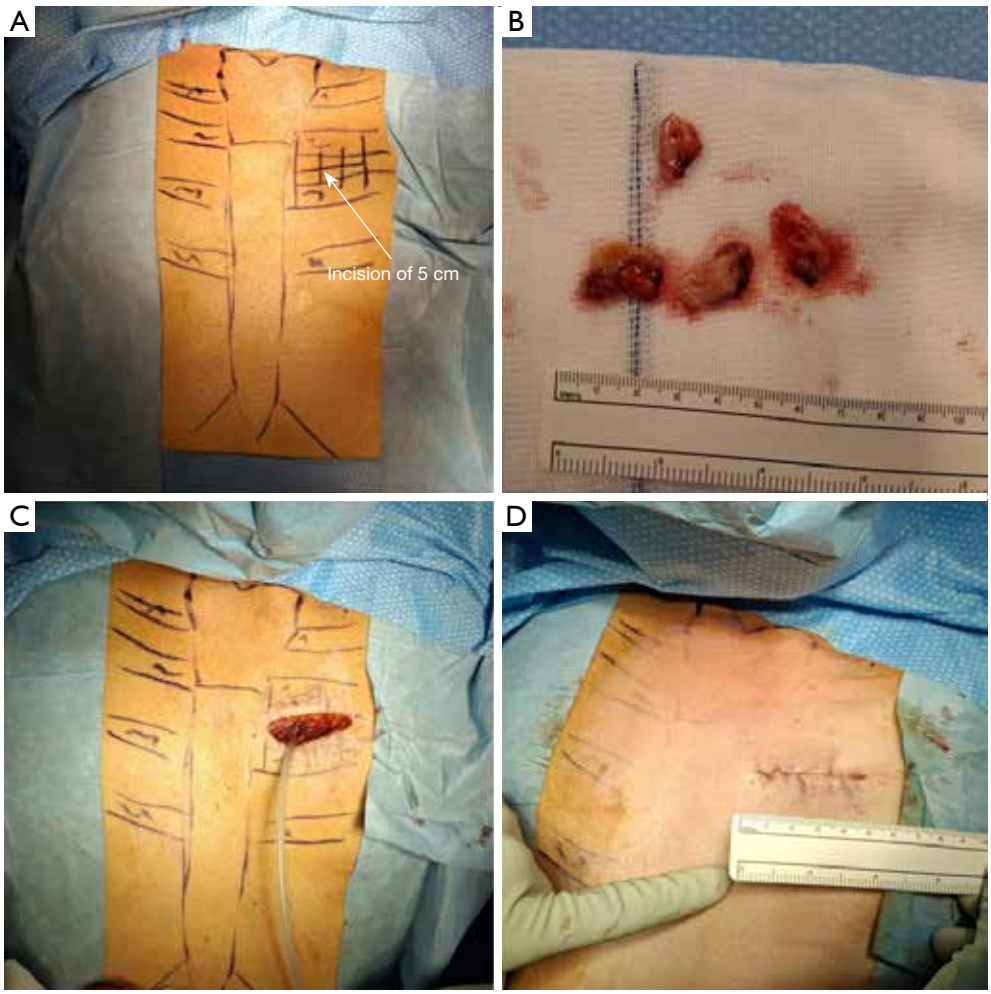

Figure 4 Surgical description of the anterior mediastinotomy according to Chamberlain. (A) Preoperative marking of the thoracic incision. (B) A picture of the 4 biopsies taken during the procedure. (C) Layer-by-layer closure of the mediastinum and skin with drainage during closure. (D) Final scar.

Video 1 Anterior mediastinotomy according to Chamberlain procedure under local anesthesia and hypnosis.

Discussion

Hypnosis began to take its place in surgery in the 19th century for breast surgery (6). In recent years, surgery under hypnosis has become increasingly widespread also in other surgical fields including thoracic surgery. However, this technique is limited for carefully selected patients with a good understanding for risks involved to undergo general anesthesia and for the great advantages of hypnosis. As in our clinical case, general anesthesia carried too much risk for the patient. Due to the size of the tumor, several risks related to general anesthesia were highlighted by the anesthesia team including risk of airway collapse, bronchospasm and compression of the superior vena cava

(2-4,7). In the case of compression of the superior vena cava, the consequences would include an alteration of blood flow from the superior vena cava to the right atrium and venous congestion of the face and upper limbs (4). However, recent literature has shown that, under direct visualization, general anesthesia does not necessarily worsen airways collapse in patient with anterior mediastinal masses (8). Nevertheless, given the heterogeneity of clinical presentations and variability institutional experience, the multidisciplinary team in our case was opted for an awake surgical approach with hypnosis, as general anesthesia was considered to carry excessive risk for the patient.

In this context, surgery under local anesthesia with hypnosis was proposed and accepted by the patient. Hypnosis is a non-invasive and safe alternative to general anesthesia for certain procedures and selected patients. In order to conduct this procedure, the surgeon must be experienced and competent, as well as every medical professional involved in the operation.

Conclusions

In order to avoid airway and circulatory collapse, due to its feasibility, anterior mediastinotomy according to Chamberlain under local anesthesia and hypnosis should be considered by thoracic surgeons. It has been established that it reduces the risks associated with general anesthesia in patients with an anterior mediastinal mass requiring surgical biopsy. This operation, however, must be performed by an experienced surgeon and with prescreened patients in medical centers with anesthesiologists trained in hypnosis.

Acknowledgments

This study would not have been possible without the support of the Hematology, Anesthesiology, and Surgery Departments of the Cantonal Hospital of Fribourg. And we sincerely thank the Cantonal Hospital of Fribourg for its financial support.

Footnote

Reporting Checklist: The authors have completed the CARE reporting checklist. Available at https://med.amegroups.com/article/view/10.21037/med-25-25/rc

Peer Review File: Available at https://med.amegroups.com/article/view/10.21037/med-25-25/prf

Funding: The study was supported by the Cantonal Hospital of Fribourg.

Conflicts of Interest: All authors have completed the ICMJE uniform disclosure form (available at https://med.amegroups.com/article/view/10.21037/med-25-25/coif). J.L. reports receiving payments/honoraria for lectures from Medtronic and serving on a Data Safety Monitoring Board or Advisory Board for AstraZeneca. The other authors have no conflicts of interest to declare.

Ethical Statement: The authors are accountable for all aspects of the work in ensuring that questions related to the accuracy or integrity of any part of the work are appropriately investigated and resolved. All procedures performed in this study were in accordance with the ethical standards of the institutional and/or national research committee(s) and with the Declaration of Helsinki and its subsequent amendments. Informed consent was obtained from the patient for publication of this case report and accompanying images and video documented in her medical record. A copy of the written consent is available for review by the editorial office of this journal.

References

1. McNeill TM, Chamberlain JM. Diagnostic anterior mediastinotomy. Ann Thorac Surg 1966;2:532-9.
2. Azizkhan RG, Dudgeon DL, Buck JR, et al. Life-threatening airway obstruction as a complication to the management of mediastinal masses in children. J Pediatr Surg 1985;20:816-22.
3. Sarkiss M, Jimenez CA. The evolution of anesthesia management of patients with anterior mediastinal mass. Mediastinum 2023;7:16.
4. Chaudhary K, Gupta A, Wadhawan S, et al. Anesthetic management of superior vena cava syndrome due to anterior mediastinal mass. J Anaesthesiol Clin Pharmacol

2012;28:242-6.
5. Kiarsis V. Understanding Ericksonian Hypnotherapy: Selected Writings of Sidney Rosen. Routledge; 2020.
6. Fuge CA. Bedford Square. A connexion with mesmerism. Anaesthesia 1986;41:726-30.
7. Belknap AR, Krause JR. Myeloid sarcoma causing airway obstruction. Proc (Bayl Univ Med Cent) 2017;30:195-6.
8. Hartigan PM, Karamnov S, Gill RR, et al. Mediastinal Masses, Anesthetic Interventions, and Airway Compression in Adults: A Prospective Observational Study. Anesthesiology 2022;136:104-14.

doi: 10.21037/med-25-25
Cite this article as: Simioni L, Stiennon O, Lutz J, Efthymiou A, Rouiller B. Case report: awake Chamberlain mediastinotomy under hypnosis to prevent complete airway obstruction and cardiovascular collapse. Mediastinum 2025;9:29.

Retraction: Postoperative complications of mediastinal cyst resection and their management

Hana Ajouz, Nestor Villamizar

Section of Thoracic Surgery, Department of Surgery, Leonard M. Miller School of Medicine University of Miami, Miami, FL, USA

Correspondence to: Nestor Villamizar, MD. Section of Thoracic Surgery, Department of Surgery, Leonard M. Miller School of Medicine University of Miami, Miami, FL, USA. Email: nvillamizar@med.miami.edu.

Received: 01 July 2025; Accepted: 11 July 2025; Published online: 10 September 2025.

doi: 10.21037/med-25-36

View this article at: https://dx.doi.org/10.21037/med-25-36

Retraction to: Mediastinum 2023;7:20.

The authors have requested the retraction of the article (1) titled "Postoperative complications of mediastinal cyst resection and their management" (doi: 10.21037/med-22-30) due to citation errors, which may have arisen from a disruption in the reference order during the writing process. As the original file containing the embedded references is no longer available, the authors have decided to withdraw the article from publication.

The authors apologize for any inconvenience caused.

This retraction was submitted by the authors and approved by the editorial office of *Mediastinum*.

Footnote

Conflicts of Interest: Both authors have completed the ICMJE uniform disclosure form (available at https://med.amegroups.com/article/view/10.21037/med-25-36/coif). N.V. serves as an unpaid editorial board member of *Mediastinum* from August 2024 to July 2026. The other author has no conflicts of interest to declare.

Ethical Statement: The authors are accountable for all aspects of the work in ensuring that questions related to the accuracy or integrity of any part of the work are appropriately investigated and resolved.

References

1. Ajouz H, Villamizar N. Postoperative complications of mediastinal cyst resection and their management. Mediastinum 2023;7:20.

doi: 10.21037/med-25-36

Cite this article as: Ajouz H, Villamizar N. Retraction: Postoperative complications of mediastinal cyst resection and their management. Mediastinum 2025;9:30.